Self-assembling polycations for gene delivery: Effects of polymer structure and environmental pH

Dissertation

zur

Erlangung des Doktorgrades

der Naturwissenschaften

(Dr. rer. nat)

dem Fachbereich Pharmazie

der Philipps-Universität Marburg

vorgelegt von

Olga Samsonova

aus Charkiw / Ukraine

Marburg / Lahn 2012

Vom Fachbereich Pharmazie der Philipps-Universität Marburg als Dissertation

Am 14.02.12 angenommen.

Erstgutachter: Prof. Dr. Thomas Kissel

Zweitgutachter: Prof. Dr. Carsten Culmsee

Tag der mündlichen Prüfung am 15.02.2012

Die vorliegende Arbeit entstand auf Anregung und unter der Leitung von

Herrn Prof. Dr. Thomas Kissel

am Institut für Pharmazeutische Technologie und Biopharmazie

der Philipps-Universität Marburg.

Gewidmet meinen Eltern & Mitstreitern
in Liebe und Dankbarkeit

Table of Contents

Chapter 1

Introduction

THERAPEUTIC GENE DELIVERY

Several basic terms and definitions tightly connected with **therapeutic gene delivery** need to be addressed prior to discussing polymeric gene delivery systems, which are subject of this dissertation. Polycations were synthesized and characterized here with the perspective to generate therapeutic tools in the biomedical field in the foreseeable future.

What is gene therapy?

It is a rather young therapeutic direction, which bases its curative attempts on causal principles, namely on correction of gene malfunction or the absence of functional gene. A broad variety of diseases which have their origin in some hereditary or acquired gene defects can be treated more directly and effectively with gene therapy. If this therapeutical gene "reparation" approach is successful, the disease symptoms will be eliminated more productively than it could be done via traditional medicinal methods, directed against the consequences of gene malfunction. The correction of gene defects can be achieved by gene replacement, removal or silencing of genes in the tissue of interest. Therapeutic gene delivery is a practical tool for achieving the goals of gene therapy.

Where can therapeutic gene delivery be applied?

Here are some examples from the broad range of severe diseases which can be potentially treated or even cured with gene therapy: cystic fibrosis [1], HIV [2], haemophilia [3], cardiovascular disorders [4], Wiskott-Aldrich Syndrom [5] and cancer [6, 7].

Two basic principles of gene "reparation" in the cell:

To address the defect gene some agent should be brought into the cell. The process of deliberate introduction of nucleic acids into the eukaryotic cell is usually defined as **transfection**. Material transfected, or introduced, into the cell can be DNA or RNA. Depending on the type of nucleic acid their further desired destination is different. So DNA needs to reach and enter the nucleus (Figure 1), whereas RNA is performing its function already in cytosol (Figure 2).

The transfected gene in form of **DNA**, would be as well supposed to perform "gene expression" after locating itself in cell nucleus, whereas **RNA** introduction mostly results in "**gene silencing**", or in other words would be blocking some "gene expression" or gene expression products at the level of translation. The process within living cells that moderates the activity of their genes is called **RNA interference** (**RNAi**) and was first described in live experiment in 1998 [8].

Both, gene expression after DNA, and gene silencing after RNA delivery are considered to be equivalent therapeutic approaches in the scope of gene therapy.

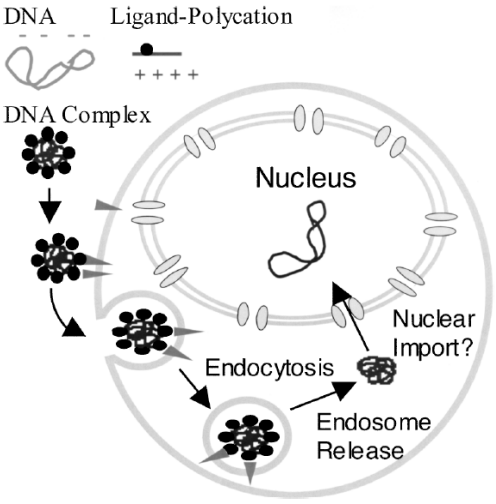

Figure 1: DNA delivery to the cell by polycationic vectors, the DNA needs to reach nucleus, where it follows the biological amplification mechanism (coding DNA › mRNA › therapeutic protein) to achieve required therapeutic effect. [9]

Nevertheless RNA is evaluated as a more long lasting gene therapy tool [10].

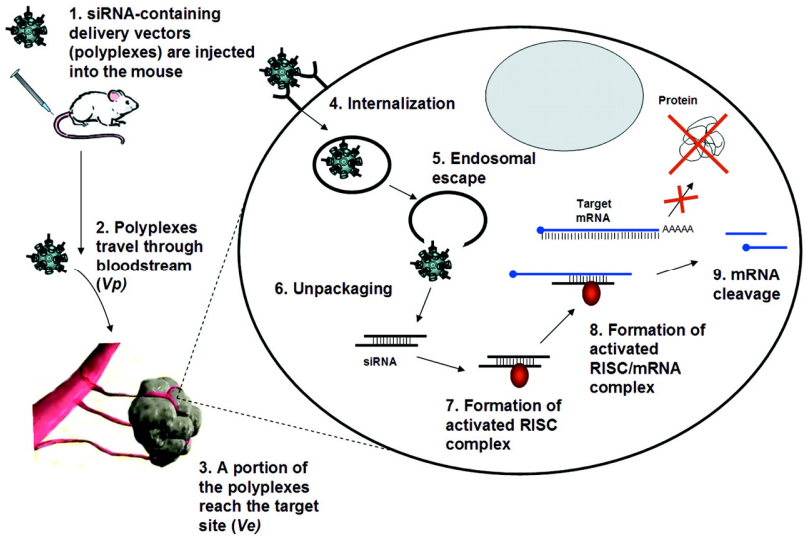

Figure 2: key steps of siRNA delivery into the cell and its "silencing" action pattern [10]

In our study we use plasmid DNA (pDNA) of a Luciferase coding gene (or reporter gene) as a model gene for transfection. The stably transfected cells which can produce Luciferase enzyme due to successful pDNA delivery into the nucleus, are treated with anti-Luceferase small interfering RNA (siRNA). The delivery efficacy of DNA and siRNA with polycationic carriers can be monitored as increased or decreased luminescence of the cells after treatment respectively.

CHARACTERISTICS OF CANCER TISSUE AS ONE OF GENE DELIVERY OBJECTIVES

Here some specific characteristics of cancer tissue, as one of the mainstream interests for therapeutic gene delivery, will be discussed in short.

Acidification of tumor tissue

One of tumor tissue characteristics is an increased acidity 6.72 - 7.01 in comparison to a healthy tissue with pH 7.3-7.4. Tumors metabolize glucose to acidic products faster than normal cells, hence increasing their acidity very rapidly [11]. Nevertheless such condition can appear in pathological state only at simultaneous lack of oxygen.

Apart of acidification of tumor tissue due to accumulating metabolite products, which can be exploited for targeting with pH-sensitive vehicles, there is also acidification inside the tumor cell compartments, which is not being straight forward and has a disadvatageous impact on chemotherapy. For example the MDR breast cancer cells have less acidic cytoplasm than drug sensitive cells, but more acidic compartmental system. In this way, among others, tissues achieve their multi drug resistance (MDR) in tumor therapy due to capturing antitumor agents in endosomes and lysosoms [12]. Another self-protecting mechanism of MDR tumor cells is P-glycoprotein efflux-pump counteracting the accumulation of chemotherapeutical agents at the site of action [13].

On the other hand tumor acidity as a specific tissue feature can be exploited for therapeutic gene delivery issues, selectively tuning the disruptive activity of nano-vehicles in targeted cells [14, 15].

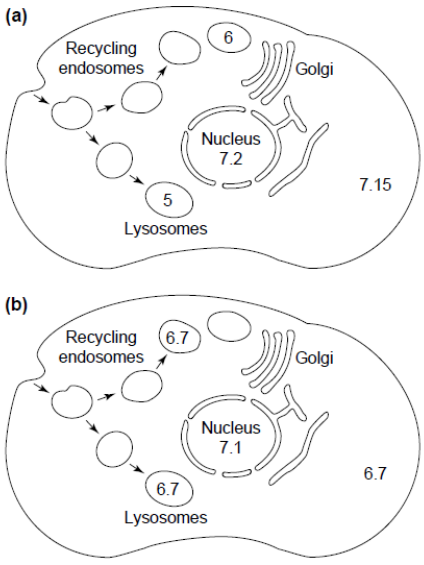

Figure 3: Schematic view of (a) a drug-resistant cell and (b) a drug-sensitive tumor cell showing the pH values measured in the various compartments [16].

Tumor cell growth phases

The control mechanism orchestrating the cell growth cycle is a factor which has to be involved in cell tumorogenic activity, as one of the features of cancer is an excessive cell proliferation with reduced control over differentiation or cell death [17]. After mitosis the daughter cells may grow to non-dividing cells or turn to another cell life cycle with G1, S and G2 phase. In case of tumor cells the farther multiple division cycles will be pursuit after mitosis.

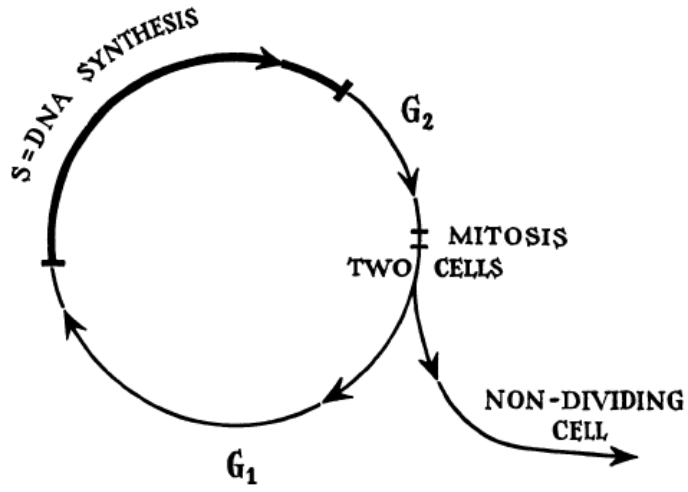

Figure 4: Cell life cycle [18].

Dependant on the cell-cycle phase of the cells to be transfected, their internalization ability, endocytosis and thus the transfection efficacy of gene carriers can vary [19-22]. The example below shows the following distribution of model gene expression after transfection performed in different cell cycle phases. Depandant on proportion of cells in different cell cycle phases in tumor tissue as a unit, the efficacy of a therapeutic agent would vary.

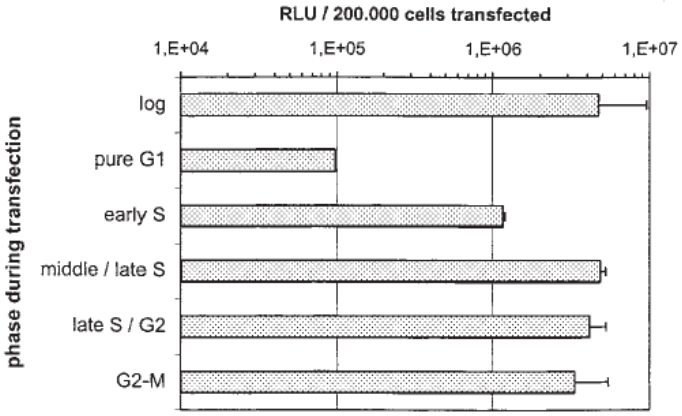

Figure 5: Cell cycle dependence of DNA-PEI transfection efficacy [19].

There is another rather converse finding of Tseng et al., where during late G1 phase 1.5 times more polyplexes are uptaken than during G2/M phases [22]. But if the cells were at S or G_2/M phases at the beginning of transfection process, approximately 30-fold or more than 500-fold higher transgene expression could be achieved than with the cells in G1 phase [19]. The cell nature should be taken into account during evaluation of cell cycle impact on transfection results.

Enhanced Permeation and Retention (EPR) Effect

Tumor tissue is known for its extensively fast growth. Due to this fact, the vessels which need to be built for blood supply of the new tissue are growing in accelerated regime. The vessel walls in tumor area are not as tightly constructed as in healthy tissue, showing multiple openings able to let through some nano-scaled objects. The grade of tumor tissue vascularisation is also above normal. Moreover the lymphatic drainage of tumor tissue is absent, herewith limiting the evacuation of infiltrated objects.

Enhanced Permeation and Retention (EPR) Effect occurs as follows: a nano-sized object, possessing no special attraction forces to a certain tissue, or predisposition to conglutinate or to be absorbed during circulation in blood steam, would not be able to get into the tissue

surrounded with healthy vessels and would not be lost from circulation till it billiary or renally eliminated. The journey through the cardiovascular system would continue till the nano-object meets the leaky vessels of tumor. Here it can passively leave the vessel and enter the malignant tissue, accumulating there due to intensified blood perfusion of tumor and lacking lymphatic drainage [23]. On this principle gene carriers without targeting moiety can be to some extent addressed to the tumor tissue "ignoring" healthy organs, in this way reducing the off-target toxicity. This passive targeting can in no case completely replace the targeting moeties but can only give some assistance to generalized drug application indicated for tumor tissue.

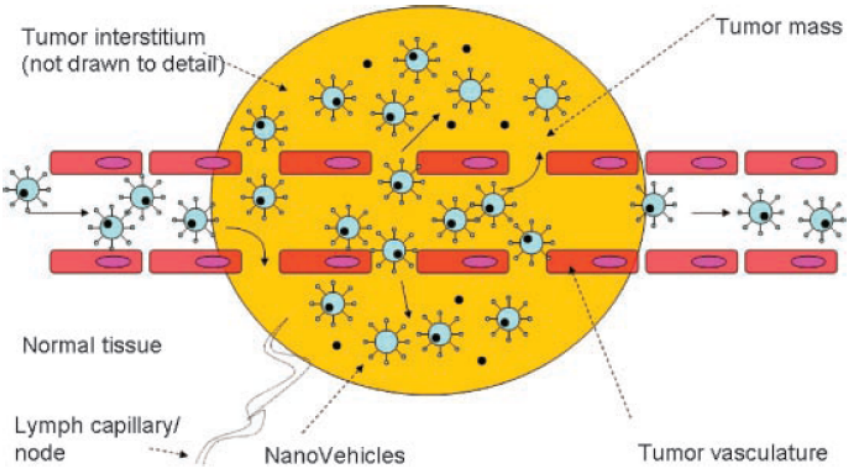

Figure 6: Enhanced Permeation and Retention Effect. Passive targeting of tumor tissue due to enhanced fenestration of tumor vasculature: preferential extravasation of nanovehicles from circulation into tumor and acculmulation there due to absent lymphatic drainage [23]

CLASSICAL EXAMPLES OF POLYCATIONIC MATERIALS FOR GENE PACKAGING

Advantages of polymeric gene carriers over viruses and liposomes

An ideal polymeric vector should combine the advantages of high performance gene delivery of viral vectors, and at the same time show reduced toxicity in comparison with cationic lipids. Immuno- and pathogenicity as latent risk of viral carriers should be eliminated, as well as sufficient load capacity for genetic cargo should be ensured [24-26].

Another advantage of polymeric vectors is the possibility to tailor them individually according to the delivery system design needs, enjoying the privilege of synthesis controllability, reproducibility and potentially easier up-scale-ability of manufacturing process.

Self-assembly principle

Most water soluble polycations have protonated nitrogens in their structure which interact with negative phosphates of nucleic acids due to charge to charge interaction. In this manner self-assembled nano-carriers are created by common pipetting of two solutions together. The polymer complexes with DNA, or **polyplexes**, gain more or less positively charged surface, depending on polymer structure and excess of polymeric nitrogen in nitrogen to phosphate ratio of the final nano-scaled construct (N/P).

Classical representatives of polycationic materials for gene delivery

A short overview of well known mainstream polycations with alterating branching grade, deriving from different polymeric classes is presented below.

Poly(ethylene imine) (branched PEI 25 kDa)

PEI was described 1995 by Boussif et al. [27] as “proton sponge”, where every third polymer atom is a protonable amino nitrogen. The primary amines are preferably protonated already at physiological pH, the higher order amines have a broader protonation capacity [28]. This feature is favourable for endosomal escape, so that no additional transfection helpers like chloroquin are needed for PEI-DNA complexes [29, 30].

PEI is a branched polymer but it lacks a definite symmetrical central point [28], the construct retains a spherical form and is rather inflexible in its interactions with nucleic acids [31].

The highest efficacy of PEI in transfection was observed for polymer molecular weights (Mw) between 5 and 25 kDa [32], whereas higher Mw appeared to be more toxic [33].

Microcalorimetric data support the charge based self-assembly process with DNA [34].

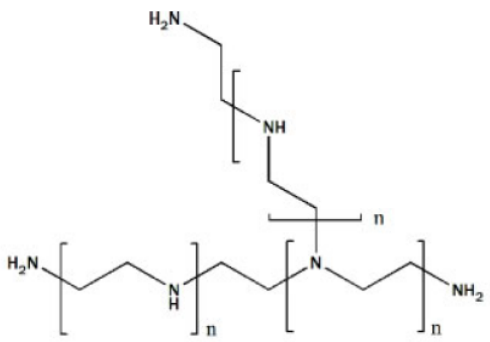

Figure 7: Branched PEI [32]

Poly(L-Lysine) (linear PLL)

Leammli et al. first visualized the ability of polylysine to compact DNA into a tight structure 1975 [35]. PLL is a liner polycation built from lysine repeating units. It has rather poor buffering capacity under pH 8, as only primary amines are available for protonation. The ability to transfect cells is also lower than those of branched PEI [28]. Transfection efficacy was correlating with toxicity of PLL increasing towards higher Mw [29]. The reduced

transfection efficiency in some cases is believed to be caused by the cell death of transfected cells, lowering the general expression rate of a model gene.

The complexation ability of linear PLL assessed with ethidium bromide assay was less pronounced than in case of PEI [28]. The ability to disrupt endosomes is very low in comparisson to proton-sponge active polymers like PEI [36].

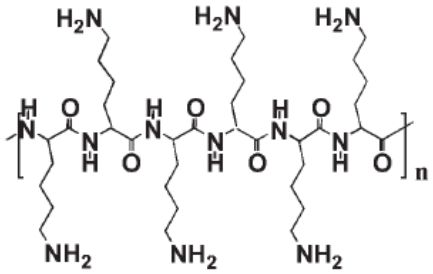

Figure 8: Polylisine [25]

Poly(2-(dimethyl amino)ethyl methacrylate), pDMAEMA

pDMAEMA is a linear polymer, its acrylate backbone is non-biodegradable, the ester group in the side chain can be hydrolysed. The hydrolytic stability of polycation increases with growing polymerization grade [37]. The average pKa is about 7.5, so the charge availability at physiological pH is available not in full extent [37]. This charge intensity is however sufficient for polymer-DNA complex formation and DNA protection, but easily dissociable once entering the cytosol [38]. Transfection efficacy of pDMAEMA Mw 309 kDa was better than of PLL 120 kDa in COS-7 cells. The toxicity of long chain polymers is growing accordingly, setting a limit for using them as non-viral vectors [39].

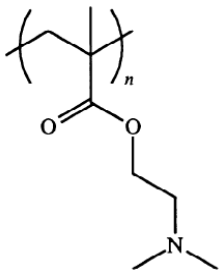

Figure 9: pDMAEMA [39]

STRATEGIES FOR IMPROVEMENT OF POLYMERIC CARRIERS

"The **ideal nanovehicular vector** would achieve long circulation time, low immunogenicity, good biocompatibility, selective targeting, efficient penetration of physiological barriers such as vascular endothelium and the blood–brain barrier, external activation or self-regulating drug release, and have no clinical side-effects"[23].

Ideal vector has not been created yet, but the approaches to lend some of its properties to already existing polymers can be traced in optimization attempts of different working groups.

Some of improvement strategies are discussed below:

Prolonged circulation time

Poly(ethylene glycol) (PEG) is a linear polyether diol, which combines several essential properties like biocompatibility, good water and organic medium solubility; it is non-toxic and was approved by FDA for internal administration [40].

Conjugation of PEG to different kinds of polycations was found to be beneficial. So e.g. the masking effect of PEG in PEG-PLL conjugate was demonstrated previously resulting to decreased cell adherence of polyplexes [41]. This effect resulted in transfection reduction in vitro, but in more physiological conditins PEG-PLL conjugates were more successful and

prevented polyplex aggregation [42, 43]. Longer circulation time of polyplexes with “indifferent” behavior in blood stream would enlarge their accumulation in tumor due to EPR effect [44]. Nevertheless activation of anti-PEG IgM after multiple exposition to PEGylated vectors was reported [45]. It resulted in “accelerated blood clearance” (ABC) phenomenon, the second dose of vector was removed from circulation much more rapidly, so that the vector could not develop the expected performance achieved initially.

Increased biocompatibility

It was manifold stated previously that transfecting agents with high molecular weight are being more effective, but also more toxic. How can transfection performance be retained whereas toxicity reduced?

One of the approaches is to reduce the Mw of involved polycation, as the most toxicity is charge associated [33]. Problematic of this toxicity reduction approach is a lower capability of low molecular weight vectors to compact and protect DNA from enzymatic degradation. To avoid this handicap of short chain polycations, most authors design complex polymeric constructs containing low toxic polycationic parts reversibly bound via biodegradable link to each other or an alternative backbone with good biocompatibility. Some examples could be: the S-S bound PEI-PEG vector, where PEI of 2 kDa was playing role of element for DNA complexation [46] or pDMAEMA side chains of pDMAEMA under 30 kDa bound via hydrolysable linkers to pHEMA backbone [47]. In both cases the linked structure had a higher gene delivery performance than its components taken apart, as well as a potential to be degraded into smaller products eliminable from the body and hence less toxic.

Increased membrane activity

Under membrane activity both outer cellular membrane and intracellular compartment membrane (endosomal and lysosomal membrane) are interaction surfaces which will be involved in discussion.

Attraction to and interaction with cellular membrane are of critical importance for productive carrier uptake into the cell. At least partial positive charge of polyplex surface is needed to attract nano-vehicle to negatively charged cell membranes. Neutral or negatively charged polymers would have difficulties to do so. After the gene delivery system and cell surface get in contact the uptake into the cell is needed for further processing of polymer protected gene. Endocytosis is believed to be the most frequent uptake mechanisms [48], whereas local destabilisation of membrane leading to enchanced penetrability is also considered to be important (e.g. for pDMAEMA [39]).

When the polyplex is taken up it meets next hurdle – it is captured in endosomal compartment and needs to escape before it is digested. To break out it needs certain disruptive forces, e.g. buffering capacity, which is based on ability of polymer to act as “proton sponge” and finally disrupt swollen compartment [49]. Broad buffering capacity is considered to be a good prerequisite of disruption activity.

Another way to increase membrane activity is the introduction of hydrophobic component, which may integrate itself in membrane phospholipid bilayer, hence serving as anchorage and membrane penetrability enhancer. This feature was borrowed from the liposomal structure, known for its excellent membrane penetrability due to membrane fusion [50, 51].

OBJECTIVE OF THE STUDY

Chapter 1 gives a short introduction on therapeutic gene delivery, defining constituent parts associated with it, explaining differences in DNA and siRNA approach to “curing” of gene

malfunction. Among the variety of severe diseases building a scope of gene therapy, special focus is given on cancer tissue characteristics, such as acidification and EPR-effect, which have essential impact on nano-carrier delivery. Classical representatives of branched and linear polycationic vectors are shortly introduced: PEI, PLL and pDMAEMA. Basic strategies for polymeric carriers' improvement are also being discussed in this chapter.

Chapter 2 aimes to investigate the alterations in polymeric transfection caused by changes in the extracellular pH during both uptake and culture phases. The study focuses on polymeric and cellular characteristics and their respond to pH decrease. The model polycations with different physicochemical properties PEI 25 kDa and PLL 27 kDa are being monitored according to their proton buffering capacity and ionization, polyplex size, surface charge, and decomplexation ability. The pH induced cellular characteristic alterations, reflected in cellular uptake, cell cycle phases, and intracellular pH environment, are also investigated.

Chapter 3 explores the impact of hydrophilic-hydrophobic-polycationic composition in tri-block polymer on its physicochemical properties. The aim of the study is to establish correlation between polymer structure and siRNA transfection efficacy. A library of PEG-PCl-PEI block-copolymers was synthesized, modifying the branching grade and PCL-segment length, in order to increase the carrier colloidal stability and ability to escape from endosomal compartments.

Chapter 4 deals with transfection efficacy optimization of low molecular weight pDMAEMA-vectors for DNA delivery. It is hypothesized that minimizing of polycationic chain length leads to a better vector biocompatibility, at the same time the pHEMA-grafting to short polycationic chain can improve its poor performance in vitro. A library of pDMAEMA-b-pHEMA diblock-copolymers with varying co-block proportions is tested towards their

ability to enhance transgenic expression in comparison to a low molecular weight homo-pDMAEMA.

In **Chapter 5** it is hypothesized that the conformational rearrangements of polymeric carriers in aqueous solution have impact on thermodynamics of polymer-DNA binding, what could be a reason for transfection efficacy alterations within the low molecular weight pDMAEMA-b-pHEMA diblock-copolymer family. The pHEMA co-part is supposed to increase the glas transition temperature of diblock-copolymers, reducing the chain mobility and hence impeding the folding readiness of a linear construct. The better surface assesibility of polycation nitrogens in a non-folded rigid construct is supposed to result in more energetically favourable polymer interaction with DNA.

REFERENCES

[1] Pringle IA, Hyde SC and Gill DR. Expert Opin. Biol. Ther. 2009;9(8):991-1003.
[2] Marathe JG and Wooley DP. Genet. Vaccines Ther. 2007;5:No pp. given.
[3] Schwaab R, Albert T, Brackmann H, Srour M, and Oldenburg J. BIOspektrum 2002;8(2):148-152.
[4] Metcalfe BL, Sellers KW, Jeng MJ, Huentelman MJ, Katovich MJ, and Raizada MK. Ann. N. Y. Acad. Sci. 2001;953(New Vistas in Therapeutics and Drug-Resistant Tuberculosis):31-42.
[5] Galy A and Thrasher AJ. Curr. Opin. Allergy Clin. Immunol. 2011;11(6):545-550.
[6] Scholl SM, Michaelis S and McDermott R. J. Biomed. Biotechnol. 2003(1):35-48.
[7] Gough MJ and Vile RG. Oxford Monogr. Med. Genet. 2003;48(Genetics of Renal Disease):515-555.
[8] Fire A, Xu S, Montgomery MK, Kostas SA, Driver SE, and Mello CC. Nature (London) 1998;391(6669):806-811.
[9] Ogris M and Wagner E. Somatic Cell Mol. Genet. 2002;27(1-6):85-95.
[10] Bartlett DW and Davis ME. Nucleic Acids Res. 2006;34(1):322-333.
[11] Volk T, Jaehde E, Fortmeyer HP, Gluesenkamp KH, and Rajewsky MF. Br. J. Cancer 1993;68(3):492-500.
[12] Altan N, Chen Y, Schindler M, and Simon SM. J. Exp. Med. 1998;187(10):1583-1598.
[13] Broxterman HJ, Sonneveld P, Van Putten WJL, Lankelma J, Eekman CA, Ossenkoppele GJ, Pinedo HM, Lowenberg B, and Schuurhuis GJ. Leukemia 2000;14(6):1018-1024.
[14] Kang HC and Bae YH. Endolysosomolytically active pH-sensitive polymeric nanotechnology. Organelle-Specific Pharm. Nanotechnol., 2010. pp. 247-262.
[15] Orr G. Organelle-specific pharmaceutical nanotechnology: active cellular transport of submicro- and nanoscale particles. Organelle-Specific Pharm. Nanotechnol., 2010. pp. 337-356.
[16] Simon SM. Drug Discovery Today 1999;4(1):32-38.
[17] Collins K, Jacks T and Pavletich NP. Proc. Natl. Acad. Sci. U. S. A. 1997;94(7):2776-2778.
[18] Baserga R. Cancer Res 1965;25:581-595.
[19] Brunner S, Sauer T, Carotta S, Cotten M, Saltik M, and Wagner E. Gene Ther. 2000;7(5):401-407.
[20] Brunner S, Furtbauer E, Sauer T, Kursa M, and Wagner E. Mol. Ther. 2002;5(1):80-86.
[21] Mortimer I, Tam P, MacLachlan I, Graham RW, Saravolac EG, and Joshi PB. Gene Ther. 1999;6(3):403-411.
[22] Tseng W, Haselton FR and Giorgio TD. Biochim. Biophys. Acta, Gene Struct. Expression 1999;1445(1):53-64.
[23] Prokop A and Davidson JM. J. Pharm. Sci. 2008;97(9):3518-3590.
[24] Kaneda Y and Tabata Y. Cancer Sci. 2006;97(5):348-354.
[25] Han S, Mahato RI, Sung YK, and Kim SW. Mol. Ther. 2000;2(4):302-317.
[26] Mintzer MA and Simanek EE. Chem. Rev. (Washington, DC, U. S.) 2009;109(2):259-302.
[27] Boussif O, Lezoualc'h F, Zanta MA, Mergny MD, Scherman D, Demeneix B, and Behr JP. Proc Natl Acad Sci U S A 1995;92(16):7297-7301.
[28] Tang MX and Szoka FC. Gene Ther. 1997;4(8):823-832.
[29] Kang HC, Lee M and Bae YH. Crit. Rev. Eukaryotic Gene Expression 2005;15(4):317-342.
[30] Forrest ML and Pack DW. Mol. Ther. 2002;6(1):57-66.
[31] Merkel OM, Zheng M, Mintzer MA, Pavan GM, Librizzi D, Maly M, Höffken H, Danani A, Simanek EE, and Kissel T. J Control Release 2011;153(1):23-33.
[32] Neu M, Fischer D and Kissel T. J. Gene Med. 2005;7(8):992-1009.
[33] Fischer D, Li Y, Ahlemeyer B, Krieglstein J, and Kissel T. Biomaterials 2003;24(7):1121-1131.
[34] Bronich T, Kabanov AV and Marky LA. J. Phys. Chem. B 2001;105(25):6042-6050.
[35] Laemmli UK. Proc. Natl. Acad. Sci. U. S. A. 1975;72(11):4288-4292.
[36] Putnam D, Gentry CA, Pack DW, and Langer R. Proc. Natl. Acad. Sci. U. S. A. 2001;98(3):1200-1205.
[37] van de Wetering P, Zuidam NJ, van Steenbergen MJ, van der Houwen OAGJ, Underberg WJM, and Hennink WE. Macromolecules 1998;31(23):8063-8068.
[38] Arigita C, Zuidam NJ, Crommelin DJA, and Hennink WE. Pharm. Res. 1999;16(10):1534-1541.
[39] van de Wetering P, Cherng J, Talsma H, and Hennink WE. J. Controlled Release 1997;49(1):59-69.
[40] Monfardini C and Veronese FM. Bioconjugate Chem. 1998;9(4):418-450.
[41] Mishra S, Webster P and Davis ME. Eur. J. Cell Biol. 2004;83(3):97-111.
[42] Liu G, Li D, Pasumarthy MK, Kowalczyk TH, Gedeon CR, Hyatt SL, Payne JM, Miller TJ, Brunovskis P, Fink TL, Muhammad O, Moen RC, Hanson RW, and Cooper MJ. J. Biol. Chem. 2003;278(35):32578-32586.
[43] Mennesson E, Erbacher P, Piller V, Kieda C, Midoux P, and Pichon C. J. Gene Med. 2005;7(6):729-738.
[44] Stolnik S, Illum L and Davis SS. Adv. Drug Delivery Rev. 1995;16(2,3):195-214.
[45] Tagami T, Nakamura K, Shimizu T, Yamazaki N, Ishida T, and Kiwada H. J. Controlled Release 2010;142(2):160-166.

[46] Zhao N, Roesler S and Kissel T. Int. J. Pharm. 2011;411(1-2):197-205.
[47] Jiang X, Lok MC and Hennink WE. Bioconjugate Chem. 2007;18(6):2077-2084.
[48] Minchin RF and Yang S. Expert Opin. Drug Delivery 2010;7(3):331-339.
[49] Godbey WT, Wu KK and Mikos AG. Proc. Int. Symp. Controlled Release Bioact. Mater. 1999;26th:220-221.
[50] Felgner PL, Gadek TR, Holm M, Roman R, Chan HW, Wenz M, Northrop JP, Ringold GM, and Danielsen M. Proc. Natl. Acad. Sci. U. S. A. 1987;84(21):7413-7417.
[51] Smith JG, Walzem RL and German JB. Biochim. Biophys. Acta, Rev. Biomembr. 1993;1154(3-4):327-340.
[52] Liu Y, Nguyen J, Steele T, Merkel O, and Kissel T. Polymer 2009;50(16):3895-3904.
[53] Sun C, Tang T, Uludag H, and Cuervo JE. Biophys. J. 2011;100(11):2754-2763.
[54] Schallon A, Jerome V, Walther A, Synatschke CV, Mueller AHE, and Freitag R. React. Funct. Polym. 2010;70(1):1-10.
[55] Alatorre-Meda M, Taboada P, Hartl F, Wagner T, Freis M, and Rodriguez JR. Colloids Surf., B 2011;82(1):54-62.
[56] Endres TK, Beck-Broichsitter M, Samsonova O, Renette T, and Kissel TH. Biomaterials 2011;32(30):7721-7731.
[57] Liu Y, Samsonova O, Sproat B, Merkel O, and Kissel T. J. Controlled Release 2011;153(3):262-268.
[58] Wiseman T, Williston S, Brandts JF, and Lin LN. Anal. Biochem. 1989;179(1):131-137.
[59] Bouchemal K. Drug Discovery Today 2008;13(21/22):960-972.
[60] Choosakoonkriang S, Lobo BA, Koe GS, Koe JG, and Middaugh CR. J. Pharm. Sci. 2003;92(8):1710-1722.
[61] Nandy B and Maiti PK. J. Phys. Chem. B 2011;115(2):217-230.
[62] Jensen LB, Mortensen K, Pavan GM, Kasimova MR, Jensen DK, Gadzhyeva V, Nielsen HM, and Foged C. Biomacromolecules 2010;11(12):3571-3577.
[63] Samsonova O, Pfeiffer C, Hellmund M, Merkel OM, and Kissel T. Polymers (Basel, Switz.) 2011;3(2):693-718.
[64] Collet O. J. Chem. Phys. 2011;134(8):85101-85107.
[65] Kichler A, Leborgne C, Coeytaux E, and Danos O. J Gene Med 2001;3(2):135-144.
[66] Kim W, Yamasaki Y, Jang W, and Kataoka K. Biomacromolecules 2010;11(5):1180-1186.
[67] Prevette LE, Lynch ML and Reineke TM. Biomacromolecules 2010;11(2):326-332.
[68] Henriksen JR and Andresen TL. Biophys. J. 2011;101(1):100-109.
[69] Lobo BA, Davis A, Koe G, Smith JG, and Middaugh CR. Arch. Biochem. Biophys. 2001;386(1):95-105.
[70] Kataoka K, Ito H, Amano H, Nagasaki Y, Kato M, Tsuruta T, Suzuki K, Okano T, and Sakurai Y. J. Biomater. Sci., Polym. Ed. 1998;9(2):111-129.
[71] Keszler B, Kennedy JP and Mackey PW. J. Controlled Release 1993;25(1-2):115-121.
[72] Santini CMB, Johnson MA, Boedicker JQ, Hatton TA, and Hammond PT. J. Polym. Sci., Part A: Polym. Chem. 2004;42(11):2784-2814.
[73] Weyts KF and Goethals EJ. Polym. Bull. (Berlin) 1988;19(1):13-19.

CHAPTER 2

The Effect of Environmental pH on Polymeric Transfection Efficiency

Han Chang Kang [a,b,1], Olga Samsonova [a,c,1], Sun-Woong Kang [a], You Han Bae [a,d]

[a] Department of Pharmaceutics and Pharmaceutical Chemistry, The University of Utah, 421 Wakara Way, Suite 318, Salt Lake City, UT 84108, USA

[b] Department of Pharmacy, College of Pharmacy, The Catholic University of Korea, 43 Jibong-ro, Wonmi-gu, Bucheon-si, Gyeonggi-do 420 743, Republic of Korea

[c] Department of Pharmaceutical Technology and Biopharmacy, Philipps-Universität Marburg, Ketzerbach 63, D-35032 Marburg, Germany

[d] Utah-Inha Drug Delivery Systems (DDS) and Advanced Therapeutics Research Center, 7-50 Songdo-dong, Yeonsu-gu, Incheon 406 840, Republic of Korea

[1] HCK and OS equally contributed to this work.

Experimental contribution of OS: in vitro transfection and toxicity, acid-base titration of polycations

Accepted in Biomaterials 33 (2012) 1651-1662

ABSTRACT

Although polymers, polyplexes, and cells are exposed to various extracellular and intracellular pH environments during polyplex preparation and polymeric transfection, the impact of environmental pH on polymeric transfection has not yet been investigated. This study aims to understand the influence of environmental pH on polymeric transfection by modulating the pH of the transfection medium or the culture medium. Changes in the extracellular pH affected polymeric transfection by way of complex factors such as pH induced changes in polymer characteristics (e.g., proton buffering capacity and ionization), polyplex characteristics (e.g., size, surface charge, and decomplexation), and cellular characteristics (e.g., cellular uptake, cell cycle phases, and intracellular pH environment). Notably, acidic medium delayed endocytosis, endosomal acidification, cytosolic release, and decomplexation of polyplexes, thereby negatively affecting gene expression. However, acidic medium inhibited mitosis and reduced dilution of gene expression, resulting in increased transfection efficiency. Compared to pH 7.4 medium, acidic transfection medium reduced gene expression 1.6~7.7-fold whereas acidic culture medium enhanced transfection efficiency 2.1~2.6-fold. Polymeric transfection was affected more by the culture medium than by the transfection medium. Understanding the effects of extracellular pH during polymeric transfection may stimulate new strategies for determining effective and safe polymeric gene carriers.

1. Introduction

A great effort for developing effective polymeric vectors has focused primarily on cellular receptor targeting [1-3], endosomal escape [4-6], cytosolic transport [7-9], nuclear import [8, 10, 11], and decomplexation [12-17]. The effects of the transfection environment with respect to proteins [18-20], ions [3, 18, 21-23], pH [13, 16, 17, 24, 25], reduction/oxidation potentials [14, 15, 26], and hypoxia [14, 27-29] have also been investigated in relation to polyplex

preparation and polymeric transfection. Among these effectors, we focused on pH because the solution (or medium) pH, extracellular pH, and intracellular pH can all modify characteristics of polymers, polyplexes, and cells.

When dissolving polycations and pDNA or preparing polycation/pDNA complexes, buffer solutions, saline, and/or deionized water have all been routinely used. These solutions can be artificially modulated by adjusting the pH, which can affect the ionization of polycations and pDNA. A change in ionization influences the physicochemical characteristics (*e.g.*, particle size and surface charge) and complexation/decomplexation behavior of polyplexes [30].

The aforementioned solution can be described as the "extracellular medium," especially when the medium surrounds cells *in vitro* and *in vivo*. The extracellular medium used for laboratory cell cultures can be modulated by adding or removing various components and by adjusting the pH to fit specific purposes. However, *in vivo* extracellular environments are predominantly affected by pathological differences. The extracellular pH of healthy organs is close to pH 7.4 (*e.g.*, pH 7.4 for normal blood, pH 7.2 for brain [31], and pH 7.5 for heart [32]). Under certain pathological conditions, the extracellular pH can become acidic (*e.g.*, approximately pH 6.4-6.8 for solid tumors [33], pH 6.4 for brain ischemia [31], and pH 6.8 for heart ischemia [32]). The extracellular pH can modulate various biological functions, such as gene expression [34], growth rate [35], viability [36], cellular uptake [37], endocytosis [37, 38], exocytosis [38], and lysosomal trafficking [39]. However, the effects of pH on polymeric transfection have rarely been studied.

The intracellular environment is not fixed at a specific pH value. Subcellular compartments such as endosomes (pH 5-7), lysosomes (pH 4-5), the cytosol (pH 6.7-7.1), and the nucleus (pH 7.1-7.2) have separate pH environments [40-42]. Upon endosomal formation, the pH drops with maturation from early to late forms. In particular, the late endosomal and lysosomal pHs are quite distinctive depending on a cell's drug resistance and/or sensitivity

(*e.g.*, approximately pH 6.0 and pH < 5.8, respectively, for drug-resistant MCF7 cells and pH 6.5 and pH > 5.8, respectively, for drug-sensitive MCF7 cells) [40, 41].

Regarding intracellular pH, polymers for polymeric vectors have been designed primarily to target endolysosomal pathways by either disrupting endolysosomal membranes [4-6] or degrading polycations [16, 17].

As described, the pH environment affects characteristics of polymers, polyplexes, and cells. However, after polyplexes or cells are exposed to certain medium or extracellular pH values, it is unknown how the changed pH environments influence polymers, polyplexes, or cells during cellular internalization and intracellular trafficking of polyplexes. Thus, this research aims to understand how extracellular pH affects polyplexes and polymeric transfection. This study examines whether the effects of extracellular pH on transfection efficiency are caused by polyplex/polymer characteristics (*e.g.*, pH-induced changes in surface charge, particle size, and decomplexation of polycation/pDNA complexes and proton buffering capacity of polymers) and/or cellular characteristics (*e.g.*, cellular uptake of polyplexes, cell cycle phases, and cell viability). Branched polyethyleneimine (PEI) and poly(L-lysine) (PLL) were selected as model polymers due to their different degrees of ionization in response to environmental pH changes. Four pHs (*i.e.*, pHs 7.4, 7.0, 6.7, and 6.3) were selected between the physiological pH 7.4 and the pathological lowest possible acidic pH 6.3.

2. Materials and methods

2.1. Materials

PLL hydrobromide (M_w(viscosity) 27.4 kDa), branched PEI (M_w 25 kDa, M_n 10 kDa), 3- (4,5-dimethylthiazol-2-yl)-2,5-diphenyltetrazolium bromide (MTT), RPMI1640 medium, Ca^{2+}-free and Mg^{2+}-free Dulbecco's phosphate buffered saline (DPBS), fluorescein isothiocyanate (FITC), rhodamine B isothiocyanate (RITC), triethylamine (TEA), dimethyl sulfoxide

(DMSO), 4-(2-hydroxy-ethyl)-1-piperazine (HEPES), 2-(*N*morpholino) ethanesulfonic acid (MES), nigericin, monensin, glucose, sodium bicarbonate, propidium iodide (PI), doxorubicin (DOX) (or adriamycin (ADR)), Triton®X-100, recombinant human insulin, and paraformaldehyde (PFA) were purchased from Sigma- Aldrich Companies (St. Louis, MO). Plasmid DNA (pDNA) encoding firefly luciferase (gWiz-Luc or pLuc) was purchased from Aldevron, Inc. (Fargo, ND). Fetal bovine serum (FBS), penicillin-streptomycin antibiotics, trypsin-EDTA, RNase, and YOYO-1 were purchased from Invitrogen, Inc. (Carlsbad, CA). The luciferase assay kit and BCA^{TM} protein assay kit were bought from Promega Corporation (Madison, WI) and Pierce Biotechnology, Inc. (Rockford, IL), respectively.

2.2. Cells and cell culture

MCF7 cells (a human breast adenocarcinoma cell line), MCF7/ADR-RES cells (a DOX induced multidrug resistant subline of MCF7), and MES-SA cells (a human uterus sarcoma cell line) were used. The cells were cultured in RPMI1640 medium supplemented with glucose (2 g/L) and 10% heat-inactivated FBS under humidified air containing 5% CO_2 at 37°C. Additionally, insulin (4 mg/L) was added to RPMI1640 medium for MCF7 and MCF7/ADR-RES cells. As previously reported [43], to maintain multidrug resistance (MDR) of MCF7/ADR-RES cells, DOX (400 ng/mL) was added once weekly.

2.3. Acid-base titration of polycations

Acid-base titration was performed to monitor the proton buffering capacity of polymeric gene carriers as previously reported [4]. PLL·HBr and PEI (10 mg) were dissolved in NaCl aqueous solution (150 mM; 10 mL) with 1 N NaOH (aq.) (100 μL). The polymer solution (1 mg/mL; 3 mL) was titrated with 0.1 N HCl at room temperature (RT). The pH changes of polymer solutions were monitored.

2.4. Preparation and physicochemical characteristics of polyplexes

As previously reported [3, 43], polyplexes were prepared using pDNA and polycations (*i.e.*, PEI and PLL) in HEPES buffer (20 mM, pH 7.4) supplemented with 5% glucose (HBG). After mixing pDNA and polycations using predetermined complexation conditions, the polyplexes (20 μL for 1 μg pDNA) were incubated for 30 min at RT. Complexation ratios of polyplexes were calculated by counting the amines (N) of polycations and the phosphate groups (P) of pDNA.

Particle size and surface charge of polyplexes were monitored under different medium pHs to understand whether medium pH affects these polyplex characteristics. The polyplex solution was added to HBG with different pHs (*i.e.*, pHs 7.4, 7.0, 6.7 and 6.3). The concentration of pDNA in the polyplex solution was 2.5 μg/mL for surface charge measurements and 5 μg/mL for particle size measurements. Surface charge and particle size of polyplexes were measured using a Zetasizer 3000HS (Malvern Instrument, Inc., Worcestershire, UK) at a wavelength of 677 nm with a constant angle of 90^{o} at RT.

The pH-induced dissociation kinetics of polyplexes under different pH environments were evaluated with a dye-dequenching method. PLL/pDNA and PEI/pDNA complexes were prepared with YOYO-1-intercalated pDNA (YOYO-1:pDNA = 1 molecules:5 base pair). After adding polyplexes (20 μL; 1 μg pDNA) into different pH RPMI1640 media (180 μL; adjusted to pHs 7.4, 7.0, 6.7, and 6.3), the fluorescence intensity of YOYO-1 in the polyplexes was monitored at 491 nm (excitation) and 509 nm (emission) every 5 min for 4 hr. To evaluate the time-dependent fluorescence change of each polyplex exposed to different pH media, the relative fluorescence units (RFU) of each polyplex at each pH were measured and t=0 was set to 100%.

2.5. In vitro transfection

MCF7, MCF7/ADR-RES, and MES-SA cells were used for in vitro transfection studies. As reported previously [1, 18, 43], transfections were performed in 6-well plates, and cells were seeded at a density of 5×10^5 cells/well. The seeded cells were cultured for 24 hr prior to adding polyplexes. One hour before transfection, the complete culture medium was replaced with serum-free and insulin-free medium. After dosing the polyplexes (20 μL; 1 μg pDNA), the cells were incubated with transfection mixtures for 4 hr, followed by an additional 44 hr incubation in complete culture medium. After transfection, the cells were rinsed twice with DPBS and then lysed using a reporter lysis buffer. Measurements of relative luminescence units (RLU) and protein content of transfected cells were performed per the manufacturer's instructions.

To investigate the effects of extracellular pH on polymeric transfection, four different pHs, pH 7.4, 7.0, 6.7, and 6.3, were used. Transfection procedures were separated into two periods (*i.e.*, the 4 hr transfection period and 44 hr incubation period) as follows:

Condition A: 4-hr transfection period at different pHs (pH 7.4, 7.0, 6.7, and 6.3) followed by the 44-hr incubation period fixed at pH 7.4.

Condition B: 4-hr transfection period at pH 7.4 followed by the 44-hr incubation period at different pHs (pH 7.4, 7.0, 6.7, and 6.3).

Condition AB: 48-hr transfection period and incubation period both at different pHs (7.4, 7.0, 6.7, and 6.3).

2.6. In vitro metabolic activity

The MTT-based metabolic activity of polyplex-transfected cells was assessed using MCF7, MCF7/ADR-RES, and MES-SA cells. Cells were seeded in 12-well plates at a density of 2.5×10^5 cells/well and cultured for 24 hr prior to polyplex addition. The experimental procedure was the same as previously described for *in vitro* transfection except for the polyplex loading dose (10 μL; 0.5 μg pDNA). After the 48-hr transfection procedure, MTT

solution (0.1 mL; 5 mg/mL) was added to the cells in 1 mL of culture medium. After 4 hr, the MTT-containing medium was removed. Living cells produced formazan crystals that were dissolved in DMSO; crystal absorbance was measured at 570 nm with a microplate reader.

2.7. Cellular uptake of polyplexes

As previously described for *in vitro* transfection, cells were prepared in 6-well plates. Polyplexes (20 μL; 1 μg pDNA) prepared using YOYO-1-intercalated pDNA were added to the cells. After a 4-hr incubation under 4 different pH environments (pH 7.4, 7.0, 6.7, and 6.3), the cells were detached and then fixed using 4% PFA solution. The cells containing fluorescent polyplexes were monitored using flow cytometry (FACScan Anaylzer, Becton-Dickinson, Franklin Lakes, NJ) with a primary argon laser (488 nm) and fluorescence detector (530±15 nm) for YOYO-1. Polyplex uptake was analyzed using a gated population containing at least 5,000 cells.

2.8. Cell cycle phases

The cell-cycle phases of MCF7, MCF7/ADR-RES, and MES-SA cells incubated in different pH media were assessed. Cells were seeded in 6-well plates at a density of 5×10^5 cells/well and cultured for 24 hr prior to treatment with different pH media. Then, cells were exposed to 4 different pH transfection media (*i.e.*, pH 7.4, 7.0, 6.7 and 6.3) for 4 hr and then 4 different pH culture media (*i.e.*, pH 7.4, 7.0, 6.7 and 6.3) for 44 hr. During the transfection process, cells were sampled at predetermined time points (*i.e.*, 0, 2, 4, 12, 24, 36, and 48 hr post-transfection). The cells were rinsed twice with DPBS and detached with trypsin-EDTA solution. The rinsed and suspended cells were fixed with cold 70% (v/v) ethanol (aq.). Fixed samples were rinsed twice with DPBS and incubated with 1 mL of a PI-containing DPBS solution (50 μg/mL PI, 0.1% Triton®X-100 solution, and 15 μg/mL RNase) for 30 min at RT. The stained samples were analyzed by flow cytometry with a primary argon laser (488 nm)

and fluorescence detector (668 nm long pass); at least 15,000 cells were counted per condition.

2.9. Intracellular pH measurement of polyplexes

The intracellular pH environment of polyplexes was monitored using fluorescent dye labeled polymers as previously reported [43]. PLL and PEI were labeled with pH-sensitive FITC and pH-insensitive RITC dyes using a simple coupling reaction. PLL and PEI were each labelled with both FITC and RITC, creating FITC-PLL-RITC (2.3 mol% (based on L-lysine units) FITC; 1.2 mol% RITC), and FITC-PEI-RITC (1.6 mol% (based on amines) FITC; 0.4 mol% RITC), respectively [43].

As previously described for *in vitro* transfections [43], cells were prepared in 6-well plates. Polyplexes (20 μL; 1 μg pDNA) were prepared using FITC-PLL-RITC or FITC-PEI-RITC, and added to cells. At predetermined time points (*i.e.*, 0.5, 1, 1.5, 2, 3, and 4 hr posttransfection), the cells were detached and then resuspended in DPBS 1% PFA solution. To create a pH calibration curve, the transfected cells were resuspended in 0.5 mL of pH clamp buffers (approximately pH 7.4, 6.8., 6.0, 5.0, and 4.0) that were prepared by mixing DPBS (pH 7.4) or MES (pH 4.0; 50 mM MES, 150 mM NaCl, 4 mM KCl, and 1 mM $MgSO_4$).

Monensin (20 μM) and nigericin (10 μM) were added into pH clamp buffers to ensure homogeneity of the pH environment for cells. The cells harboring fluorescent polyplexes were monitored using flow cytometry (FACScan Anaylzer, Becton-Dickinson) with a primary argon laser (488 nm) and fluorescence detectors (530±15 nm for FITC and 585±21 nm for RITC). The average intracellular pH of polyplexes was assessed by analyzing the ratio of FITC to RITC intensity from a gated population of at least 5,000 cells. In order to identify and assign the major intracellular compartments holding the polyplexes from the intracellular pH, the entire fluorescent cell population was divided into four areas based on the cellular pH

calibration curve. The nucleus, and potentially the cytoplasm, was designated by pH values greater than pH 6.8, early endosomes were approximated between pH 6.0 and pH 6.8, late endosomes were between pH 5.0 and pH 6.0, and lysosomes were classified with a pH less than 5.0 [43].

3. Results and discussion

Prior to applying extracellular media of various pH values (*i.e.*, culture medium and transfection medium) for *in vitro* polymeric transfection, the optimum conditions for PEI- and PLL-based transfection of MCF7, MCF7/ADR-RES, and MES-SA cells were determined using less toxic polymer/pDNA complexation ratios. For PEI/pDNA complexes, N/P 5 was applied to all cell lines used in this study because, in general, higher N/P values cause cytotoxicity [19, 22, 44]. For PLL/pDNA complexes, N/P 5 was used for MCF7 and MCF7/ADR-RES cells based on our previous report [43]. For MES-SA cells, N/P 10 was used as the optimum transfection condition based on results from a test of N/P values between 3 and 15 (Fig. S1).

3.1. Effects of extracellular pH on transfection efficiency

PEI- and PLL-mediated transfection efficiencies are shown in Fig. 1 for cells exposed to specific extracellular pHs. Luciferase expression of the cells transfected with 4 different medium pHs (*i.e.*, transfection medium and culture medium) for 48 hr (Condition AB) was polyplex- and cell-dependent. The medium pH strongly influenced transgene expression of PEI/pDNA-transfected MCF7, MCF7/ADR-RES, and MES-SA cells ($p<0.001$, $p<0.001$, and $p=0.004$ by one-way ANOVA, respectively). Using pH 7.4 medium, PEI/pDNA-transfected MCF7 cells had approximately 2-fold to 3-fold higher transfection efficiency than those at pH 7.0, 6.7, and 6.3 ($p=0.01$, $p=0.02$, and $p=0.09$ by one-way ANOVA with Tukey HSD test, respectively). Interestingly, PEI/pDNA-transfected MCF7/ADR-RES and MES-SA cells

showed increased transgene expression with decreasing medium pH values. Specifically, gene expression in medium pH 6.3 was approximately 2-fold higher than in medium pH 7.4 ($p<0.001$ for MCF7/ADR-RES cells and $p=0.01$ MES-SA cells by one-way ANOVA with Tukey HSD test).

PLL/pDNA-transfected cells experienced approximately 2-fold lower (for MES-SA cells) or higher (for MCF7 and MCF7/ADR-RES cells) gene expression with medium pH 7.4 than medium pH 6.3. However, PLL-mediated transfections were less sensitive to medium pH ($p=0.27$ for MCF7, $p=0.07$ for MCF7/ADR-RES, and $p<0.05$ for MES-SA cells by one-way ANOVA) than PEI-mediated transfections. Also, transfection results conducted at medium pH 7.4 and medium pH 6.3 showed less significant differences ($p=0.03$ for MES-SA, $p=0.21$ for MCF7, and $p=0.06$ for MCF7/ADR-RES cells by one-way ANOVA with Tukey HSD test) for PLL versus PEI. These medium pH-induced polymeric transfection results were further analyzed to understand which steps of polymeric transfection are strongly affected by the extracellular pH. Thus, pH-controlled medium treatment was divided into transfection medium for 4-hr transfection periods and culture medium for 44-hr incubation periods. When applying Condition A (transfection media of various pHs) as shown in Fig. 1, acidic transfection media caused either decreased or nearly equal transfection efficiencies compared with neutral transfection medium. For PEI/pDNA-transfected MCF7 and MCF7/ADR-RES cells, transfection medium pH 6.3 reduced transfection efficiency by as low as 7.7-fold and 2.1-fold, respectively, compared with transfection medium pH 7.4 (for both, $p=0.004$ by one-way ANOVA with Tukey HSD test). Acidic transfection medium (pH 6.3) also caused approximately 25-35% reduced transgene expression of MES-SA cells compared to transfection medium pH 7.4, although transfection efficiency was less affected by medium pH ($p=0.23$ by one-way ANOVA). PLL-mediated transfections were also influenced by transfection medium pH ($p=0.04$ for MCF7, $p=0.02$ for MCF7/ADR-RES, and $p<0.001$ for MES-SA by one-way ANOVA). MCF7/ADR-RES and MES-SA cells transfected with

transfection medium pH 6.3 had 2.4- fold and 2.7-fold lower transfection efficiencies than those with transfection medium pH 7.4 ($p<0.05$ and $p=0.001$ by one-way ANOVA with Tukey HSD test, respectively). For PLL/pDNA-transfected MCF7 cells, transfection medium pH 7.0 caused the highest transfection efficiency, which was approximately 2-fold higher than those from other pH transfection media. However, unlike the pH effects of transfection media, transfection efficiencies increased in acidic culture media (called as Condition B) (Fig. 1). The pH of the culture medium significantly influenced transfection efficiencies for PEI/pDNA-transfected MCF7/ADR-RES and MES-SA cells (for both, $p<0.001$ by one-way ANOVA), and their transfection efficiencies in culture medium pH 6.3 were 1.9-fold and 2.6-fold higher than those in culture medium pH 7.4 (for both, $p<0.001$ by one-way ANOVA with Tukey HSD test). For PEI/pDNA-transfected MCF7 cells, although the effect of culture medium pH on PEImediated transfection efficiency was not statistically significant ($p=0.31$ by one-way ANOVA), transfection efficiencies using culture medium pH 6.3 were 1.6-fold higher than those at culture medium pH 7.4 ($p=0.49$ by one-way ANOVA with Tukey HSD test). When transfecting cells with PLL/pDNA using Condition B, there was no statistically significant influence of decreased culture medium pH values on transfection efficiencies ($p=0.22$ for MCF7, $p=0.28$ for MCF7/ADR-RES, and $p=0.30$ for MES-SA cells by one-way ANOVA). However, the culture medium pH 6.3 induced approximately 1.6-fold higher transfection efficiencies for PLL/pDNA-transfected MCF7 and MCF7/ADR-RES cells than culture medium pH 7.4 ($p=0.33$ and $p=0.34$ by one-way ANOVA with Tukey HSD test, respectively).

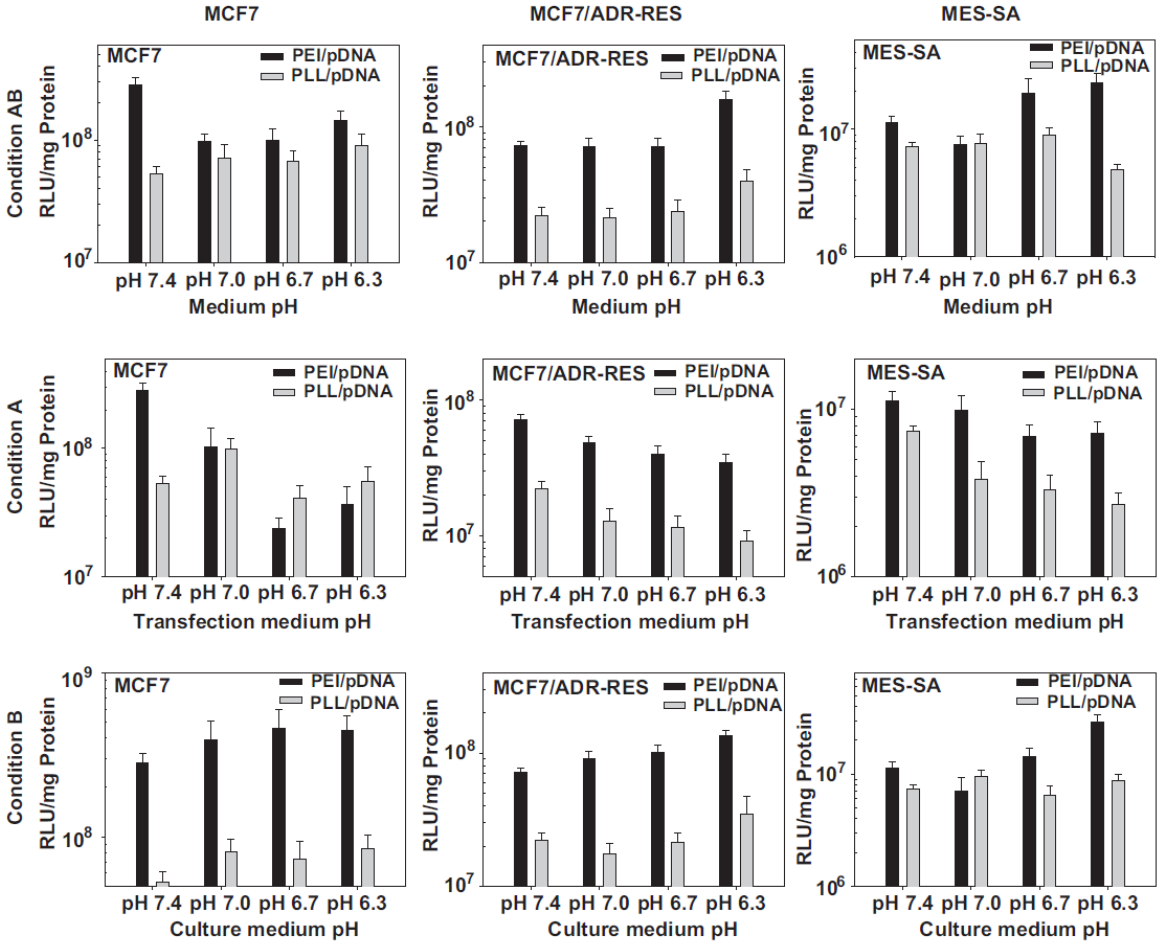

Fig. 1. Effects of extracellular pH (*e.g.*, medium pH for Condition AB, transfection medium pH for Condition A, and culture medium pH for Condition B) on the transfection efficiency of PEI/pDNA- and PLL/pDNA-transfected MCF7, MCF7/ADR-RES, and MES-SA cells. ($n \geq 8$; mean ± SEM).

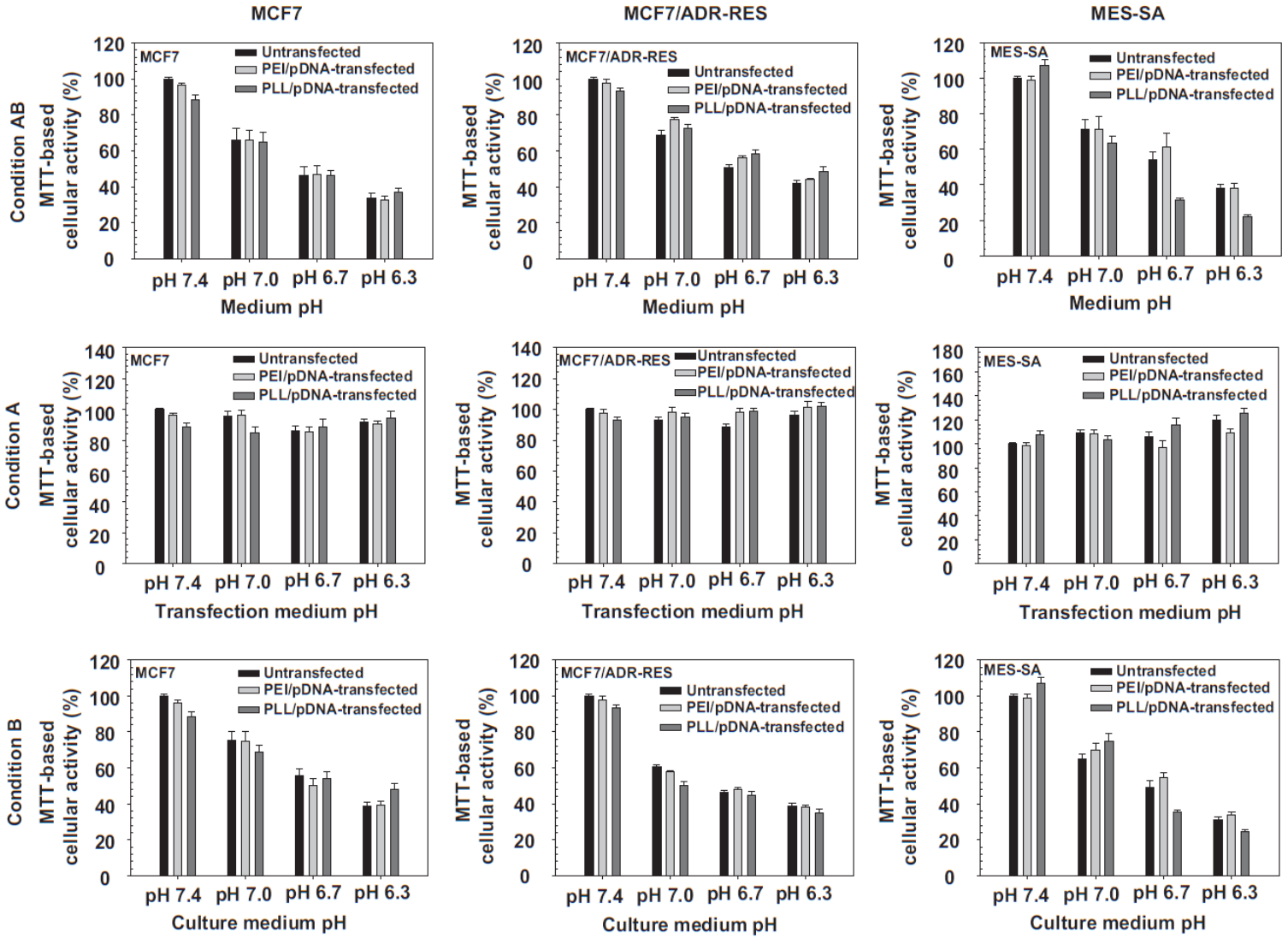

Fig. 2. Effects of extracellular pH (*e.g.*, medium pH for Condition AB, transfection medium pH for Condition A, and culture medium pH for Condition B) on MTT-based cellular activity of PEI/pDNA- and PLL/pDNA-transfected MCF7, MCF7/ADR-RES, and MES-SA cells. ($n = 6$; mean ± SEM).

3.2. Effects of extracellular pH on MTT-based cellular activity

MTT-based cellular activity assays were applied to understand how the extracellular pH influences cell number, cell viability, metabolic activity, and the cell proliferation rate of polyplex-transfected cells. When different medium pHs were applied to untransfected cells (Condition AB), the cellular activities significantly decreased with decreasing pHs, regardless of cell type (for all cell lines, $p<0.001$ by one-way ANOVA) as shown in Fig. 2. These results are consistent with previous studies [35, 45]. However, regardless of the type of polyplex used, the cellular activity of most transfected cells was almost the same as untransfected cells at the same pH. In Fig. 2, 4-hr treatment of acidic transfection media (Condition A) did not significantly damage the cellular activities of untransfected or transfected cells versus neutral transfection media treatment. On the other hand, longer treatment (44 hr) of acidic medium (Condition B) induced similar cellular activities to Condition AB treatment. However, it is not clear whether acidic medium caused reduced cell viability and/or metabolic activity or inhibited cell proliferation (without cell death).

3.3. Effects of medium pH on polymers and polyplexes

When polymers and polyplexes are exposed to different pH environments, their chemical, physical and electrochemical properties can be changed. First, the proton buffering capacity of PEI and PLL were monitored by acidic titration. As shown in Fig. S2, a PLL solution had no proton buffering capacity like a NaCl aqueous solution (150 mM) because the primary amines of PLL stay protonated within the range of basic to acidic pHs. On the contrary, a PEI solution exhibited proton buffering throughout a broad pH range (approximately pH 3-10) due to continuous protonation of primary, secondary, and tertiary amines upon acidification. These results are consistent with previous reports [46]. During acidification, protonation of amines increases the net positive charge character, and the altered charge could affect electrostatic interactions between polymers and pDNA. In this way, medium pH (*i.e.*, buffer

pH) could influence complexation and decomplexation between polymers and pDNA as well as particle size and surface charge of polyplex. Nevertheless, Godbey *et al*., reported that PEI-mediated transfection efficiencies were not different when PEI/pDNA complexes were prepared in different pH solutions [47]. Thus, this study excluded the effects of medium pH on complexation. All polyplexes were prepared at pH 7.4.

When polyplexes were exposed to different medium pHs, the changes of PEI/pDNA and PLL/pDNA complexes' particle size, surface charge, and decomplexation were investigated. As expected, the particle size and surface charge of PLL/pDNA complexes were not affected by HBG with different pHs ($p=0.88$ and $p=0.96$ by one-way ANOVA, respectively) (Fig. 3(a) and 3(b)). These results may be attributed to unaltered primary amine protonation of PLL within the pH range of 6.3 to 7.4; the side chain of L-lysine has pK_a 8.95. In the case of PEI/pDNA complexes (Fig. 3(a) and 3(b)), particle sizes were around 80-90 nm in solutions pH 6.7-7.4, although the size at pH 6.3 (106±19 nm) was somewhat increased compared to those at other pHs. Surface charges ranged between 10-15 mV without statistical significance related to pH effects.

The effects of medium pH on decomplexation were monitored over time as shown in Fig. 3(c). Medium pH 7.4 resulted in increased decomplexation (*i.e*., increased fluorescent intensity) with time, regardless of polyplex type. However, acidic medium (pH 6.3 to 7.0) compared to medium pH 7.4 showed decreasing or constant fluorescent intensity over time. These results may be caused by increasing (+/-) charge ratios of polyplexes because the phosphate groups of pDNA (approximately pK_a 6.3) are less negatively charged at acidic pH than pH 7.4. This phenomenon may be similar to tight complexation of polyplexes at high (+/-) charge ratios.

Our findings suggest that polyplexes may be stable in acidic extracellular environments and during endosomal acidification, but could be dissociated in neutral pH environments such as the cytoplasm or the nucleus. If medium pH 7.4 can induce a weak attraction between

polycations and pDNA in polyplexes within 4 hr, before cellular internalization, this may facilitate pDNA release from polyplexes after endosomal release, thereby enhancing polymeric transfection efficiency. That is, high pH-induced decomplexation could generate higher transfection efficiency than low pH-induced decomplexation.

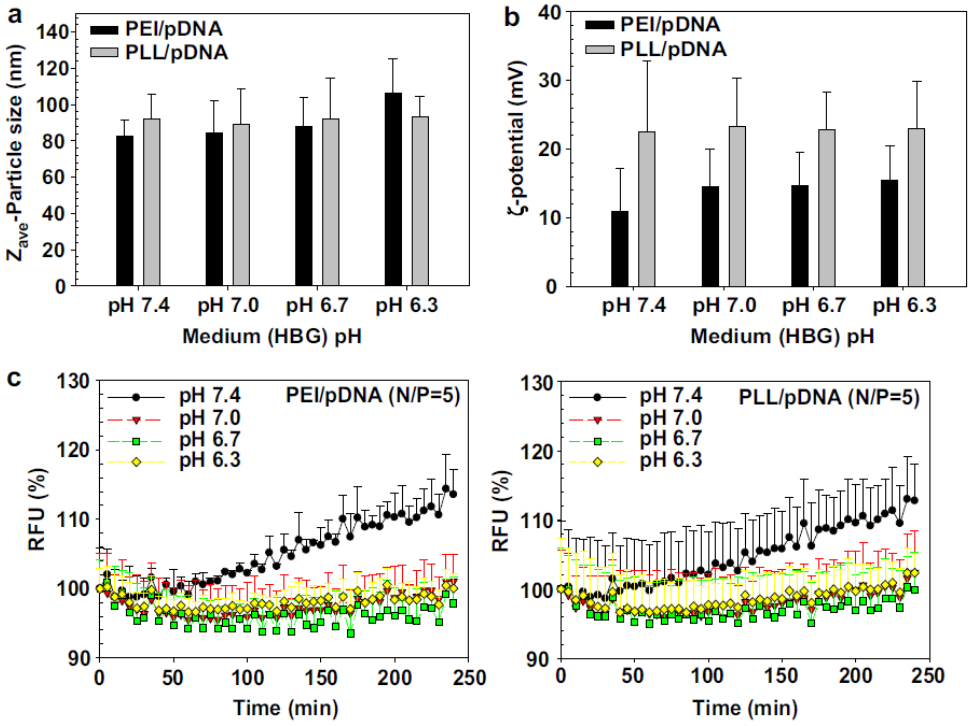

Fig. 3. Effects of medium pH on (a) Particle size, (b) Surface charge, and (c) decomplexation of PEI/pDNA (N/P = 5) and PLL/pDNA (N/P = 5) complexes. (n = 3; mean ± SD).

3.4. Effects of medium pHs on polyplex uptake

In transfection experiments, transfection medium was applied for 4 hr and then replaced with culture medium. At 4 hr post-transfection, the polyplexes that were not endocytosed will be removed. Thus, only internalized polyplexes will be available for gene expression. During the first 4 hr post-transfection, the different pHs of transfection medium for Conditions AB and A could affect cellular polyplex uptake, whereas the same pH of transfection medium under Condition B could cause the same cellular uptake.

Thus, when different medium pHs were applied, cellular uptake 4 hr post-transfection was monitored by flow cytometry. As shown in Fig. S3, PEI/pDNA uptake in MCF7 cells in transfection medium pH 7.4 was somewhat lower than uptake under other transfection

medium pHs. A similar amount of PLL/pDNA complexes was internalized into transfected MCF7 cells regardless of the transfection medium pH. However, MCF7/ADR-RES and MES-SA cells showed negligible effects of altered transfection medium pH for PEI/pDNA and PLL/pDNA uptake.

3.5. Effects of medium pH on cell cycle phases

The cell-cycle phase of transfected cells affects cellular internalization, endocytosis, and transfection efficiency of gene complexes [48-51]. Cellular internalization of nonviral gene complexes during the G2/M phases was 1.5-fold lower than during late G1 [51]. Polymeric transfection initiated at the S or G2/M phases caused approximately 30-fold or more than 500-fold higher transgene expression than transfections beginning at G1, respectively [48]. Thus, we monitored the effect of medium pH on cell cycle phases. During the first 4 hr posttransfection, the G1, S, and G_2 phases of cells from different medium pHs were not significantly different (Fig. S4). This may support the similar cellular internalization of polyplexes shown in Fig. S3. Under Condition A, the effects of different tranfection pHs on polymeric transfection efficiency may be caused by other effectors, but not the cell-cycle phase.

However, after the first 4 hr post-transfection, cell-cycle phases were indeed influenced by medium pH. Even though the impact of acidic medium is cell-dependent, the medium at pH 6.3 induced more G1 phase and less S and G2 phases than other pHs, regardless of the cell type (Fig. 4). In MCF7 cells, medium at pH 6.3 slightly inhibited cellular functions such as cell proliferation (G2 phase) and DNA duplication (S phase) compared with other medium pHs. Compared to MCF7 cells, MCF7/ADR-RES and MES-SA cells were strongly influenced by medium pH. In the case of MCF7/ADR-RES cells, medium at pH 6.7, 7.0 and 7.4 did not show any significant changes on cell cycle phases within the first 12 hr posttransfection.

However, acidic (pH 6.3) medium-treated MCF7/ADR-RES cells had remarkably increased G1 phases and reduced S and G2 phases 24 hr post-transfection, unlike treatment with the other pH media. For MES-SA cells, acidic medium clearly showed higher G1 phases and lower S and G2 phases than neutral medium 4 hr post-transfection. These findings indicate that the cytoskeletal network for endocytosis of polyplexes may be maintained. Also, the lower proportion of mitotic cells in acidic medium could prevent dilution of gene expression per cell so long as the acidic medium does not damage cell viability. These two possibilities indicate that acidic culture media induces better transgene expression than neutral culture media under Condition B.

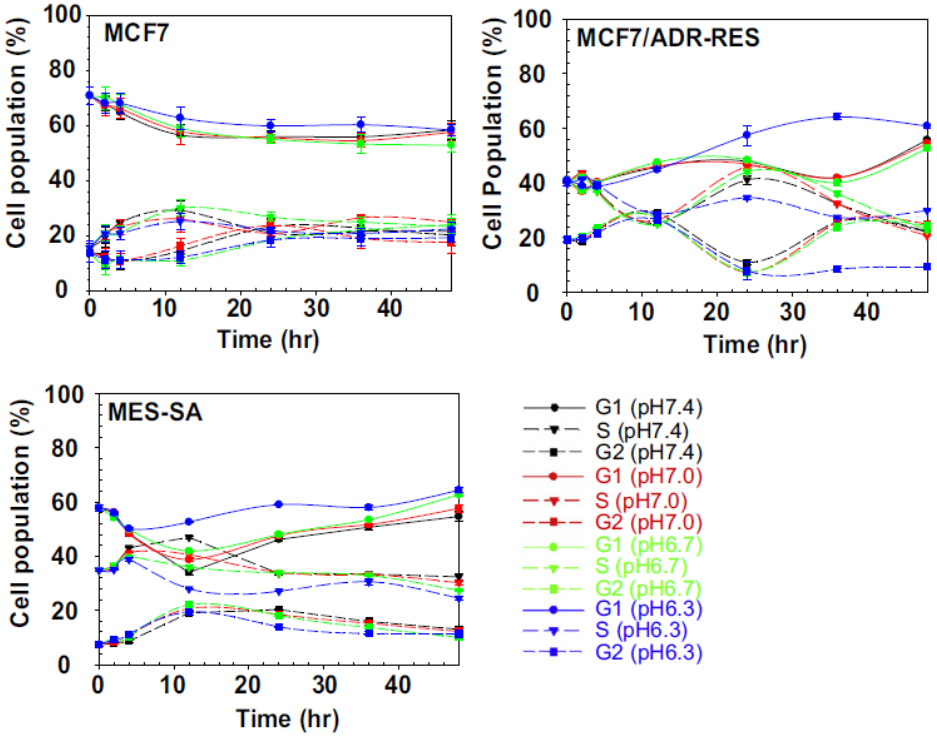

Fig. 4. G_1, S, and G_2 phases of MCF7, MCF7/ADR-RES, and MES-SA cells after treatment with transfection media of varying pH (48 hr incubation).

3.6. Intracellular environment of polyplexes

The intracellular location and pH of polyplexes or pDNA strongly affect polymeric transfection efficiency [43, 52]. Thus, we estimated how the medium pH influences the intracellular environment of polyplexes using flow cytometry as previously reported [43]. In

cells transfected with PEI/pDNA and PLL/pDNA complexes, the average intracellular pH environment was monitored during the first 4 hr post-transfection (Fig. 5). Polyplexes continuously internalize until they are used up from the extracellular medium. Therefore, polyplexes could be exposed to different subcellular locations, and the transfected cells having these polyplexes may experience different intracellular pHs over time. Thus, as shown in Fig. 6 and Fig. 7, it was estimated how many polyplex-transfected cells had average intracellular pHs conducted from polyplexes exposed to the pH of subcellular compartments (*e.g.*, the cytosol, the early and late endosomes, the lysosomes, and the nucleus) over time. As shown in Fig. 5, the effects of transfection medium pH on the average intracellular pH of polyplex-transfected cells were cell- and polyplex-dependent. The average intracellular pH of PLL-mediated MCF7 transfected cells was not significantly influenced by the medium pH, whereas the intracellular pH for MCF7/ADR-RES and MES-SA transfections was affected by medium pH. In PLL/pDNA-transfected MCF7/ADR-RES cells, acidic medium induced a slow drop in intracellular pH within the first 2 hr post-transfection. Recovery of intracellular pH, which was caused by endosomal escape of polyplexes [43], was somewhat lower (approximately 0.1~0.2 pH units). Furthermore, the time points for intracellular pH recovery were delayed (2 hr post-transfection for medium pH 6.3 vs. 0.5-1 hr post-transfection for medium pH 7.4). Similarly, MES-SA cells transfected with PLL/pDNA complexes showed an acidic medium (pH 6.3)-mediated slow intracellular pH recovery (1.5 hr post-transfection vs. 0.5-1 hr post-transfection at medium pH 7.4) and low recovered intracellular pH (~ pH 6.5 vs. pH 6.7 at medium pH 7.4). These results are probably not attributed to polymer characteristics because PLL does not have proton buffering capacity in the pH range experienced during intracellular polyplex trafficking. One significant contribution could be the acidic medium-induced changes to cell characteristics; acidic extracellular medium lowered intracellular (cytoplasmic) pHs [37], and acidic cytosolic pHs are known to inhibit/delay the endocytosis of therapeutics such as proteins [38, 53-55].

Delayed endosomal acidification rates and lower intracellular recovery pHs of PLL/pDNA-transfected cells in acidic medium could be supported by the population data of cells with average intracellular pHs related to subcellular compartments. As shown in Fig. 6, it seems that medium pH does not significantly affect time-dependent polyplex uptake (column plots) or the average intracellular pH (dot plots) relevant to subcellular compartments. Regardless of the medium pH, PLL/pDNA-transfected MCF7 cells had an average intracellular pH between pH 7.25-7.35 (relevant to the cytosol/the nucleus), pH 6.55- 6.70 (relevant to the early endosomes), pH 5.40-5.55 (relevant to the late endosomes), and ~ pH 4 (relevant to the lysosomes). The pH ranges of PLL/pDNA-transfected MCF7/ADR-RES cells were pH 7.01-7.13, pH 6.18-6.47, pH 5.40-5.57, and pH 4.00-4.10, and were lower than those of MCF7 transfected cells due to the fast endosomal acidification rates of MDR cells [43]. Also, PLL/pDNA-transfected MES-SA cells had pH 7.17-7.27, pH 6.44-6.64, pH 5.48- 5.65, and pH 4.00-4.15. However, in PLL/pDNA-transfected MCF7/ADR-RES cells and MES-SA cells, the peak cell populations relevant to late endosomes and lysosomes (from column plots of Fig. 6) were delayed with acidic medium treatment. This acid mediuminduced delayed acidification process could cause delayed cytosolic release of polyplexes. Also, the lower intracellular pH may slow down decomplexation rates. Together, these phenomena may influence the acidic transfection medium-induced decrease in polymeric transfection efficiency. When applying PEI/pDNA complexes (having endosomal disruption capability) to the cells, the intracellular pH of transfected cells was higher (> ~pH 6.7) than those of PLL/pDNA-transfected cells (Fig. 5) because the proton buffering capacity of PEI can break endosomal membranes, quickly releasing PEI/pDNA into the cytoplasm. Like PLL/pDNAtransfected cells, PEI/pDNA-transfected cells were influenced by delayed endocytosis and endosomal acidification of polyplex-trapped endosomes when treated with acidic transfection medium. This was clearly demonstrated by the fast endosomal acidification rates (*e.g.*, MCF7/ADR-RES cells in this study). As shown in Fig. 7, transfection

medium pH 6.3 caused more cells to be exposed to early endosomal pHs than transfection medium pH 7.4. Also, the delayed endosomal acidification may negatively influence the endosomal release of PEI/pDNA complexes because the proton buffering capacity of PEI is strongly affected by decreasing pH.

Based on the transfection results of Conditions AB, A, and B (as summarized in Table 1), acidic transfection media decreased polymeric transfection efficiencies, whereas acidic culture media enhanced efficiencies. The effects of transfection media on transfection efficiency may be mediated by the delayed acidification rates of polyplex-trapped endolysosomes and the decomplexation rates during the transfection period. Delayed endosomal acidification caused by acidic transfection media resulted in delayed cytosolic release of polyplexes (*i.e.*, sequestrated in the late endosomes and lysosomes). In addition, polyplexes in acidic extracellular environments and slightly acidic cytosol could be tightened and then slowly release pDNA. These reasons might explain why acidic transfection media decreased polymeric transfection efficiencies.

On the other hand, the culture medium affected the cell cycle phase and metabolic activity of transfected cells. Under acidic conditions, the metabolic activity of transfected cells was reduced. Although these results may have been caused by a reduction in viable cells, the metabolic functions of transfected cells could be limited by cellular arrest (*i.e.*, increased G_1 phase and decreased G_2 and S phases) without cell death. Cellular arrest could delay mitosis, leading to less dilution of gene expression in transfected cells. As a result, acidic culture medium can enhance polymeric transfection efficiencies. Thus, the impact of transfection media and culture media on cells may determine the effects of medium pH on transfection efficiency. Nevertheless, in regard to the effects of extracellular pH on polymeric transfection, the pH of the culture medium could be more influential than the pH of the transfection medium because transfected cells are exposed to culture medium longer (44 hr) than transfection medium (4 hr). The findings in this study may be helpful for developing effective

polymeric vectors for solid tumors and ischemia because these cells pathologically feature acidic extracellular environments.

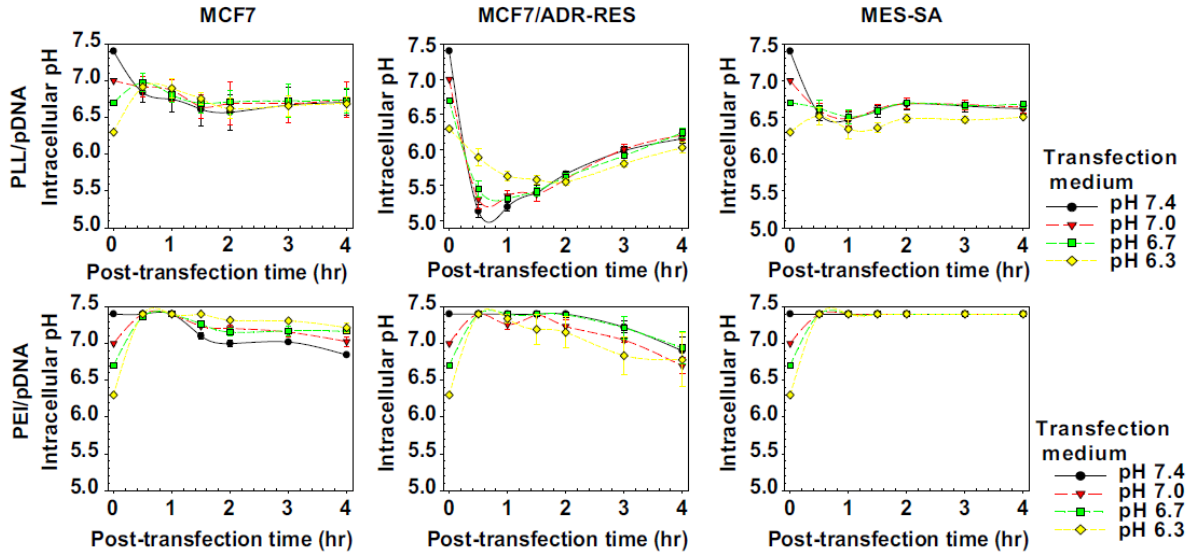

Fig. 5. Average intracellular pH of PEI/pDNA- or PLL/pDNA-uptake in MCF7, MCF7/ADR-RES, and MES-SA cells within 4 hr after polymeric transfection (mean ± SEM; $n = 3$).

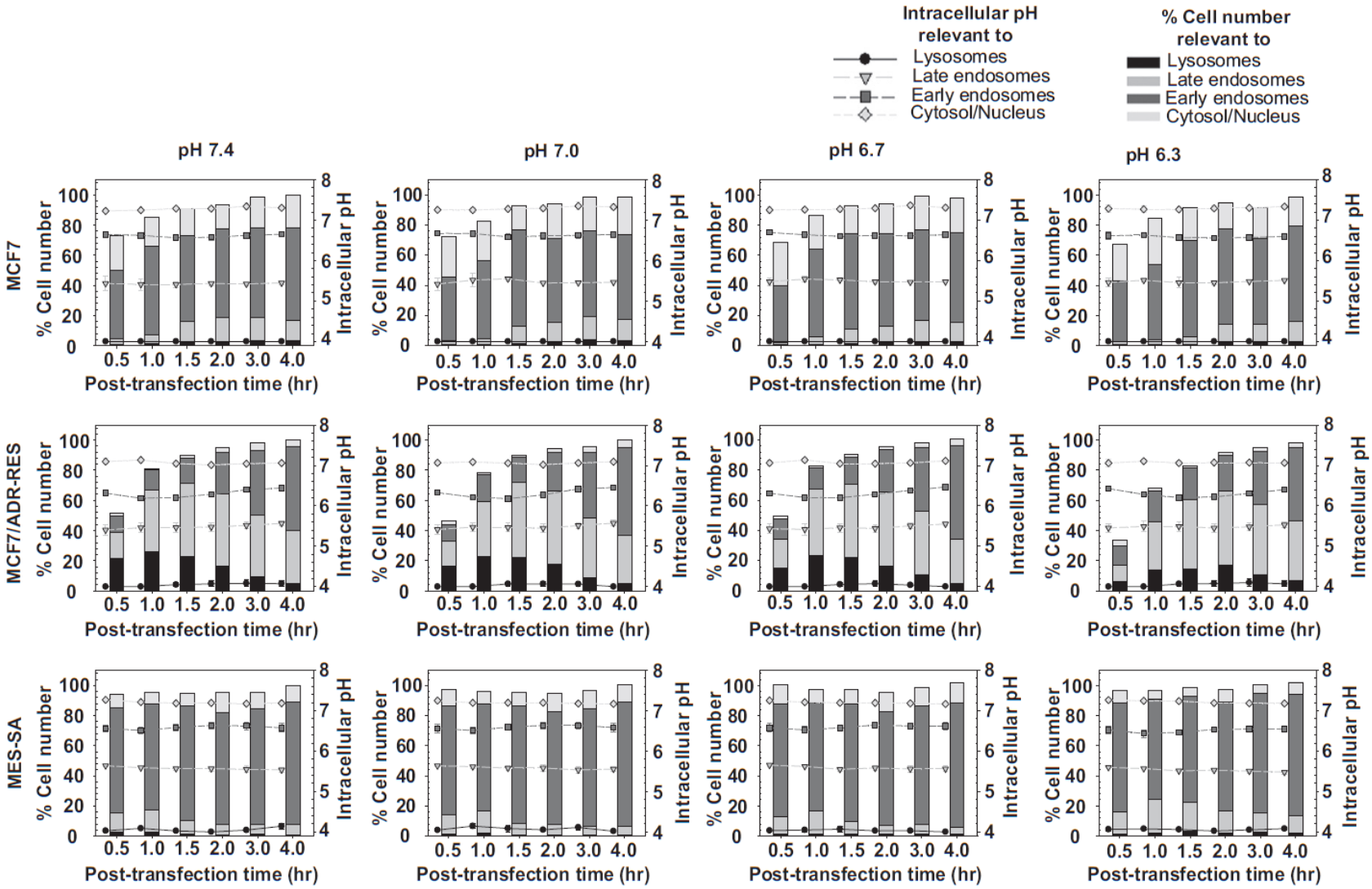

Fig. 6. Subcellular pH distributions of PLL/pDNA-uptake in MCF7, MCF7/ADR-RES, and MES-SA cells within 4 hr after polymeric transfection. The pH of each subcellular compartment in polyplex-transfected cells and the number of cells in each subcellular compartment at a given time point following transfection are represented in the following dot plots and column plots, respectively. The intracellular pH for polyplex-transfected cells relevant to the pH of lysosomes (black circle, ●), late endosomes (gray inverse triangle, ▼), early endosomes (dark gray square, ■), and the cytosol/nucleus (bright gray diamond, ◆) are represented in dot plots. The corresponding % cell numbers are represented as ■, ■, ■, and ■ in the column plots. The cell number at 4 hr post-transfection was set to 100% (mean ± SEM; $n = 3$).

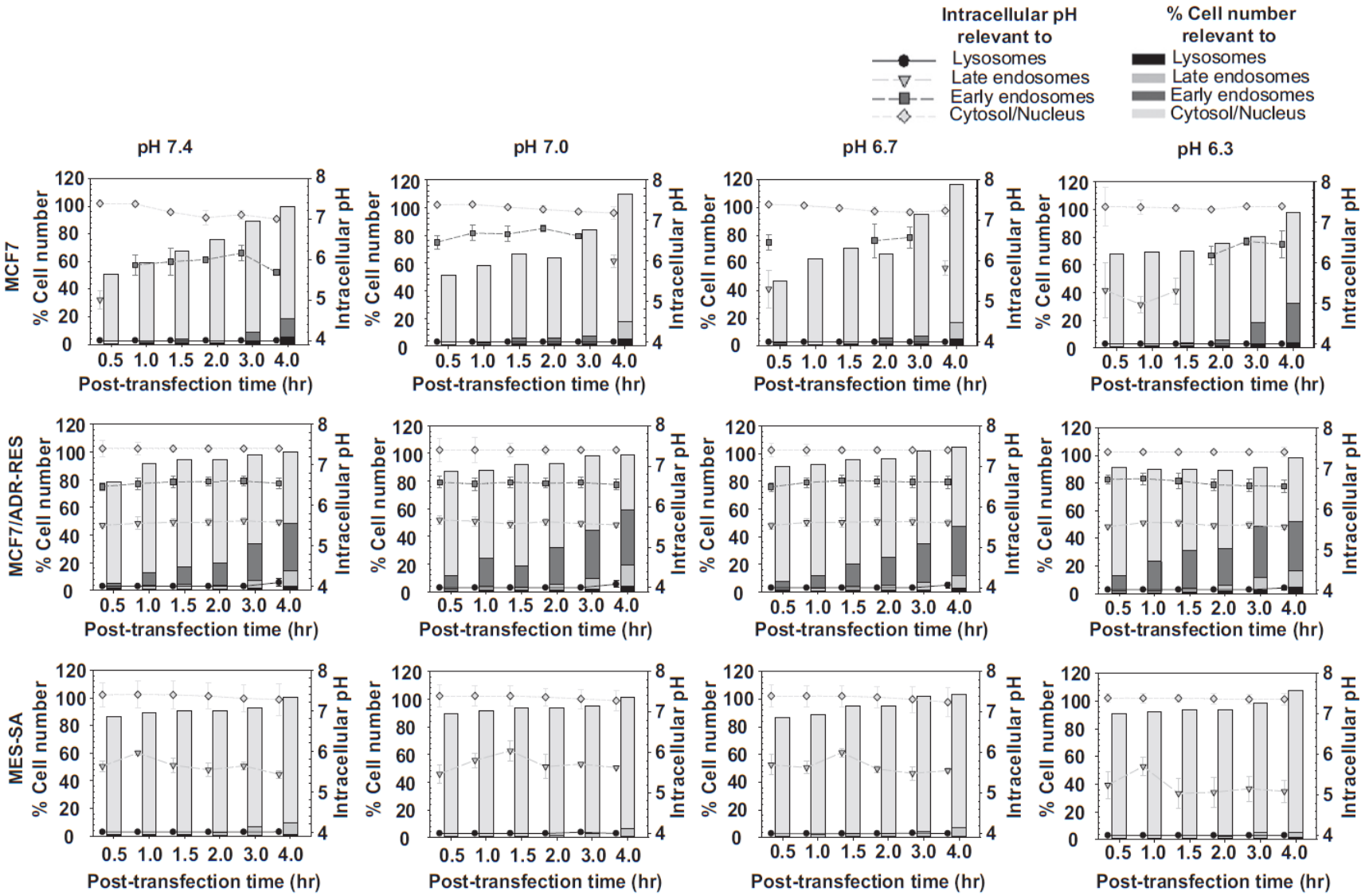

Fig. 7. Subcellular pH distributions of PEI/pDNA-uptake in MCF7, MCF7/ADR-RES, and MES-SA cells within 4 hr after polymeric transfection (mean ± SEM; $n = 3$).

4. Conclusion

In vitro polymeric transfection was strongly affected by the extracellular pH. Transfection media modulated both polymer/polyplex characteristics (*e.g.*, proton buffering and decomplexation) and cellular characteristics (*e.g.*, endocytic trafficking), whereas culture medium affected only cellular characteristics (*e.g.*, cell proliferation, cell cycle phase, and mitosis). In conclusion, acidic transfection medium reduced and acidic culture medium enhanced polymeric transfection efficiency. When treating with a specific extracellular pH during polymeric transfection, the impact of transfection medium and culture medium may determine the effect of medium pH on transfection efficiency.

Table 1. Summary of cell transfection enhancement or reduction with extracellular pH 6.3 compared to extracellular pH 7.4.

		MCF7	MCF7 /ADR-RES	MES-SA
PEI/pDNA-mediated transfection	**Condition AB**	2-fold ↓	2.2-fold ↑	2-fold ↑
	Condition A	7.7-fold ↓	2.1-fold ↓	1.6-fold ↓
	Condition B	1.6-fold ↑	1.9-fold ↑	2.6-fold ↑
PLL/pDNA-mediated transfection	**Condition AB**	1.7-fold ↑	1.8-fold ↑	1.5-fold ↓
	Condition A	1-fold	2.4-fold ↓	2.7-fold ↓
	Condition B	1.6-fold ↑	1.6-fold ↑	1.2-fold ↑

↓ and ↑ mean lower and higher, respectively.

ACKNOWLEDGEMENTS

This work was supported by NIH GM82866.

SUPPLEMENTARY INFORMATION

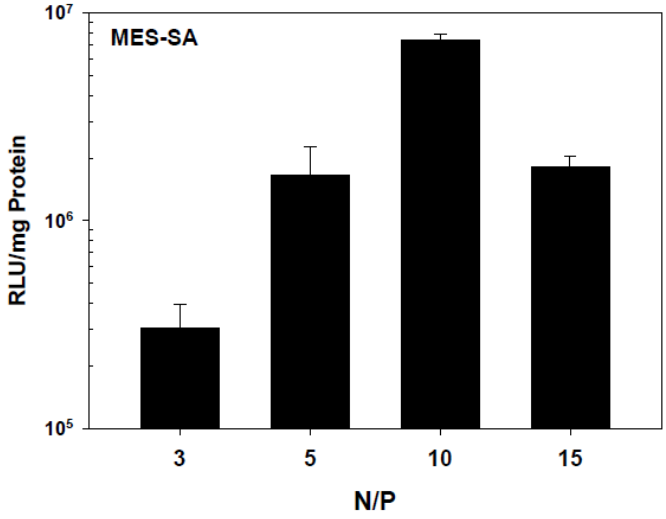

Fig. S1. N/P-dependent transfection efficiency of PLL/pDNA-transfected MES-SA cells (n≥4; mean±SEM).

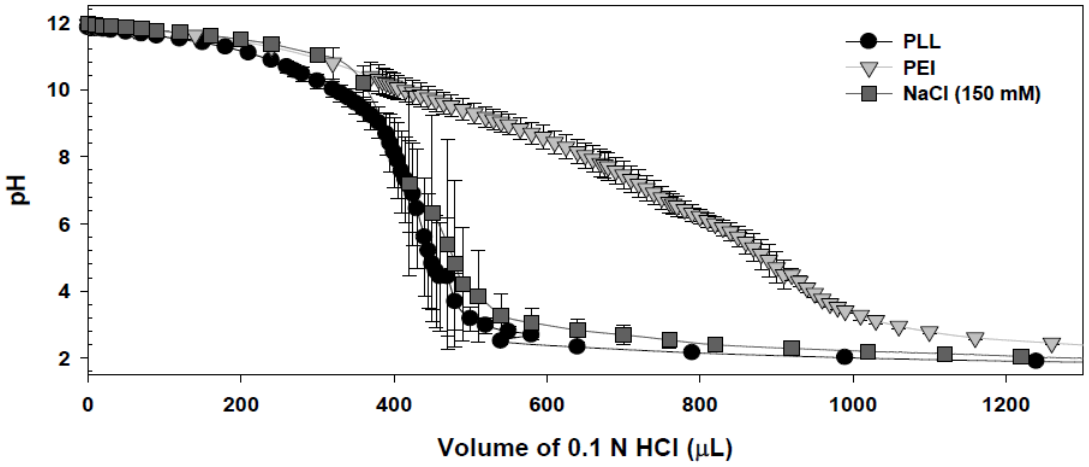

Fig. S2. Acid-base titration of PEI and PLL (n=3, mean±SD)

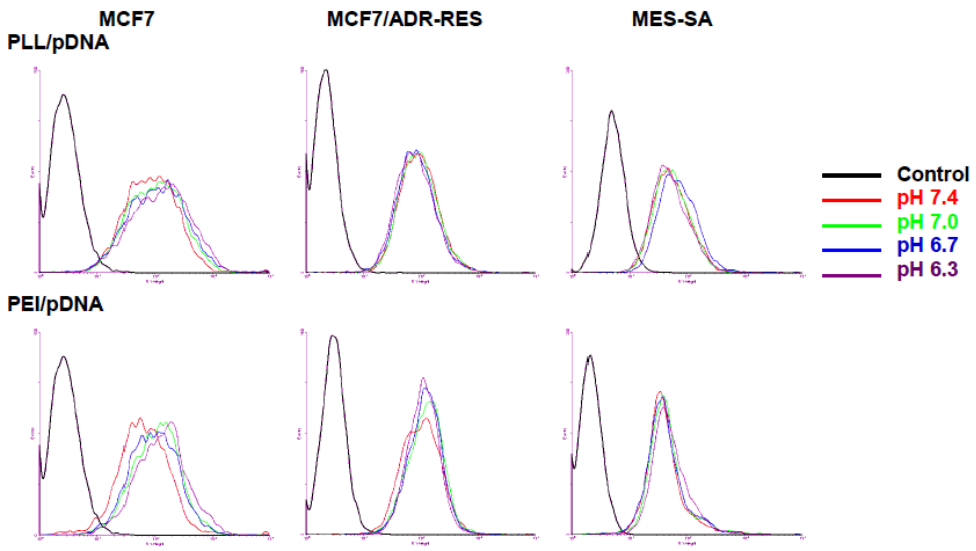

Fig. S3. Cellular uptake of PEI/pDNA and PLL/pDNA complexes under transfection media with different pHs (7.4, 7.0, 6.7, and 6.3) at 4 hr post-transfection.

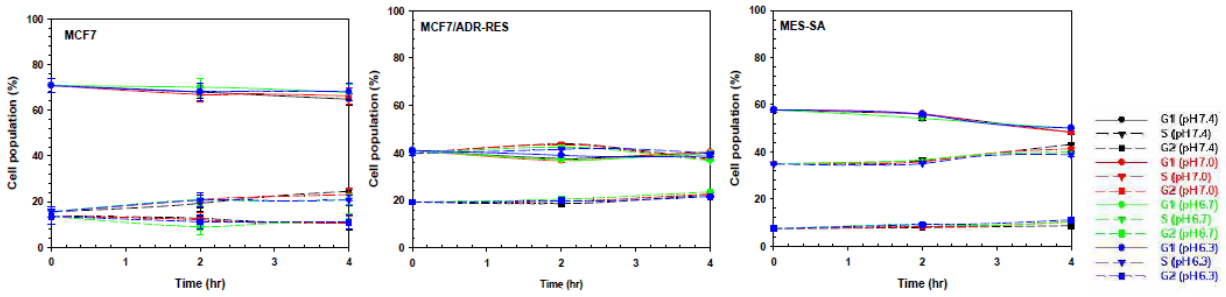

Fig. S4. G_1, S, and G_2 phases of MCF7, MCF7/ADR-RES, and MES-SA cells after treating transfection media having different pHs (4 hr incubation).

REFERENCES

[1] Kang HC, Kim S, Lee M, Bae YH. Polymeric gene carrier for insulin secreting cells: Poly(l-lysine)-g-sulfonylurea for receptor mediated transfection. J Control Release 2005;105:164-176.

[2] Kawakami S, Higuchi Y, Hashida M. Nonviral approaches for targeted delivery of plasmid DNA and oligonucleotide. J Pharm Sci 2008; 97:726-745.

[3] Kang HC, Bae YH. Transfection of insulin-secreting cell line and rat islets by functional polymeric gene vector. Biomaterials 2009;30:2837-2845.

[4] Kang HC, Bae YH. pH-Tunable endosomolytic oligomers for enhanced nucleic acid delivery. Adv Funct Mater 2007; 17:1263-1272.

[5] Jones RA, Cheung CY, Black FE, Zia JK, Stayton PS, Hoffman AS, et al. Poly(2- alkylacrylic acid) polymers deliver molecules to the cytosol by pH-sensitive disruption of endosomal vesicles. Biochem J 2003; 372:65-75.

[6] Kiang T, Bright C, Cheung CY, Stayton PS, Hoffman AS, Leong KW. Formulation of chitosan-DNA nanoparticles with poly(propyl acrylic acid) enhances gene expression. J Biomater Sci Polym Ed 2004; 15:1405-1421.

[7] Ng CP, Goodman TT, Park IK, Pun SH. Bio-mimetic surface engineering of plasmid- loaded nanoparticles for active intracellular trafficking by actin comet-tail motility Biomaterials 2009; 30:951-958.

[8] Choi JS, Ko KS, Park JS, Kim YH, Kim SW, Lee M. Dexamethasone conjugated poly(amidoamine) dendrimer as a gene carrier for efficient nuclear translocation. Int J Pharm 2006; 320:171-178.

[9] Drake DM, Pack DW. Biochemical investigation of active intracellular transport of polymeric gene-delivery vectors. J Pharm Sci 2008; 97:1399-1413.

[10] Wagstaff KM, Jans DA. Nuclear drug delivery to target tumour cells. Eur J Pharmacol 2009;625:174-180.

[11] Park KM, Kang HC, Cho JK, Chung IJ, Cho SH, Bae YH, et al. All-trans-retinoic acid (ATRA)-grafted polymeric gene carriers for nuclear translocation and cell growth control. Biomaterials 2009;30:2642-2652.

[12] Kang HC, Kang HJ, Bae YH. A reducible polycationic gene vector derived from thiolated low molecular weight branched polyethyleneimine linked by 2-iminothiolane. Biomaterials 2011; 32:1193-1203.

[13] Kim YH, Park JH, Lee M, Kim YH, Park TG, Kim SW. Polyethylenimine with acidlabile linkages as a biodegradable gene carrier. J Control Release 2005; 103:209-219.

[14] Christensen LV, Chang CW, Yockman JW, Conners R, Jackson H, Zhong Z, et al. Reducible poly(amido ethylenediamine) for hypoxia-inducible VEGF delivery. J Control Release 2007;118:254-261.

[15] Ou M, Xu R, Kim SH, Bull DA, Kim SW. A family of bioreducible poly(disulfide amine)s for gene delivery. Biomaterials 2009; 30:5804-5814.

[16] Shim MS, Kwon YJ. Acid-transforming polypeptide micelles for targeted nonviral gene delivery. Biomaterials 2010; 31:3404-3413.

[17] Shim MS, Kwon YJ. Controlled cytoplasmic and nuclear localization of plasmid DNA and siRNA by differentially tailored polyethylenimine. J Control Release 2009;133:206-213.

[18] Kang HC, Bae YH. Polymeric gene transfection on insulin-secreting cells: sulfonylurea receptor-mediation and transfection medium effect. Pharm Res 2006;23:1797- 1808.

[19] Florea BI, Meaney C, Junginger HE, Borchard G. Transfection efficiency and toxicity of polyethylenimine in differentiated Calu-3 and nondifferentiated COS-1 cell cultures. AAPS PharmSci 2002; 4:E12.

[20] Dash PR, Read ML, Barrett LB, Wolfert MA, Seymour LW. Factors affecting blood clearance and in vivo distribution of polyelectrolyte complexes for gene delivery. Gene Ther 1999;6:643-650.

[21] Spitnik P, Lipshitz R, Chargaff E. Studies in nucleoproteins. III. Deoxyribonucleic acid complexes with basic polyelectrolytes and their fractional extraction. J Biol Chem 1954; 215:765-775.

[22] Kang HC, Bae YH. Transfection of rat pancreatic islet tissue by polymeric gene vectors. Diabetes Technol Ther 2009; 11:443-449.

[23] Dautzenberg H, Karibyants N. Polyelectrolyte complex formation in highly aggregating systems. Effect of salt: response to subsequent addition of NaCl. Macromol Chem Phys 1999; 200:118-125.

[24] Poon Z, Chang D, Zhao X, Hammond PT. Layer-by-Layer Nanoparticles with a pH Sheddable Layer for in Vivo Targeting of Tumor Hypoxia. ACS Nano 2011;5:4284-4292.

[25] Sethuraman VA, Na K, Bae YH. pH-responsive sulfonamide/PEI system for tumor specific gene delivery: In vitro study. Biomacromolecules 2006; 7:64-70.

[26] Meng F, Hennink WE, Zhong Z. Reduction-sensitive polymers and bioconjugates for biomedical applications. Biomaterials 2009;30:2180-2198.

[27] Kim HA, Lee BW, Kang D, Kim JH, Ihm SH, Lee M. Delivery of hypoxia-inducible VEGF gene to rat islets using polyethylenimine. J Drug Target 2009; 17:1-9.
[28] Liu ML, Oh JS, An SS, Pennant WA, Kim HJ, Gwak SJ, et al. Controlled nonviral gene delivery and expression using stable neural stem cell line transfected with a hypoxiainducible gene expression system. J Gene Med 2010;12:990-1001.
[29] Kim HA, Lim S, Moon HH, Kim SW, Hwang KC, Lee M, et al. Hypoxia-inducible vascular endothelial growth factor gene therapy using the oxygen-dependent degradation domain in myocardial ischemia. Pharm Res 2010; 27:2075-2084.
[30] hm JE, Han KO, Hwang CS, Kang JH, Ahn KD, Han IK, et al. Poly (4- vinylimidazole) as nonviral gene carrier: in vitro and in vivo transfection. Acta Biomater 2005;1:165-172.
[31] Sarantopoulos C, McCallum B, Sapunar D, Kwok WM, Hogan Q. ATP-sensitive potassium channels in rat primary afferent neurons: the effect of neuropathic injury and gabapentin. Neurosci Lett 2003; 343:185-189.
[32] Hunjan S, Mason RP, Mehta VD, Kulkarni PV, Aravind S, Arora V, et al. Simultaneous intracellular and extracellular pH measurement in the heart by 19F NMR of 6- fluoropyridoxol. Magn Reson Med 1998; 39:551-556.
[33] Volk T, Jahde E, Fortmeyer HP, Glusenkamp KH, Rajewsky MF. pH in human tumour xenografts: effect of intravenous administration of glucose. Br J Cancer 1993; 68:492-
500.
[34] Bumke MA, Neri D, Elia G. Modulation of gene expression by extracellular pH variations in human fibroblasts: a transcriptomic and proteomic study. Proteomics
2003; 3:675-688.
[35] Bear MP, Schneider FH. The effect of medium pH on rate of growth, neurite formation and acetylcholinesterase activity in mouse neuroblastoma cells in culture. J Cell Physiol 1977;91:63-68.
[36] Petronini PG, Alfieri R, Campanini C, Borghetti AF. Effect of an alkaline shift on induction of the heat shock response in human fibroblasts. J Cell Physiol 1995; 162:322-329.
[37] Davoust J, Gruenberg J, Howell KE. Two threshold values of low pH block endocytosis at different stages. EMBO J 1987; 6:3601-3609.
[38] Cosson P, de Curtis I, Pouyssegur J, Griffiths G, Davoust J. Low cytoplasmic pH inhibits endocytosis and transport from the trans-Golgi network to the cell surface. J Cell Biol 1989; 108:377-387.
[39] Glunde K, Guggino SE, Solaiyappan M, Pathak AP, Ichikawa Y, Bhujwalla ZM. Extracellular acidification alters lysosomal trafficking in human breast cancer cells. Neoplasia 2003; 5:533-545.
[40] Altan N, Chen Y, Schindler M, Simon SM. Defective acidification in human breast tumor cells and implications for chemotherapy. J Exp Med 1998; 187:1583-1598.
[41] Simon SM. Role of organelle pH in tumor cell biology and drug resistance. Drug Discov Today 1999; 4:32-38.
[42] Kang HC, Bae YH. Endolysosomolytically active pH-sensitive polymeric nanotechnology. In: Weissig V, D'Souza GGM, editors. Organelle-specific pharmaceutical nanotechnology. Hoboken, NJ: John Wiley & Sons, Inc., 2010. p. 247-262.
[43] Kang HC, Samsonova O, Bae YH. Trafficking microenvironmental pH of gene vector polycation in drug-sensitive and multidrug-resistant MCF7 breast cancer cell.
Biomaterials 2010; 31:3071-3078.
[44] Morimoto K, Nishikawa M, Kawakami S, Nakano T, Hattori Y, Fumoto S, et al.
Molecular weight-dependent gene transfection activity of unmodified and galactosylated polyethyleneimine on hepatoma cells and mouse liver. Mol Ther 2003; 7:254-261.
[45] Overgaard J. Influence of extracellular pH on the viability and morphology of tumor cells exposed to hyperthermia. J Natl Cancer Inst 1976; 56:1243-1250.
[46] Suh J, Paik HJ, Hwang BK. Ionization of poly(ethyleneimine) and poly(allylamine) at various pH's. Bioorg Chem 1994; 22:318-327.
[47] Godbey WT, Wu KK, Mikos AG. Size matters: molecular weight affects the efficiency of poly(ethylenimine) as a gene delivery vehicle. J Biomed Mater Res 1999; 45:268-275.
[48] Brunner S, Sauer T, Carotta S, Cotten M, Saltik M, Wagner E. Cell cycle dependence
of gene transfer by lipoplex, polyplex and recombinant adenovirus. Gene Ther 2000; 7:401- 407.
[49] Brunner S, Furtbauer E, Sauer T, Kursa M, Wagner E. Overcoming the nuclear barrier: cell cycle independent nonviral gene transfer with linear polyethylenimine or electroporation. Mol Ther 2002; 5:80-86.
[50] Mortimer I, Tam P, MacLachlan I, Graham RW, Saravolac EG, Joshi PB. Cationic lipid-mediated transfection of cells in culture requires mitotic activity. Gene Ther
1999; 6:403-411.
[51] Tseng WC, Haselton FR, Giorgio TD. Mitosis enhances transgene expression of plasmid delivered by cationic liposomes. Biochim Biophys Acta 1999; 1445:53-64.
[52] Kang HC, Lee M, Bae YH. Polymeric gene carriers. Crit Rev Eukaryot Gene Expr 2005;15:317-342.

[53] Smith RM, Baibakov B, Lambert NA, Vogel SS. Low pH inhibits compensatory endocytosis at a step between depolarization and calcium influx. Traffic 2002; 3:397-406.
[54] Sandvig K, Olsnes S, Petersen OW, van Deurs B. Acidification of the cytosol inhibits endocytosis from coated pits. J Cell Biol 1987; 105:679-689.
[55] Sandvig K, Olsnes S, Petersen OW, van Deurs B. Inhibition of endocytosis from coated pits by acidification of the cytosol. J Cell Biochem 1988; 36:73-81.

CHAPTER 3

Biophysical characterization of hyper-branched polyethylenimine-graftpolycaprolactone-block-mono-methoxyl-poly(ethylene glycol) copolymers (hy-PEI-PCL-mPEG) for siRNA delivery

Yu Liu [a,1], Olga Samsonova [a,1], Brian Sproat [b,2], Olivia Merkel [a], Thomas Kissel [a]

[a] Department of Pharmaceutics and Biopharmacy, Philipps-Universität Marburg, Ketzerbach 63, D-35037 Marburg, Germany

[b] Integrated DNA Technologies BVBA, Interleuvenlaan 12A, 3001 Leuven, Belgium

[1] These two authors contributed equally to this paper

Experimental contribution of OS: MTT assay, siRNA transfections, complexation assay

Published in Journal of Controlled Release 153 (2011) 262-268

2.1. ABSTRACT

A library of mono-methoxyl-poly(ethylene glycol)-block-poly(ε-caprolactone) (mPEG-PCL) modified hyperbranched PEI copolymers (hy-PEI-PCL-mPEG) was synthesized to establish structure function relationships for siRNA delivery. These amphiphilic block-copolymers were thought to provide improved colloidal stability and endosomal escape of polyplexes containing siRNA. The influence of the mPEG chain length, PCL segment length, hy-PEI molecular weight and the graft density on their biophysical properties was investigated. In particular, buffer capacity, complex formation constants, gene condensation, polyplex stability, polyplex size and zeta-potential were measured. It was found that longer mPEG chains, longer PCL segments and higher graft density beneficially affected the stability and formation of polyplexes and reduced the zeta-potential of siRNA polyplexes. Significant siRNA mediated knockdown was observed for hy-PEI25k-(PCL900-mPEG2k)1 at N/P 20 and 30, implying that the PCL hydrophobic segment played a very important role in siRNA transfection. These gene delivery systems merit further investigation under in vivo conditions.

2.2. INTRODUCTION

Gene silencing by short interfering RNA (siRNA) offers tremendous promise for the treatment of many genetic and acquired diseases. The discovery of siRNA in mammalian cells [1] provides a new and much more effective strategy to induce the degradation of specific mRNA sequences that may regulate diseased cells [2]. Similar to plasmid DNA (p-DNA), siRNA also consists of double-stranded nucleic acids. They possess a phosphodiester backbone with the same negative charge to nucleotide ratio, and can interact electrostatically with cationic agents [3]. The duration of siRNA therapeutic effects was reported to be longer than that of p-DNA [4]. Additionally, siRNA needs to be delivered to the cytosol only [5]. The development of safe and efficient non-viral carriers for siRNA remains a challenging task. Among the vast family of non-viral gene delivery systems, poly (ethylenimine) (PEI)

and its derivatives have taken a prominent position due to their high positive charge density. They are able to effectively condense nucleic acids into homogenous polyplexes with sizes of d100 nm, which are capable of transfecting cells efficiently in vitro as well as in vivo [6]. Recent reports showed that PEI can facilitate efficient delivery of siRNA both in vitro and in vivo [7]. The molecularweight of PEI was a critical factor influencing the toxicity and transfection efficiency [8]. PEI with higher molecular weight, for example, 25 kDa, exhibited both higher transfection efficiency and higher toxicity than other smaller PEIs [9, 10]. The dilemma of the correlation of toxicity with transfection efficiency has been the key obstacle for the application of PEI in vivo. Many strategies to overcome these problems have been proposed. For instance, the introduction of hydrophilic and hydrophobic segments in PEI molecules [11–13], the cross-linking of small PEI molecules via disulfide bonds [14] or ester bonds and/ or amide-based PEI derivatives [15, 16], the modification of polyplexes' surface to shield the positive charge [17], and the conjugation of PEI with ligands [18]. Amphiphilic polymer structures containing mPEG as the hydrophilic component and PCL as flexible hydrophobic segments grafted onto branched PEI (hy-PEI) molecules could hypothetically form micelles exhibiting a core-corona structure. These carriers could improve the solubility and colloidal stability of polyplexes in aqueous solution and biological fluids. Also transfection efficiency could be improved due to facilitated transmembrane transport [19, 20]. Moreover, the core corona arrangement could offer the possibility of multi-functionality [21] whereby the co-delivery of siRNA (corona) and hydrophobic markers or drugs (core) could be envisaged. Previous results demonstrated that this strategy could be promising. The cytotoxicity decreased with increasingmolecularweights of the PCL and mPEG segments. Hy-PEI-PCL-mPEG with very short PCL segments displayed higher transfection efficiency compared to hy-PEI25k. The hy-PEI-PCL-mPEG copolymers also exhibited the cleavage of ester bonds in aqueous solution [20, 22]. Despite these initial results knowledge about relationships between the copolymer structure and function as a gene delivery vector is still

limited. To demonstrate that these copolymers can be used for efficient siRNA delivery, further investigations were required. We hypothesized that hy-PEI-PCL-mPEG might show controllable stability of polyplexes, and transfection properties for siRNA as a function of different polymer compositions. Hence a library of hy-PEI-PCL-mPEG copolymers with varying mPEG length, short PCL segments, graft density and two molecular weights of hy-PEI (10 kDa and 25 kDa) was synthesized to explore the influence of polymer compositions on the physicochemical properties of the polymers as well as the relationship to efficiency of siRNA transfection to enable successful application of this type of polymer for siRNA delivery in the future.

2.3. MATERIALS AND METHODS

2.3.1. Materials

Poly(ethylene glycol)-mono-methyl-ether (mPEG) (MW, 550 Da, 2 kDa, 5 kDa) and caprolactone were purchased from Fluka (Taufkirchen, Germany). Acryloyl chloride and tin (II) 2-ethylhexanoate ($SnOct_2$) were from Sigma-Aldrich (Taufkirchen, Germany). Hy-PEIs with molecular weights of 25 kDa (hy-PEI25k) and 10 kDa (hy-PEI10k) were obtained from BASF (Ludwigshafen, Germany) and Polysciences Inc. (Eppelheim, Germany) respectively. 2´-O-Methylated 25/27mer DsiRNA targeting Firefly Luciferase and a Non-Coding control DsiRNA were obtained from Integrated DNA Technologies (Leuven, Belgium). Other reagents of analytical quality were used without further purification. As abbreviations hy PEIα, PCLβ, mPEGγ, mPEGγ-PCLβ and hy-PEIα-(PCLβ-mPEGγ)n were used. Herein n represents the graft density of mPEG-PCL on PEI while α, β and γ describe the molecular weight of PEI, PCL and mPEG segments, respectively.

2.3.2. Synthesis and characterization

Hy-PEI-PCL-mPEG was synthesized as described previously [20]. Briefly, mPEG, ε caprolactone and $SnOct_2$ were reacted in a roundbottom flask at 120 °C under stirring for 24 h. One mmol of dried products was mixed with 2 mmol of triethylamine and 2 mmol of acryloyl chloride in 40 ml of toluene and stirred for 8 h at 80 °C, followed by the removal of triethylamine hydrochloride and precipitation of the polymer by addition of cold n-hexane. The dried precipitate (based on the molar ratio of hy-PEI) was finally reacted with PEI in chloroform at 45 °C for 8–24 h (higher graft density required longer reaction time). The copolymer was characterized by 1H NMR and ^{13}C NMR spectroscopy, which verified its structure and enabled calculation of its composition. Gel permeation chromatography (GPC) demonstrated the absence of unreacted mPEG-PCL diblock copolymer and PEI homopolymers. No further purification steps were necessary. Details of the characterization are shown in Table 1 of the supplementary materials.

2.3.3. Buffer capacity of hyPEI-PCL-mPEG

1 ml of polymer aqueous solution at the concentration of 0.01 and 0.05 M (based on the repeat unit of PEI) was titrated by aliquots of standard 0.1 M HCl at each time point and the pH response was monitored at room temperature [23] by a Hanna bench top pH meter 210 (Hanna Instrument, Germany) fitted with a microelectrode Model 421 (Inlab, Mettler Toledo, Schwerzenbach, Switzerland). The titration was stopped at pH 2. All samples were titrated in triplicate. The buffer capacity (β) was calculated from the titration curves as reported earlier, $\beta=dC_{HCl}/dpH$ [24, 25]. The individual amino group of the copolymers was considered as a mono-protic base B. So $pK_a=pH+\log([BH^+]/[B])$. The concentration fractions of [B] and $[BH^+]$ in the copolymer solution were defined as [23, 24]

$$\alpha_{BH^+} = \alpha_1 = \frac{[BH^+]}{[BH^+] + [B]} = \frac{[H^+]}{[H^+] + Ka}$$

$$\alpha_B = \alpha_0 = \frac{[B]}{[BH^+] + [B]} = \frac{Ka}{[H^+] + Ka}$$

Here, α_1 and α_0 represent the percentage of protonated and unprotonated nitrogen atoms respectively.

2.3.4. Complex stability of copolymers

The complex stability of copolymers was described by the complex formation constant (K), which was calculated as follows: K=[Cu-PEI]/[Cu] [PEI] [24], where, [Cu-PEI] stands for the concentration of copper and PEI bound in the complex. Titration was performed with 0.1 M copper sulfate as titrant [26]. All solutions used in this assay were prepared in 5% potassium acetate at pH 5.5. Copper sulfate solution was added to the polymer solution (1 mg/ml), and the optical density at 285 nm was recorded by an Ultrospec 3000 UV/visible spectrophotometer (GE Healthcare, Germany). To quantify the amount of PEI in copolymers, a standard titration curve was used. All samples were titrated in triplicate.

2.3.5. Preparation of polyplexes

Distilled water, PBS buffer (pH 7.4, 0.15 M), 5% glucose, HBG buffer (pH 7.4, 10 mM), and sodium acetate solution (pH 5.0, 0.10 M) were selected as media for polyplex preparation. All buffer solutions were filtered through 0.20 µm pore-size filters (Nalgene syringe filter, Sigma-Aldrich, Taufkirchen, Germany) before use. Ten µl of stock copolymer solution (1 mg/ml based on hy-PEI) were diluted with buffers to a final volume of 50 µl in microcentrifuge tubes. siRNA stock solution was also diluted in the same buffers used for copolymers to a final volume of 50 µl. Equal volumes of siRNA aliquots and the diluted copolymer solutions were mixed by pipetting and incubated for 20 minutes for complex formation.

2.3.6. Characterization of polyplexes

The particle size and zeta-potential of the polyplexes were monitored using a Malvern Zetasizer Nano ZS (Malvern Instrument, Herrenberg, Germany) as described previously [22]. The size of the polyplexes was measured in a disposable low volume cuvette (100 µl, Uvette, Eppendorf, Wesseling–Berzdorf, Germany). Zeta-potential measurements were then carried out in the standard clear capillary electrophoresis cell (Malvern, Herrenberg, Germany) at 25 °C by diluting 100 µl of polyplexes solution with an additional 600 µl of buffer to give a final siRNA concentration of 11 ng/µl. The salt stability was determined by the size changes of the polyplexes after incremental amounts of 3 M NaCl solution were added stepwise to the polyplex solution with vortexing. The total salt concentration required for aggregation of the polyplexes was recorded. All experiments were performed in triplicate.

2.3.7. Ethidium bromide complexation assay

The ethidium bromide complexation assay was performed using a PERKIN ELMER fluorescence spectrometer LS 50B (PerkinElmer Instruments, Rodgau, Germany) with an excitation wavelength of 510 nm (10 nm slit) and an emission wavelength of 590 nm (10 nm slit). 4 µg of anti-luc siRNA was mixed with various amounts of polymer in HBG (containing 5% glucose buffered with 10 mM HEPES) based on the predetermined N/P ratios using 96-well plates. After incubation for 10 min, 20 µl of ethidium bromide (0.1 mg/ml) in HBG were added and incubated with the polyplexes for 10 min in the dark. The fluorescence intensity of the solution was recorded. Triplicate samples were investigated and three consecutive measurements were performed and the intensity values were averaged and corrected for dilution. The results were transformed into relative fluorescence values (F_{sample}/F_{DNA}).

2.3.8. Cell culture

HeLa cells were purchased from Clontech (Saint-Germain-en-Laye, France) and transfected with a Luciferase Reporter Vector pTRE2hyg-Luc (Clontech, Saint-Germain-en-Laye, France) containing the luciferase reporter gene and a hygromycin resistance gene, as previously reported [27]. Stably transfected cells were maintained in DMEM (PAA Laboratories, Cölbe, Germany), supplemented with 10% fetal bovine serum (Cytogen, Sinn, Germany), in a humidified atmosphere with 5% CO_2 at 37 °C.

2.3.9. MTT assay

HeLa/Luc cells were seeded in 96-well plates at a density of 8000 cells/well and incubated at 37°C in 5% CO_2 for 24 h prior to the treatment of copolymer solutions with the concentration range from 0.00029 to 0.5 mg/ml and incubated as described previously [27]. Briefly, medium was changed after 24 h. MTT solution was added into fresh serum-free medium and incubated for 4 h. Cell viability was determined by measuring the absorbance of enzymatically formed formazan at 580 nm with 690 nm background corrections after cell lysis in 200 µl of DMSO. Results are given as mean values of a replicate of four.

2.3.10. siRNA transfections

HeLa/Luc cells, a cell culture model stably expressing Luciferase [27], were seeded at a density of 15,000 cells/well in 48-well plates and incubated at 37 °C in 5% CO_2 for 24 h prior to transfection. Transfection efficiencies of the polymers with various compositions were compared to each other and to Lipofectamine™ 2000 (Invitrogen, Karlsruhe, Germany) (LF) as a positive control. Cells were treated with polyplexes of 20 pmol of 2´-O-methylated 25/27mer DsiRNA targeting Firefly Luciferase (Integrated DNA Technologies, Leuven, Belgium) or nonspecific control DsiRNA (Integrated DNA Technologies, Leuven, Belgium) and polymers at varied N/P in a total volume of 25 µl. Polyplexeswere prepared in 10mM HEPES bymixing equal volumes of siRNA and polymer solutions and incubated for 20min

before addition to 250 µl full serum containing medium.Mediumwas changed 4 h post transfection to 500 µl, and cells were incubated for another 44 h before they were washed with PBS buffer, lysed with CCLR (Promega, Mannheim, Germany) and assayed for luciferase expression with a 10mM luciferin solution on a BMG LUMIstar OPTIMA luminometer plate reader (BMG Labtech, Offenburg, Germany). Results are shown as relative mean values (% of untreated cells with full luciferase expression) in replicates of four +/- standard deviation. Statistical analysiswas performed using the software Graph Pad Prism5.0 (Graph Pad Software, La Jolla, USA).

2.4. RESULTS AND DISCUSSION

2.4.1. Characterization of copolymers

A library of hy-PEI-PCL-mPEG copolymers with varying short PCL segments (molecular weight of 342, 570, and 900 Da), hydrophilic mPEG (molecular weight of 0.55, 2 and 5 kDa), hy-PEI (molecular weight of 10 and 25 kDa) and graft density (1 and 3) was synthesized as described previously [20]. The characteristics of the copolymers are listed in Table 1 of the supplementary materials. PCL block length was controlled by the feed ratio. The graft density, defined as the average number of mPEG-PCL chains per hy-PEI, and the copolymer composition could be calculated from the ratio of the peak area in the ^{1}H NMR spectrum corresponding to the methyl group of PCL segments at 4.06 ppm or the methyl group of mPEG chains at 3.36 ppm to that of the methyl groups at 2.4–3.0 ppm in hy-PEI. The content of hy-PEI was also confirmed by copper (II) ion titration [26], which agreed with the data calculated from the ^{1}H NMR spectra. The molecular weights of copolymers obtained by GPC confirmed those calculated from NMR spectroscopy. These data suggest that the synthesis of these copolymers is reproducible and well controlled. The amphiphilic behavior of hy-PEI-

PCL-mPEG was investigated by a comparison of the ^{1}H NMR spectra in D_2O and in $CDCl_3$ (Fig. 1 of supplementary materials). The signals of hydrophobic PCL segments at 1.35, 1.63, 2.3 and 4.06 ppm all disappeared in deuterated water while the ratios of mPEG and hy-PEI signals did not change due to the hydrophobic force of PCL segments as well as the entropy reduction. This indicated that the hydrophobic PCL segments were located inside the hydrophobic core surrounded by polar hy-PEI and non-polar mPEG, when dispersed in an aqueous environment. At a polymer concentration of 100 μg/ml (based on PEI) in HBG we measured the particle size of polymer architectures using dynamic light scattering (Fig. 1). Particle sizes from copolymers containing hy-PEI10k were significantly larger than those with hy-PEI25k due to the lower surface charge densities while increasing the block-length of mPEG and PCL length decreased sizes because of the higher flexibility of longer mPEG chains [28] and stronger hydrophobic interactions of longer PCL segments [29]. Polymers with a higher graft density exhibited larger sizes probably due to lower chain mobility caused by the higher graft density [30]. These results were consistent with earlier reports [13, 31].

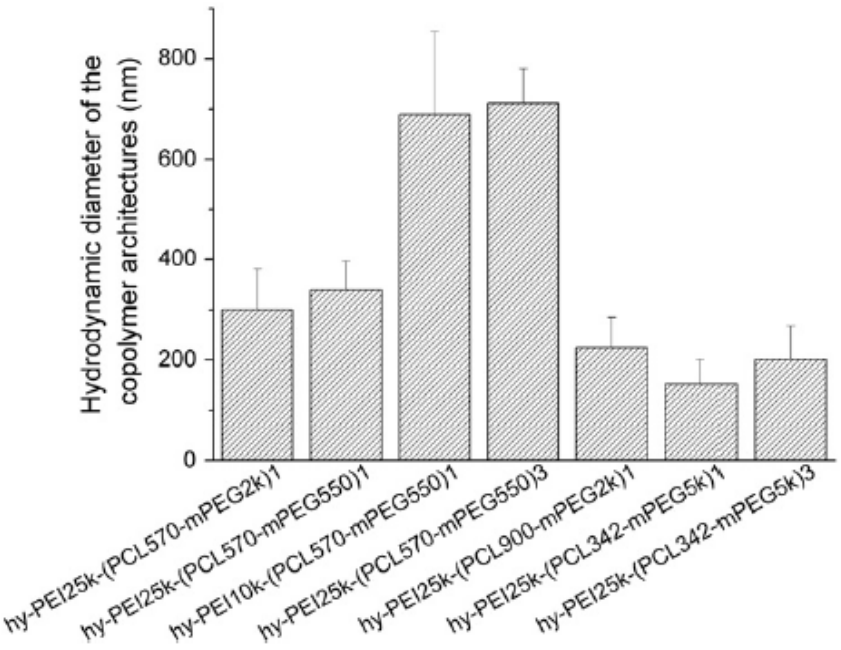

Fig. 1. The hydrodynamic diameters of micelles in HBG buffer.

2.4.2. Buffer capacity

One prominent advantage of PEI as a gene vector is its buffer capacity, which destabilizes the vesicle and releases the polyplexes from endosomes [32]. To evaluate the feasibility of modified hy-PEI as a novel gene carrier, the buffer capacity was evaluated by the titration of copolymer solutions with 0.1 M HCl. Plateaus associated with this buffer capacity can be observed on the titration curves (Fig. 2A). All the copolymers showed a broad buffer capacity ranging from pH 4.0 to 9.0. Fig. 2B shows the buffer capacity of copolymers at pH 5.0 relevant for endosomal escape by the proton sponge effect. The copolymer, hy- PEI25k (PCL570-mPEG550)1, displays the highest buffer capacity. Lower molecular weight PEI and PCL segments showed the same reduction in buffer capacity as an increase in chain length of mPEG. These results are possibly caused by the shielding effect of mPEG and lower charge densities of smaller PEI segments. Surprisingly, upon increasing the graft density from 1 to 3, the buffer capacity increased, especially for modified hy-PEI25k. As we know, each amino group of the copolymers would have a different pKa value. The pKa values calculated in this study were only the apparent ionization data, which was the value dependent on pH (Table 2 of supplementary materials). The pKa of all the copolymers decreased as pH was reduced to 5 due to the large number of positive centers present on the polymers at lower pH and consequently greater electrostatic suppression of protonation of additional amines [33]. Hy PEI25k-(PCL570-mPEG550)1 showed more protonated amino groups at pH 5 than hy-PEI25k-(PCL900-mPEG2k)1 and hy-PEI25k-(PCL342-mPEG5k)3 followed by hy-PEI25k. This behaviour suggested that the conformational stability of the hy-PEI-PCL-PEG copolymers were crucial for the buffer capacity of these copolymers [25].

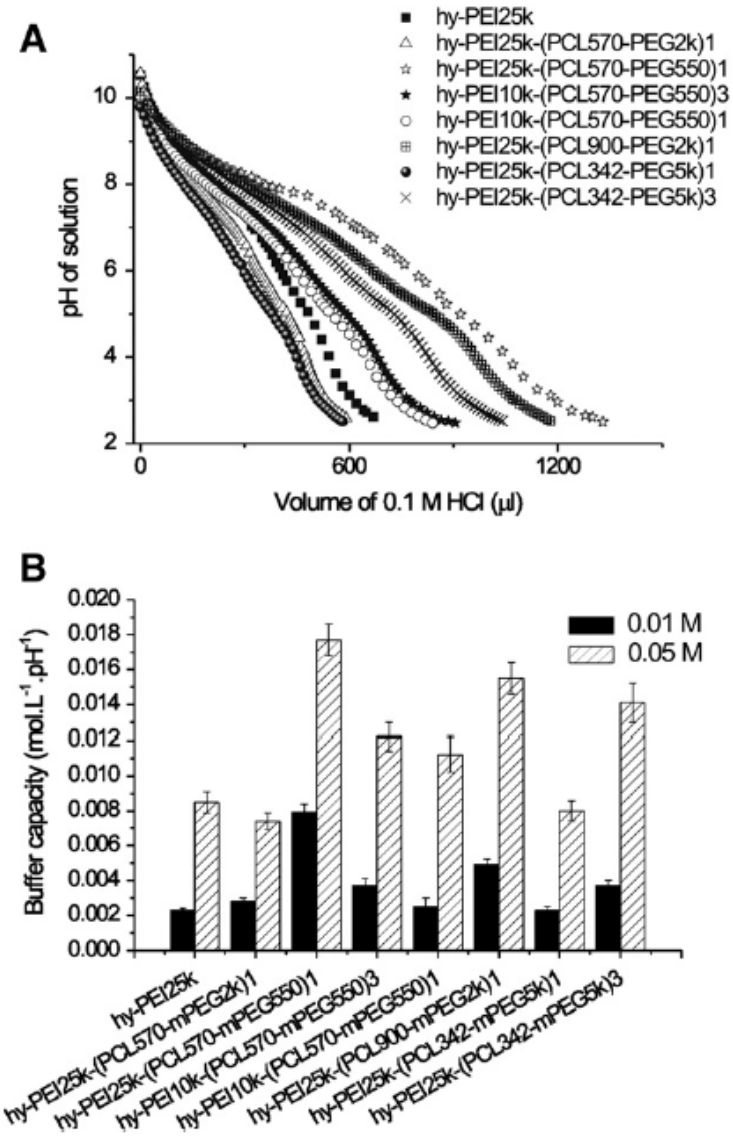

Fig. 2. The titration curve of 0.05 M copolymer solution with 0.1 M HCl (A) and the buffer capacity of polymers at concentration of 0.01 and 0.05 M at pH 5 (B); the concentrations of all the polymers represented here are based on the repeat unit of PEI.

2.4.3. Complex stability of copolymers

To further investigate the effect of copolymer composition on the formation of complexes we studied the interaction of copper (II) with different hy-PEI-PCL-mPEG copolymers. Addition of copper (II) ions to aqueous polymer solutions led to the formation of dark blue cuprammonium complexes suitable for colorimetric analysis of PEI [24, 34]. The inflection points of the titration curve represent the N/Cu ratio in the complex (supplementary section, Fig. 2). Moreover, the N/Cu ratio varied with the structure of the modified PEI due to the

different accessibility of nitrogen atoms for complex formation. Therefore the complex stability was used to monitor the stability of copolymer/gene polyplexes. Complex stability can be described using the complex formation constant (K), which is depicted in Fig. 3 based on the calculation method described above. Hy-PEI25k-(PCL900-mPEG2k)1 showed the highest complex stability followed by hy-PEI25k-(PCL570-mPEG550)1. These results demonstrated the importance of the hydrophobic core and in the stability of the complexes.

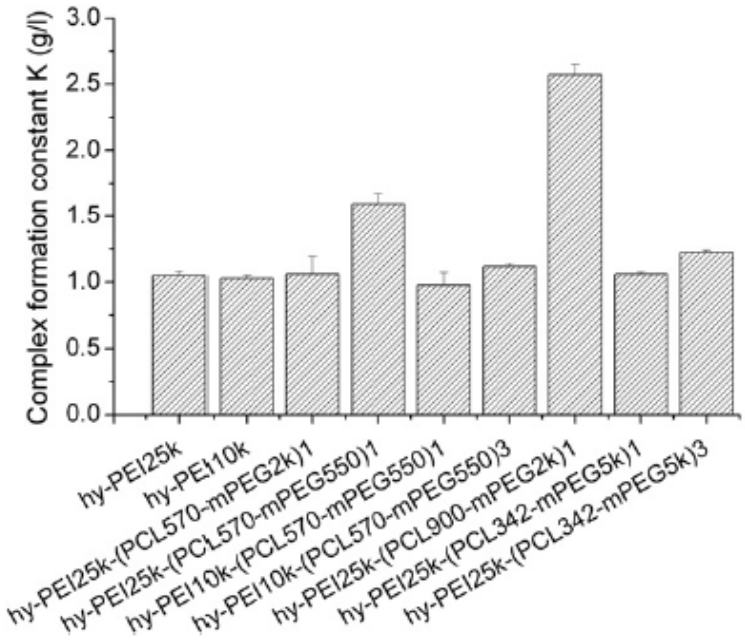

Fig. 3. Complex formation constants of polymers in 5% potassium acetate solution (pH 5.5); error bars are the standard deviation (SD) of three measurements performed on the same sample. Results shown are typical of three separate experiments.

2.4.4. siRNA binding affinity

The formation of polyplexes between siRNA and hy-PEI-PCL-mPEG occurs spontaneously based on electrostatic interactions and thermodynamic effects. The siRNA binding affinity of polymers can be assessed by an ethidium bromide (EB) assay [35]. The interaction of these polymers with siRNA was performed in HBG buffer and the results are shown in Fig. 4. All copolymers were able to bind siRNA effectively. Above an N/P ratio of 5, all copolymers showed significant fluorescence quenching for siRNA. The EB quenching data suggested a strong structural effect of the copolymers on nucleic acid-binding. Copolymers with larger hy-

PEI segments exhibited stronger binding efficiency due to higher cationic charge densities. Surprisingly, longer mPEG chains, longer PCL segments and higher graft density enhanced the interaction between copolymers and nucleic acids as well. It is well known that PEG blocks provide steric protection for nucleic acid/ polymer complexes [36]. The “conventional” PEG-grafted cationic copolymers are effectively shielded by PEG, reducing the available positive charges of the polymer for complexation [36]. However, in our studies hy-PEI10k-(PCL570-mPEG550)1, hy-PEI10k-(PCL570- mPEG550)3, hy-PEI25k-(PCL570-mPEG2k)1 and hy-PEI25k-(PCL570-mPEG2k)1 represented insignificant enhancement of binding, while hy-PEI25k-(PCL900-mPEG2k)1, hy-PEI25k-(PCL342-mPEG5k)1 and hy-PEI25k-(PCL342-mPEG5k)3 revealed a clear enhancement compared with hy-PEI25k. These results suggest that hydrophobic PCL segments and mPEG played a significant role in promoting complexation. Similar results of enhanced nucleic acid condensation have recently been reported for plasmid DNA [12], antisense oligonucleotides [36], as well as siRNA in complexation with PEGylated PEIs [37]. It seems that longer mPEG chains and suitable graft densities can separate the PEI/nucleic acid core from the mPEG chains, resulting in the effective interaction of PEI with the nucleic acid [37]. Furthermore, longer PCL segments caused association into small and stable supramolecular nano-carriers driven by hydrophobic interactions [24, 28], while higher graft density improved the stability due to a reduction in mobility of the chains [30]. Therefore higher degrees of grafting were believed to be necessary to achieve efficient nucleic acid condensation compared to unmodified PEI [37]. Moreover, only hy-PEI25k-(PCL900-mPEG2k)1 and hy-PEI25k-(PCL342-mPEG5k)3 exhibited significant affinity over the entire range of N/P ratios tested. This can be explained by the rigid rod-like behavior of the shorter siRNA molecules [3].

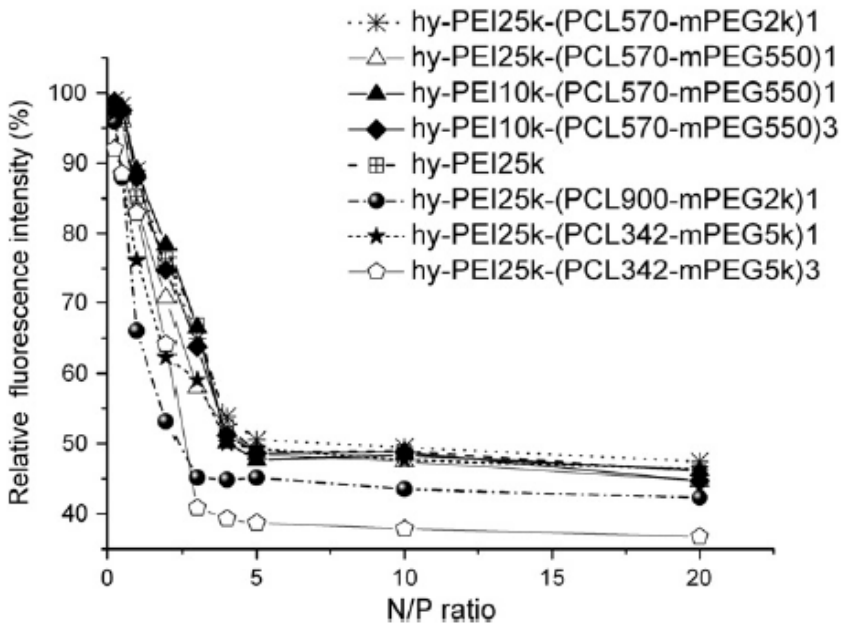

Fig. 4. Ethidium bromide binding affinity assay of copolymers with siRNA in HBG buffer (pH 7.4).

2.4.5. Characterization and stability of polyplexes (polymer/siRNA complexes)

The size and zeta-potential of polyplexes were measured at N/P 10 in HBG buffer using dynamic laser light scattering (DLS) to investigate the influence of copolymer compositions on the characteristics of the polyplexes. Fig. 5A shows difference concerning the polyplex sizes of both unmodified and modified hy-PEI10k and hy-PEI25k in HBG buffer. Smaller polyplex size was obtained for polyplexes compared with blank micelles (Fig. 1) due to the condensation effects of negatively charged nucleic acid. Higher graft density and longer mPEG chain length decreased both the size and zeta-potential of polyplexes, which is in line with earlier reports [36, 37]. This behavior was attributed to the increased steric hindrance associated with the longer PEG blocks, which maximized the space between the hydrophilic segments. The polyplexes of hy-PEI25k-(PCL900-mPEG2k)1 were larger due to the larger hydrophobic PCL core. Based on the micelle structure, the hydrophobic PCL core was expected to incorporate the water-insoluble moieties to stabilize the polyplexes in aqueous solution and protect the nucleic acid from degradation in the extracellular environment.

Electrostatic interactions between polycationic polymers and nucleic acid, largely responsible for the stability of the polyplexes, were strongly influenced by the ionic strength of the surroundings [38]. The determination of the colloidal stability was measured by the titration of polyplex solutions with concentrated NaCl solution (3 M) and polyplex size was monitored by DLS (Fig. 5B). As expected longer mPEG chains, longer PCL segments, larger hy-PEI and higher graft density increased the stability of polyplexes due to steric, electrostatic and entropic stabilization [39]. Similar results were also reported for lipoplexes [40].

In order to demonstrate the stability of polyplexes over time, the size changes of polyplexes of hy-PEI25k-(PCL570-mPEG2k)1 were monitored in HBG buffer (supplementary materials Fig. 3). The hydrodynamic diameter of polyplexes decreased a little initially and subsequently no significant increasewas noticed during the observation time. These results suggest that the siRNA polyplexes from hy-PEI-PCLmPEGcopolymers did not aggregate in HBG buffer at room temperature.

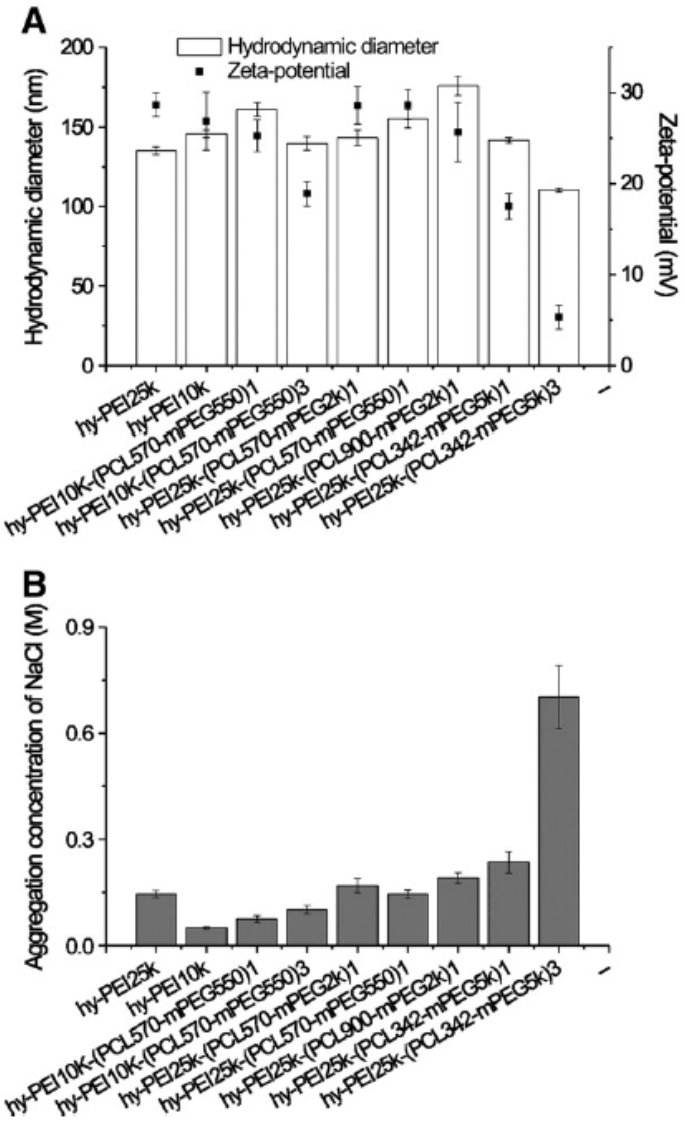

Fig. 5. Hydrodynamic diameters and zeta-potentials of siRNA polyplexes from copolymers with different compositions formed in HBG buffer (A); NaCl concentration required for aggregation of polyplexes (B), the polyplex solutions were titrated with concentrated NaCl solution (3 M) and monitored by DLS to determine the size changes. N/P ratio is 10. Error bars are the standard deviation (SD) of three measurements performed on the same sample. Results shown are typical of three separate experiments.

2.4.6. Cytotoxicity assay (MTT)

MTT-assays were performed in HeLa/Luc cells to evaluate the cytotoxicity of the copolymers. Uncomplexed copolymers were used to obtain results for the worst case scenario as reported [20]. Four copolymers were selected and hy-PEI25k was used as a control in this study. As illustrated in Fig. 6, the cytotoxicity of these copolymers in HeLa/Luc displayed a similar concentration dependency as observed in A549 cells [20]. No statistically significant

differences in cytotoxicity were found between different polymers in this particular cell line which was generated to quantify knock-down effects. However, in other cells, for instance, A549 [20] and L929 (not published), the difference can easily be observed. Additionally, a trend can be observed according to which unmodified PEIwas more cytotoxic, all copolymers with grafting degree 1 behaved very similar, and the copolymer with the highest grafting degree of 3 PCL-PEI chains caused the lowest impairment of cell viability. The same trend has been described earlierwith an IC50 value of PEI in L929 cells that supported our results in HeLa/Luc cells [11].

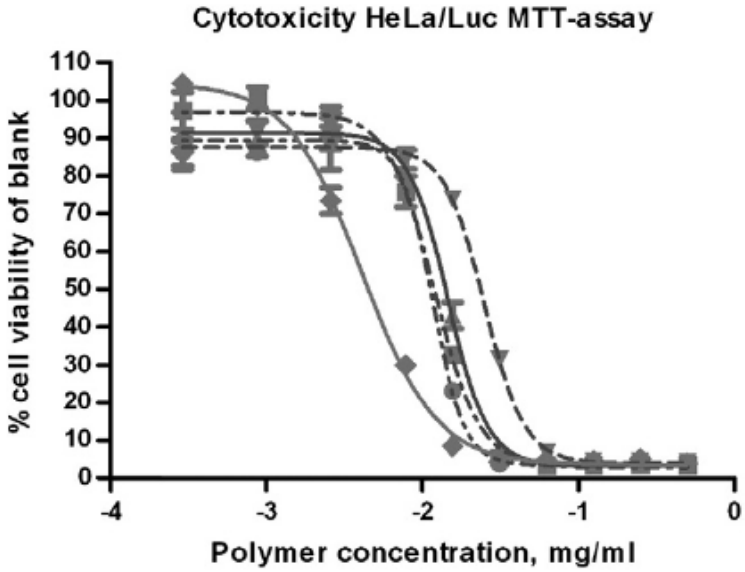

	IC50
hy-PEI25K	0.01174
hy-PEI25k-(PCL900-mPEG2k)1	0.01191
hy-PEI25k-(PCL342-mPEG5k)1	0.01460
hy-PEI25k-(PCL342-mPEG5k)3	0.02520
hy-PEI25k-(PCL570-mPEG2k)1	0.004129

Fig. 6. Cell viability of copolymers with different composition in HeLa/Luc cells. X axis represents the logarithm of polymer concentration. Experiments were performed in triplicate, and the results are given as the mean value.

2.4.7. siRNA transfection

The same panel of copolymers was then investigated with regard to siRNA transfection properties in HeLa/Luc cells under in vitro conditions. Lipofectamine was used as the reference [27]. Hy-PEI25k-(PCL900-mPEG2k)1 could be identified as the most efficient knockdown agent at N/P 20 and 30 with a statistical significance of $p<0.05$** and $p<0.001$***, respectively (Fig. 7). At N/P 40, some toxic effects decreased the luciferase expression in cells treated with non-specific control siRNA (si-NegCon), which precluded a clear statement of the significance of the specific action of the anti-Luc siRNA. However, hy-PEI25k-(PCL570-mPEG2k), showed only some luciferase silencing at N/P 20 ($p<0.01$*) (Fig. 4 of supplementary materials) although the higher DNA transfection in A549 cells at N/P 10 was achieved with the same copolymer [21]. Hy-PEI25k-(PCL900-mPEG2k)1 was shown to exhibit very good buffer capacity, the highest complex stability and higher zeta-potential within the investigated panel, and enhanced siRNA condensation without significantly decreased complex size. It is apparent that siRNA transfection efficiency cannot be directly predicted based on DNA transfection studies. In this study, the copolymers that showed no significant complex stability did not mediate efficient gene knockdown. Since the stability of electrolyte complexes in the presence of serum is a major hurdle [26], it is well understood that improved complex stability (Fig. 3) and condensation efficacy (Fig. 4), as realized with copolymer hy-PEI25k-(PCL900-mPEG2k)1, may be beneficial and apparently more important than a decrease of the hydrodynamic diameters below 150 nm. This copolymer additionally contains the longest hydrophobic PCL chain amongst the panel investigated. This emerging amphiphilic character has previously been shown to be advantageous for transfection of amphiphilic, 2´-O-methylated siRNA [41]. The sizes of siRNA polyplexes from all these polymers were below 170 nm (Fig. 5A), which was believed to be the acceptable size for endocytosis [10]. All the siRNA polyplexes presented net positive surface charges (Fig. 5B), which were considered to facilitate uptake by negatively charged cell

membranes [10]. Since the difference in gene silencing efficiency of the various complexes are not reflected in their hydrodynamic diameter, not only size and surface charge but also buffer capacity, and especially colloidal and polyplex stability, as well as cell lines jointly affect the siRNA transfection efficiency. Among these factors the stability of polyplexes was believed to play a more crucial role than others, not least because increased stability, which was earlier accomplished by modification of hyPEI with a long PEG chain of 20 kDa protects siRNA against enzymatic degradation and therefore helps the delivery of intact duplexes [12].

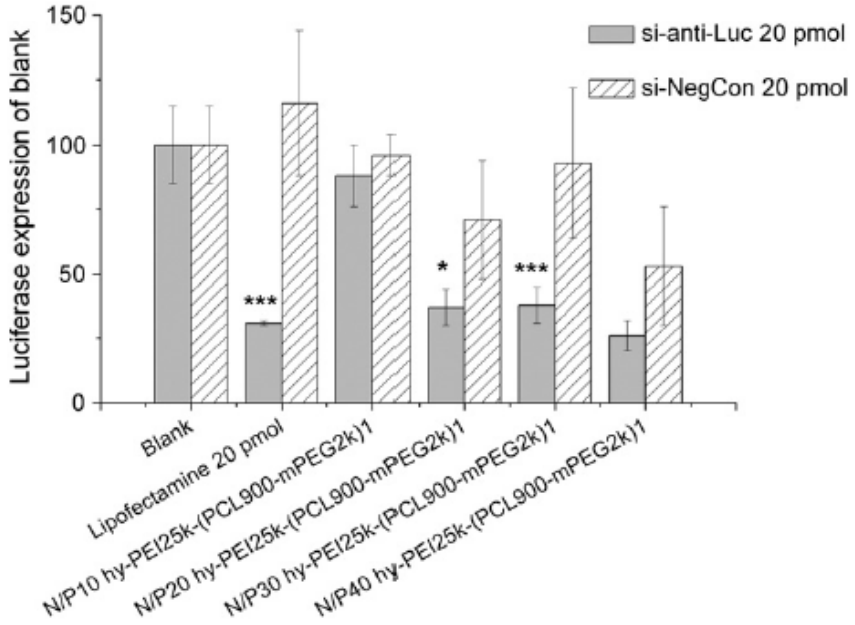

Fig. 7. Luciferase knockdown in HeLa/Luc cell lines using hy-PEI25k-(PCL900-mPEG2k)$_1$ at different N/P ratios. Solid bars represent the copolymers with anti-luciferase siRNA; diagonally striped bars stand for the copolymers with non-specific control siRNA. Error bars are the standard deviation (SD, $n = 4$; $^{*}p < 0.05$, $^{**}p < 0.01$, and $^{***}p < 0.001$).

2.5. CONCLUSIONS

The properties of branched PEI (molecular weight of 25 kDa and 10 kDa) modified with mPEG-PCL were investigated in this study. The results revealed the amphiphilic character of hy-PEI-PCL-mPEG and the composition dependency of the copolymer properties. Compared

with other published works [42], the main advantage of these polymers are the amphiphilicity and the controllable stability of polyplexes. In the case of buffer capacity, complex stability, siRNA binding affinity, and polyplex stability, the hydrophobic PCL segment and graft density exhibited the greatest impact. For instance, hy-PEI25k-(PCL900-mPEG2k)1 and hy PEI25k-(PCL342-mPEG5k)3 showed better properties tested in this study than other copolymers. Interestingly, hydrophobicity was also shown to play a role in the siRNA transfection due to the better polyplex stability despite the formation of larger particles, e.g. hy-PEI25k-(PCL900-mPEG2k)1 displayed significant knockdown at N/P 20 and 30 in HeLa/Luc cells. Although hy-PEI25k-(PCL570-mPEG2k)1 was the most promising copolymer for DNA transfection in our previous studies, no significant siRNA transfection was observed for this copolymer in our present experiments. This indicated that the principle and results of DNA transfection cannot be directly applied to siRNA transfection. Studies on siRNA transfection in vivo, the mechanism of gene transfection with hy-PEI-PCL-mPEG and the attachment of different targeting ligands onto hy-PEI-PCL-mPEG will be the subjects of our further investigations.

2.6. ACKNOWLEDGEMENTS

We are grateful to Eva Mohr (Dept. of Pharmaceutics and Biopharmacy) for the excellent technical support. MEDITRANS, an Integrated Project funded by the European Commission under the Sixth Framework (NMP4-CT-2006-026668), is gratefully acknowledged for the financial support.

2.7. SUPPLEMENTARY MATERIALS

Table 1. Characterization of copolymers in this study. All the percentage of PEI composition is based on the weight.

Polymers	Feed PEI %	NMR PEI%[a]	PEI%[b]	Mn[c]	Mw[c]	PDI[c]
Hy-PEI25k-(PCL570-mPEG2k)1	91	93	91	32270	48224	1.494
Hy-PEI25k-(PCL570-mPEG550)1	96	96	96	28500	42550	1.489
Hy-PEI10k-(PCL570-mPEG550)1	90	90	90	15530	18260	1.176
Hy-PEI10k-(PCL570-mPEG550)3	75	75	77	16320	22310	1.367
Hy-PEI25k-(PCL900-mPEG2k)1	90	90	89	28410	42690	1.502
Hy-PEI25k-(PCL342-mPEG5k)1	82	85	87	38130	54290	1.424
Hy-PEI25k-(PCL342-mPEG5k)3	49	70	78	41430	58070	1.402

a. Calculated from ^{1}H-NMR
b. Quantified from the titration of copper ions
c. Obtained From GPC

^{1}H-NMR (JEOL 500MHz, $CDCl_3$) of hy-PEI-PCL-mPEG: δ 1.36ppm (m, -$COCH_2CH_2C\underline{\boldsymbol{H_2}}CH_2CH_2O$-); δ 1.63ppm (m, -$COCH_2C\underline{\boldsymbol{H_2}}CH_2C\underline{\boldsymbol{H_2}}CH_2O$-); δ 2.02ppm (t, -CO-$C\underline{\boldsymbol{H_2}}CH_2NH$-) δ 2.30ppm (t, -$COC\underline{\boldsymbol{H_2}}CH_2CH_2CH_2CH_2O$-); δ 2.32~3.00ppm (t, -$C\underline{\boldsymbol{H_2}}C\underline{\boldsymbol{H_2}}NH$-); δ 3.37ppm (s, $C\underline{\boldsymbol{H_3}}O$-); δ 3.53-3.68ppm (m, -$C\underline{\boldsymbol{H_2}}C\underline{\boldsymbol{H_2}}O$-); δ 4.06ppm (t, -$COCH_2CH_2CH_2CH_2C\underline{\boldsymbol{H_2}}O$-); δ 4.20ppm (t, -$CH_2C\underline{\boldsymbol{H_2}}O$-$COCH_2CH_2CH_2CH_2CH_2O$); δ 4.30ppm (t, -$COCH_2CH_2CH_2CH_2C\underline{\boldsymbol{H_2}}O$- $COCH_2CH_2NH$-).

^{13}C-NMR (JEOL 500MHz, $CDCl_3$) of hy-PEI-g-PCL-b-mPEG: δ 173.08ppm (-$\underline{\boldsymbol{C}}OO$-); δ 70.49ppm (-$O\underline{\boldsymbol{C}}H_2\underline{\boldsymbol{C}}H_2O$-); δ 63.88ppm (-$OCH_2\underline{\boldsymbol{C}}H_2O$-CO-); δ 57.9ppm ($CH_3O$-$\underline{\boldsymbol{C}}H_2CH_2O$-); δ 57.44ppm ($\underline{\boldsymbol{C}}H_3O$-); δ 54.41ppm (-N-$\underline{\boldsymbol{C}}H_2CH_2NH_2$); δ 52.98ppm (-$N\underline{\boldsymbol{C}}H_2CH_2NH$-); δ 49.45ppm (-$N\underline{\boldsymbol{C}}H_2\underline{\boldsymbol{C}}H_2N$-); δ 47.54ppm (-NH-$\underline{\boldsymbol{C}}H_2CH_2NH_2$); δ 41.72ppm (-NH-$\underline{\boldsymbol{C}}H_2\underline{\boldsymbol{C}}H_2$-NH-); δ 39.82ppm (-N$\mathbf{C}H_2\underline{\boldsymbol{C}}H_2$-NH-); δ 33.92ppm (-NH-$CH_2\underline{\boldsymbol{C}}H_2$-$NH_2$); δ 31.33ppm (-CO-$\underline{\boldsymbol{C}}H_2CH_2NH$-); δ 28.18ppm (-CO-$CH_2CH_2CH_2CH_2\underline{\boldsymbol{C}}H_2O$-); δ 25.27ppm (-CO-$\underline{\boldsymbol{C}}H_2CH_2CH_2CH_2CH_2O$-); δ 24.39ppm (-CO-$CH_2\underline{\boldsymbol{C}}H_2CH_2\underline{\boldsymbol{C}}H_2CH_2O$-); δ 22.53ppm (-CO-$CH_2CH_2\underline{\boldsymbol{C}}H_2CH_2CH_2O$-); δ 14.00ppm (-CO-$CH_2\underline{\boldsymbol{C}}H_2NH$-).

Table 2. pKa values and protonation degree of polymers. α_1 stands for the percentage of protonated nitrogen atoms; the concentrations expressed here are based on the repeat unit of PEI

Polymers	original pKa		pKa at pH 5		original α_1		α_1 at pH 5	
	0.01M	0.05M	0.01M	0.05M	0.01M	0.05M	0.01M	0.05M
Hy-PEI25k	8.22	8.36	4.90	4.81	0.01272	0.00672	0.44269	0.39234
Hy-PEI10k	8.04	8.32	4.90	4.79	0.01036	0.00642	0.44269	0.38686
PEI25k-(PCL570-mPEG2k)1	7.90	7.56	5.04	4.77	0.00883	0.00268	0.52301	0.37061
PEI25k-(PCL570-mPEG550)1	7.96	7.62	5.45	4.98	0.00946	0.00288	0.73811	0.48849
PEI10k-(PCL570-mPEG550)1	7.34	7.42	5.07	4.85	0.00466	0.00229	0.54021	0.44269
PEI10k-(PCL570-mPEG550)3	7.12	7.32	5.08	4.87	0.00362	0.00204	0.54021	0.44269
PEI25k-(PCL900-mPEG2k)1	6.78	7.24	5.24	4.96	0.00245	0.00186	0.63474	0.47699
PEI25k-(PCL342-mPEG5k)1	6.74	7.04	4.87	4.74	0.00229	0.00148	0.42572	0.35465
PEI25k-(PCL342-mPEG5k)3	6.66	6.86	5.14	4.93	0.00213	0.00120	0.57990	0.45979

Figure 1. The comparison of the ^{1}H-NMR spectra of hy-PEI25k-(PCL570-mPEG2k)$_3$ and hy-PEI25k-(PCL570-mPEG2k)$_1$ in deuterated water (D_2O) and chloroform ($CDCl_3$) respectively. (A): hy-PEI25k-(PCL570-mPEG2k)$_3$ in $CDCl_3$; (B): hy-PEI25k-(PCL570-mPEG2k)$_3$ in D_2O; (C): hy-PEI25k-(PCL570-mPEG2k)$_1$ in $CDCl_3$; (D): hy-PEI25k-(PCL570-mPEG2k)$_1$ in D_2O;

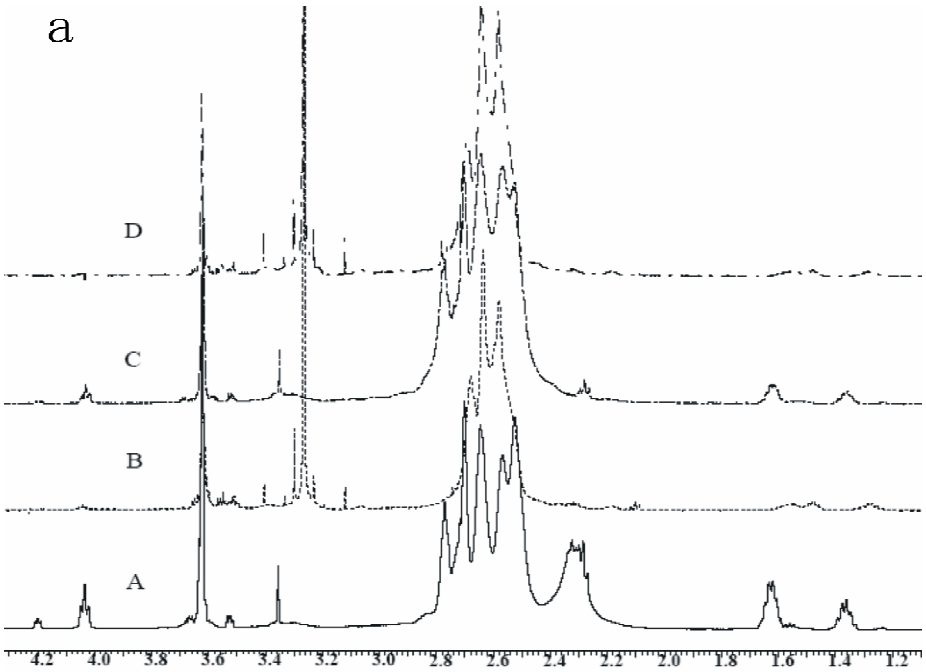

Figure 2. Raw data of a representative copper (II) titration curve (Effect of copper (II) amount upon complexes formation)

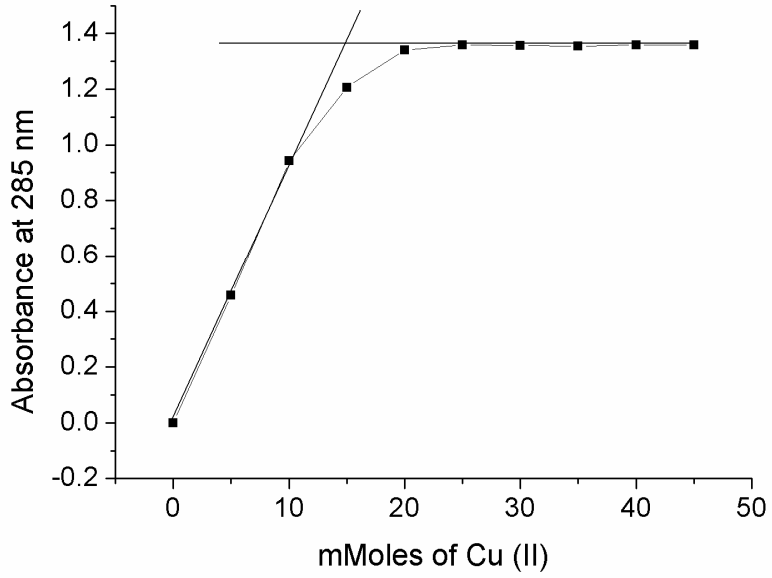

Figure 3. The stability of siRNA/ hy-PEI25k-(PCL570-mPEG2k)$_1$ complexes in HBG buffer with incubation time at room temperature. The N/P ratios of both are 10. Error bars are the standard deviation (SD) of three measurements performed on the same sample. Results shown are typical of three separate experiments.

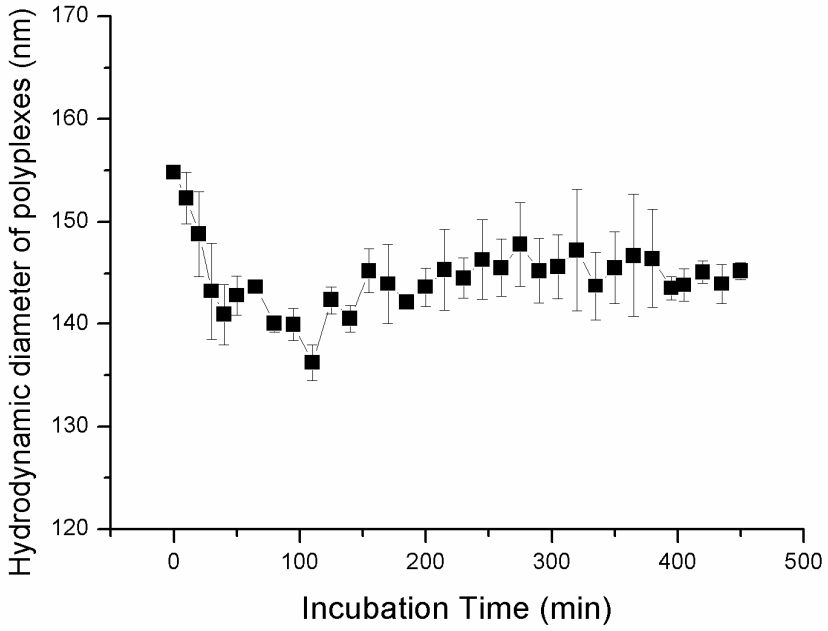

Figure 4. Luciferase knockdown in HeLa/Luc cell lines using hy-PEI-PCL-mPEG with different compositions at N/P 20 and 30. Solid bars represent the copolymers with anti-luciferase siRNA; diagonally striped bars stand for the copolymers with non-specific control siRNA. Error bars are the standard deviation (SD, n=4; *p < 0.05, **p < 0.01, and ***p < 0.001).

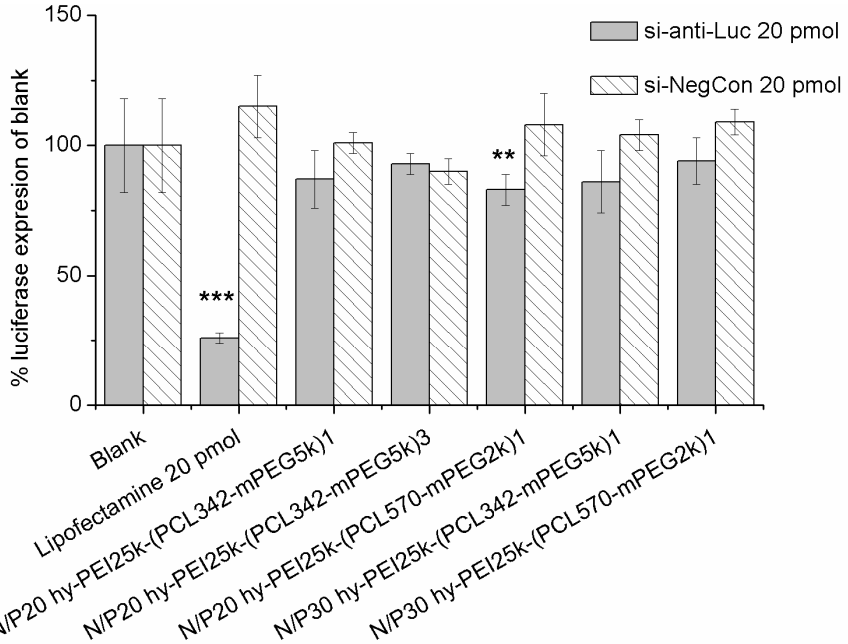

REFERENCES

[1] S. Elbashir, J. Harborth, W. Lendeckel, A. Yalcin, K. Weber, T. Tuschl, Duplexes of 21-nucleotide RNAs mediate RNA interference in cultured mammalian cells, Nature 411 (2001) 494–498.

[2] D.T. Auguste, K. Furman, A. Wong, J. Fuller, S.P. Armes, T.J. Deming, R. Langer, Triggered release of siRNA from poly(ethylene glycol)-protected, pH-dependent liposomes, J. Control. Release 130 (2008) 266–274.

[3] D.J. Gary, N. Puri, Y.-Y. Won, Polymer-based siRNA delivery: perspectives on the fundamental and phenomenological distinctions from polymer-based DNA delivery, J. Control. Release 121 (2007) 64–73.

[4] D.W. Bartlett, M.E. Davis, Insights into the kinetics of siRNA-mediated gene silencing from live-cell and live-animal bioluminescent imaging, Nucleic Acids Res. 34 (2006) 322–333.

[5] P.D. Zamore, B. Haley, Ribo-gnome: the big world of small RNAs, Science 5740 (2005) 1519–1524.

[6] T. Merdan, J. Kopeček, T. Kissel, Prospects for cationic polymers in gene and oligonucleotide therapy against cancer, Adv. Drug Deliv. Rev. 54 (2002) 715–758.

[7] B. Urban-Klein, S.Werth, S.Abuharbeid, F. Czubayko, A. Aigner, RNAi-mediated genetargeting through systemic application of polyethylenimine (PEI)-complexed siRNA in vivo, Gene Ther. 12 (2005) 461–466.

[8] W.T. Godbey, K.K. Wu, A.G. Mikos, Size matters: molecular weight affects the efficiency of poly(ethylenimine) as a gene delivery vehicle, J. Biomed. Mater. Res. 45 (1999) 268–275.

[9] D. Fischer, T. Bieber, Y. Li, H.P. Elsässer, T. Kissel, A novel non-viral vector for DNA delivery based on low molecular weight, branched polyethylenimine: effect of molecular weight on transfection efficiency and cytotoxicity, Pharm. Res. 16 (1999) 1273–1279.

[10] A.C. Grayson, A.M. Doody, D. Putnam, Biophysical and structural characterization of polyethylenimine-mediated siRNA delivery in vitro, Pharm. Res. 23 (2006) 1868–1876.

[11] S.J. Sung, S.H. Min, K.Y. Cho, S. Lee, Y.I. Yeom, J.K. Park, Effect of polyethylene glycol on gene delivery of polyethylenimine, Biol. Pharm. Bull. 26 (2003) 492–500.

[12] S. Mao, M. Neu, O. Germershaus, O. Merkel, J. Sitterberg, U. Bakowsky, T. Kissel, Influence of polyethylene glycol chain length on the physicochemical and biological properties of poly(ethylene imine)-graft-poly(ethylene glycol) block copolymer/siRNA polyplexes, Bioconjug. Chem. 17 (2006) 1209–1218.

[13] L.Y. Qiu, Y.H. Bae, Self-assembled polyethylenimine-graft-poly(ε-caprolactone) micelles as potential dual carriers of genes and anticancer drugs, Biomaterials 28 (2007) 4132–4142.

[14] M.A. Gosselin, W. Guo, R.J. Lee, Efficient gene transfer using reversibly cross-linked low molecular weight polyethylenimine, Bioconjug. Chem. 12 (2001) 989–994.

[15] R. Arote, T.H. Kim, Y.K. Kim, S.K. Hwang, H.L. Jiang, H.H. Song, J.W. Nah, M.H. Cho, C.S. Cho, A biodegradable poly(ester amine) based on polycaprolactone and polyethylenimine as a gene carrier, Biomaterials 28 (2007) 735–744.

[16] H. Petersen, T. Merdan, K. Kunath, D. Fischer, T. Kissel, Poly(ethylenimine-co-L-lactamide-co-succinamide): a biodegradable polyethylenimine derivative with an advantageous pH-dependent hydrolytic degradation for gene delivery, Bioconjug. Chem. 13 (2002) 812–821.

[17] M. Ogris, S. Brunner, S. Schüller, R. Kircheis, E. Wagner, PEGylated DNA/ transferrin-PEI complexes: reduced interaction with blood components, extended circulation in blood and potential for systemic gene delivery, Gene Ther. 6 (1999) 595–605.

[18] R. Kircheis, S. Schüller, S. Brunner, M. Ogris, K.H. Heider, W. Zauner, E. Wagner, Polycation-based DNA complexes for tumor-targeted gene delivery in vivo, J. Gene Med. 1 (1999) 111–120.

[19] X. Shuai, T. Merdan, F. Unger, M. Wittmar, T. Kissel, Novel biodegradable ternary copolymers hy-PEI-g-PCL-b-PEG: synthesis, characterization and potential as efficient nonviral gene delivery vectors, Macromolecules 36 (2003) 5751–5759.

[20] Y. Liu, J. Nguyen, T. Steele, O. Merkel, T. Kissel, A new synthesis method and degradation of hyper-branched polyethylenimine grafted polycaprolactone block mono-methoxyl poly(ethylene glycol) copolymers (hy-PEI-g-PCL-b-mPEG) as potential gene delivery vectors, Polymer 50 (2009) 3895–3904.

[21] S.M. Janib, A.S. Moses, J.A. MacKay, Imaging and dug delivery using theranostic nanoparticles, Adv. Drug Deliv. Rev. 62 (2010) 1052–1063.

[22] Y. Liu, T. Steele, T. Kissel, Degradation of hyper-branched poly(ethylenimine)-graft poly(caprolactone)-block-mono-methoxyl-poly(ethylene glycol) as a Potential Gene Delivery Vector, Macromol. Rapid Commun. 31 (2010) 1509–1515.

[23] M.P. Xiong, M.L. Forrest, G. Ton, A. Zhao, N.M. Davies, G.S. Kwon, Poly(aspartate-g- PEI800), a polyethylenimine analogue of low toxicity and high transfection efficiency for gene delivery, Biomaterials 28 (2007) 4889–4900.

[24] F. Seel, Grundlagen der analytischen Chemie, Verlag Chemie, Weinheim, 1970.

[25] J. Suh, M.-J. Kim, Microenvironments of 3-[2-imidazolylazo]-benzoyl-poly (ethylenimine): high affinity for Ni(II) and 9-anthracenecarboxylate ions, Bioorg. Chem. 20 (1992) 366–376.
[26] T.D. Perrine, W.R. Landis, Analysis of polyethylenimine by spectrophotometry of its copper chelate, J. Polym. Sci. A-1 (5) (1967) 1993–2003.
[27] O.M. Merkel, D. Librizzi, A. Pfestroff, T. Schurrat, K. Buyens, N.N. Sanders, S.C. De Smedt, M. Béhé, T. Kissel, Stability of siRNA polyplexes from poly(ethylenimine) and poly(ethylenimine)-g-poly(ethylene glycol) under in vivo conditions: effects on pharmacokinetics and biodistribution measured by Fluorescence Fluctuation Spectroscopy and Single Photon Emission Computed Tomography (SPECT) imaging, J. Control. Release 138 (2009) 148–159.
[28] D.E. Owens III, N.A. Peppas, Opsonization, biodistribution, and pharmacokinetics of polymeric nanoparticles, Int. J. Pharm. 307 (2006) 93–102.
[29] D. Attwood, C. Booth, S.G. Yeates, C. Chaibundit, N.M. Ricardo, Block copolymers for drug solubilisation: relative hydrophobicities of polyether and polyester micelle-core-forming blocks, Int. J. Pharm. 345 (2007) 35–41.
[30] G. Storm, S.O. Belliot, T. Daemen, D.D. Lasic, Surface modification of nanoparticles to oppose uptake by the mononuclear phagocyte system, Adv. Drug Deliv. Rev. 17 (1995) 31–48.
[31] K. Kunath, A. von Harpe, D. Fischer, H. Petersen, U. Bickel, K. Voigt, T. Kissel, Lowmolecular- weight polyethylenimine as a non-viral vector for DNA delivery: comparison of physicochemical properties, transfection efficiency and in vivo distribution with high-molecular-weight polyethylenimine, J. Control. Release 89 (2003) 113–125.
[32] A. Kichler, C. Leborgne, E. Coeytaux, O. Danos, Polyethylenimine-mediated gene delivery: a mechanistic study, J. Gene Med. 3 (2001) 135–144.
[33] J. Suh, H.J. Paik, B.K. Hwang, Ionization of poly(ethylenimine) and poly (allylamine) at various pH's, Bioorg. Chem. 22 (1994) 318–327.
[34] F. Ungaro, G. De Rosa, A. Miro, F. Quaglia, Spectrophotometric determination of polyethylenimine in the presence of an oligonucleotide for the characterization of controlled release formulations, J. Pharm. Biomed. Anal. 31 (2003) 143–149.
[35] A.L. Parker, D. Oupicky, P.R. Dash, L.W. Seymour, Methodologies for monitoring nanoparticle formation by self-assembly of DNA with poly(l-lysine), Anal. Biochem. 302 (2002) 75–80.
[36] H. Petersen, P.M. Fechner, A.L. Martin, K. Kunath, S. Stolnik, C.J. Roberts, D. Fischer, M.C. Davis, T. Kissel, Polyethylenimine-graft-poly(ethylene glycol) copolymers: Influence of copolymer block structure on DNA complexation and biological activities as gene delivery system, Bioconjug. Chem. 13 (2002) 845–854.
[37] M. Neu, O. Germershaus, M. Behe, T. Kissel, Bioreversibly crosslinked polyplexes of PEI and high molecular weight PEG show extended circulation times in vivo, J. Control. Release 124 (2007) 69–80.
[38] A. Zintchenko, A. Philipp, A. Dehshahri, E. Wagner, Simple modifications of branched PEI lead to highly efficient siRNA carriers with low toxicity, Bioconjug. Chem. 19 (2008) 1448–1455.
[39] U. Rungsardthong, T. Ehtezazi, L. Bailey, S.P. Armes, M.C. Garnett, S. Stolnik, Effect of polymer ionization on the interaction with DNA in nonviral gene delivery systems, Biomacromolecules 4 (2003) 683–690.
[40] M.C. Pedroso de Lima, S. Simões, P. Pires, H. Faneca, N. Düzgüneş, Cationic lipid- DNA complexes in gene delivery: from biophysics to biological applications, Adv. Drug Deliv. Rev. 47 (2001) 277–294.
[41] O.M. Merkel, M.A.Mintzer, D. Librizzi, O. Samsonova, T. Dicke, B. Sproat, H. Garn, P.J. Barth, E.E. Simanek, T. Kissel, Triazine dendrimers as nonviral vectors for in vitro and in vivoRNAi: the effects of peripheral groups and core structure onbiological activity, Mol. Pharm. 7 (2010) 969–983.
[42] H. Debus, P. Baumhof, J. Probst, T. Kissel, Delivery of messenger RNA by using poly (ethylene imine)-poly(ethylene glycol)-copolymer blends for polyplex formation: biophysical characterization and in vitro transfection properties, J. Control.
Release 148 (2010) 334–343.

CHAPTER 4

Low Molecular Weight pDMAEMA-*block*-pHEMA Block-Copolymers Synthesized via RAFT-Polymerization: Potential Non-Viral Gene Delivery Agents?

Olga Samsonova [1,†], Christian Pfeiffer [1,2,†], Markus Hellmund [1], Olivia M. Merkel [1] and Thomas Kissel [1]

[1] Department of Pharmaceutics and Biopharmacy, Philipps-Universität, Ketzerbach 63, D-35032 Marburg, Germany; E-Mails: samsonova.olga@staff.uni-marburg.de (O.S.); pfeiffeb@staff.uni-marburg.de (C.P.); hellesm@zedat.fu-berlin.de (M.H.); kissel@staff.uni-marburg.de (T.K.)

[2] Department of Physics, Philipps-Universität, Renthof 7, D-35032 Marburg, Germany

† Both authors contributed equally

Experimental contribution of OS: gel assays, DLS/LDA measurements, cytotoxicity and transfection in vitro, CLSM, flow cytometry

Published in Polymers 2011, 3, 693-718

3.1. ABSTRACT

The aim of this study was to investigate non-viral pDNA carriers based on diblock-copolymers consisting of poly(2-(dimethyl amino)ethyl methacrylate) (pDMAEMA) and poly(2-hydroxyethyl methacrylate) (pHEMA). Specifically the block-lengths and molecular weights were varied to determine the minimal requirements for transfection. Such vectors should allow better transfection at acceptable toxicity levels and the entire diblock-copolymer should be suitable for renal clearance. For this purpose, a library of linear poly(2-(dimethyl amino)ethyl methacrylate-*block*-poly(2-hydroxyl methacrylate) (pDMAEMA-*block*-pHEMA) copolymers was synthesized via RAFT (reversible addition-fragmentation chain transfer) polymerization in a molecular weight (Mw) range of 17–35.7 kDa and analyzed using ^{1}H and ^{13}C NMR (nuclear magnetic resonance), ATR (attenuated total reflectance), GPC (gel permeation chromatography) and DSC (differential scanning calorimetry). Copolymers possessing short pDMAEMA-polycation chains were 1.4–9.7 times less toxic *in vitro* than polyethylenimine (PEI) 25 kDa, and complexed DNA into polyplexes of 100–170 nm, favorable for cellular uptake. The DNA-binding affinity and polyplex stability against competing polyanions was comparable with PEI 25 kDa. The zeta-potential of polyplexes of pDMAEMA-grafted copolymers remained positive (+15–30 mV). In comparison with earlier reported low molecular weight homo pDMAEMA vectors, these diblock-copolymers showed enhanced transfection efficacy under *in vitro* conditions due to their lower cytotoxicity, efficient cellular uptake and DNA packaging. The homo pDMAEMA$_{115}$ (18.3 kDa) self-assembled with DNA into small positively charged polyplexes, but was not able to transfect cells. The grafting of 6 and 57 repeating units of pHEMA (0.8 and 7.4 kDa) to pDMAEMA$_{115}$ increased the transfection efficacy significantly, implying a crucial impact of pHEMA on vector-cell interactions. The intracellular trafficking, *in vivo* transfection efficacy and kinetics of low molecular weight pDMAEMA-*block*-pHEMA are subject of ongoing studies.

3.2. INTRODUCTION

The field of non-viral gene delivery remains a topic of intensive research efforts, and numerous polycations are under investigation [1, 2]. One prominent vector in pDNA delivery is poly(ethylene imine) (PEI) 25 kDa, a branched polycation with a high charge density well known for its effective complexation, high transfection, but also significant toxicity [3]. To improve biocompatibility of PEI, several strategies were pursued such as a reduction of the molecular weight [4] or introduction of shielding component, e.g., PEGylation [5, 6].

As the toxicity of a polymer, among other factors, is related to its charge density [3], polycations with more broadly spread charge distribution along the polymer chain, namely poly(2-(dimethyl amino)ethyl methacrylate (pDMAEMA) could be of interest. In comparison to PEI 25 kDa, pDMAEMA contains only tertiary amino groups, and the charge density is lower than in PEI. pDMAEMA shows an average pKa of 7.5 [7], and is thus sufficiently protonated at physiological pH for effective polyanion complexation. Previous reports described pDMAEMA to possess a decreased proton sponge effect compared to PEI 25 kDa [8] implying alternative mechanisms of membrane interaction, such as membrane destabilization [9]. This eventually led to reduced cell death, but the polymer retained the capacity to escape from endosomes [10].

A relationship between the polymer-DNA dissociation rate and transfection efficiency was established suggesting that pDMAEMA more readily releases DNA from polyplexes than polylysine [11]. The class of pDMAEMA was intensively investigated by Hennink and coworkers, demonstrating that homopolymers with molecular weights (Mw) of 300 kDa are effective DNA-carriers [12]. With increasing molecular weight, its transfection efficiency, complexation efficiency but also toxicity increased [10, 13]. Scarce information on the performance of low molecular weight (<43 kDa) pDMAEMA is available from the literature, although such polymers could possibly be eliminated by renal excretion [9]. Therefore, a

library of low molecular weight homo-pDMAEMAs with the chain length varying from 15 to 23.7 kDa was synthesized and grafted with pHEMA (poly(2-hydroxyethyl methacrylate)), resulting in water soluble linear diblock copolymers with a total Mw below 40 kDa. The number of tertiary amino groups of the charged copolymer-part exceeds 20 to 30-fold the minimal requirement of 4-6 groups reported to be necessary for efficient interaction with DNA [14].

Instead of applying ATRP (atom transfer radical polymerization) [10, 15], in this study, the synthesis was performed via RAFT polymerization (reversible addition-fragmentation chain transfer) to avoid the use of toxic organometallic catalysts, and to attain narrow polydispersity indices (PDIs).

To improve biocompatibility and colloidal stability, uncharged blocks consisting of pHEMA were introduced in an attempt to reduce undesirable adverse interactions such as aggregation and cytotoxicity reported previously [16]. PEGylation of pDMAEMA has resulted in a decrease of zeta-potential and good steric stabilization of polycations at the cost of poor polyplex uptake into cells [17]. Another disadvantage of PEGylation could be seen in an “accelerated blood clearance” phenomenon (“ABC”) [18], occurring after repeated application of PEGylated vectors due to anti-PEG IgM-production and activation of the complement system. The hydrogel-forming pHEMA was earlier reported to be non-toxic and water soluble if not cross-linked [19], and biodegradable in linear form [20]. So far, no complement activation by pHEMA was reported despite longtime usage in medical applications [19].

Several pDMAEMA-pHEMA vector systems have been investigated recently showing their potential as gene delivery systems: blends of pDMAEMA and pHEMA were used to obtain nanoparticles [21], polymer with brush-like structures based on short chain pDMAEMA grafted on pHEMA backbones by cleavable carbonate ester linkage were reported [15]. Also

star shaped pDMAEMAs with cleavable disulfide bonds synthesized via grafting with multiple short chain pDMAEMA-arms showed improved transfection efficiency [22].

Since high molecular weight homopolymers of pDMAEMA (300 kDa) were efficient transfection reagents, here, the molecular weight was systematically varied in the range from 290 to 15 kDa using RAFT to determine the minimal chain length required for transfection efficiency. Subsequently, such structures were modified using pHEMA to improve cytotoxicity and colloidal stability. These linear diblock copolymers, in contrast to previously studied pDMAEMA/pHEMA vectors, were designed to possess very narrow polydispersities, a less complicated steric structure and thus better accessibility for charge to charge interaction with genetic material, as well as low total molecular weight, allowing renal elimination without previous degradation.

3.3. MATERIALS AND METHODS

3.3.1. Materials

Benzyl chloride, Sulfur (80%), Potassium hexacyanoferrate(III), 2-Hydroxyethyl methacrylate (HEMA), 2-(Dimethyl amino) ethyl methacrylate (DMAEMA) and 4,4‘-Azobis (4-cyanopentanoic acid) (V-501) were purchased from Sigma-Aldrich. Silica gel 60 (0.040–0.063 mm) for column chromatography (230–400 mesh ASTM) was ordered from Merck Chemicals. The dialysis membrane Spectra /Por 6 RC (MWCO 1 kDa) was delivered from VWR International GmbH. HEMA and DMAEMA were distilled under reduced pressure before use. Poly(ethylene imine) (Polymin™, 25 kDa, abbreviated as PEI 25k) was a gift from BASF (Ludwigshafen, Germany). pCMV-Luc (Lot: PF461-090623) was amplified by The Plasmid Factory (Bielefeld, Germany). Beetle Luciferin and heparin sodium salt were bought from Sigma-Aldrich Laborchemikalien GmbH (Seelze, Germany). SYBR® Gold was

obtained from Invitrogen (Karlsruhe, Germany). The Pierce® BCA Protein Assay Kit was obtained from Thermo scientific (Schwerte, Germany). All other chemicals not listed were obtained from Sigma-Aldrich Chemie GmbH (Seelze, Germany) and used in the highest purity if not stated otherwise.

3.3.2. Synthesis

3.3.2.1 Synthesis of 4-Cyanopentanoic acid Dithiobenzoate (CPT) and Poly (2-(dimethyl amino)ethyl methacrylate) (pDMAEMA)

4-Cyanopentanoic acid dithiobenzoate (CPT), used as chain transfer agent (CTA), was synthesized as described in the literature [29]. The synthesis of pDMAEMA, which was used as a macroCTA, was performed similarly to the method of Scales *et al.* [28]. Briefly, 80 mmol of DMAEMA were mixed in an ice bath with sodium acetate buffer (pH 5.2) and adjusted to pH 5 with HCl. Subsequently, 0.8 mmol of CPT were dissolved in the mixture and either 0.1 or 0.2 mmol of 4,4´-Azobis (4-cyanopentanoic acid) (V-501) were added. The reaction was started by placing the reaction flask into the oil bath pre-heated to 70 °C. To stop the reaction, the mixture was frozen in liquid nitrogen after a predetermined time. The polymer was purified by dialysis in water, which was adjusted to pH 3–4 with acetic acid. The dialysate was changed three times a day during a period of 4 days. The slightly pink-colored polymer was dried by lyophilization.

3.3.2.2. Synthesis of Poly (2-(dimethyl amino)ethyl methacrylate)-block-Poly-2-Hydroxyethyl Methacrylate Block Copolymers (pDMAEMA-block-pHEMA)

To synthesize the block copolymer, 0.05 mmol of the macroCTA were dissolved in 5 mL sodium acetate buffer and 5 mmol HEMA were added. The amount of 0.125 mmol of V-501 was added by pipetting 0.25 mL of a freshly prepared stock solution (14 mg/mL) into the flask. The reaction was started by placing the reaction flask into in oil bath, which was pre-

heated to 70 °C. To stop the reaction after a certain time, the mixture was frozen in liquid nitrogen. The purification and drying of the block copolymer was performed by dialysis and lyophilization as described above.

3.3.2.3. Synthesis of Poly(2-(dimethyl amino)ethyl methacrylate)-Poly-2-Hydroxyethyl Methacrylate Random Copolymers (r-pDMAEMA-pHEMA)

The random copolymers were prepared by mixing different ratios of DMAEMA and HEMA in a final volume of 10 mL sodium acetate buffer (pH 5.2) with 0.03 mmol V-501. The DMAEMA was therefore dissolved in 5 mL buffer first and adjusted to pH 5 with HCl. The reaction was started by placing the reaction flask in an oil bath, which was pre-heated to 70 °C. After 2.5 h, the reaction mixture was frozen in liquid nitrogen. The copolymer was precipitated in THF and dried over night at room temperature. Afterwards, the slightly pink-colored polymer was dissolved in water and dried by lyophilization.

3.3.2.4. Impurities

Residues of monomers could be a reason for toxicity of prepared polymers although all residues which may originate from the synthesis of the homo polymers and block copolymers were removed by dialysis of 40 mL of polymer solution in 10 L distilled water. The water was changed three times a day over a period of four days. Monomers left over in the polymer solution of random copolymers were separated from the polymer by precipitation of the polymer in THF. Residual THF was removed by lyophilization.

3.3. Characterization of Polymers

The CPT was characterized by ^{1}H, ^{13}C nuclear magnetic resonance (NMR) and attenuated total reflectance (ATR) spectroscopy whereas the polymers were also characterized by gel permeation chromatography (GPC) and differential scanning calorimetry (DSC). The NMR

spectra were obtained with a JEOL GX 400D in either $CDCl_3$, deuterated water, or methanol-d4. ATR measurements were performed on a Spectrometer of the Excalibur series from Digi-Lab containing an ATR unit with the WinIR Pro Version 3.3 software in a range between 600 and 4,000 cm^{-1}. The GPC system contained a Duratec7505 degasser, Merck-Hitachi HPLC system (L6000 pump, AS-2000 auto sampler, T6300 column thermostat), Wyatt Dawn-EOS multi-angle laser light scattering detector (calibrated with toluene and normalized with 22 kDa pullulan standard) and an Optilab DSP refractometer. The columns used for sample separation were a PSS 10µ Novema pre-column and two PSS 10µ Novema 30 columns of 8 × 300 mm. The measurements were performed at 35 °C using 1% formic acid as eluent with a flow rate of 0.5 mL/min (laser wavelength: 690 nm, cell type: K5). The analysis and the calculation of the refractive indices of the copolymers were performed using the Wyatt Astra software V5.1.9. The refractive index of pDMAEMA was obtained from the literature [34]. The DSC measurements were performed using a DSC 7 unit with TAC7/DX controlling station from Perkin-Elmer in a range between -40 °C and 120 °C and a heat rate of 10 °C/min.

3.3.3. Polyplex Formation

For transfection, 0.5 µg plasmid DNA (pDNA) in a total of 25 µL polyplex solution was applied per well. The polyplexes were prepared by mixing equal volumes of pDNA and copolymer in isotonic glucose, calculated to afford the desired N/P ratios (positively charged polymer nitrogen atoms per phosphate groups in DNA) as described previously by Liu *et al.* [35]. After mixing by vigorous pipetting, the polyplexes were incubated for 20 min at room temperature for complete self-assembly and used freshly. The preparation was scaled up for several replicates, so that the total volume (max. 112.5 µL) was later divided into single aliquots of 25 µL after incubation, if not stated otherwise. The charge density involved in DNA-complexation defined as factor A (g polymer per mol nitrogen) was calculated to be

157 g/mol for homo-pDMAEMA and increased with larger percentage of the pHEMA part. PEI 25k polyplexes as control were prepared as stated above (factor A = 43 g/mol).

3.3.4. Retardation Efficiency on Agarose Gel & Heparin Competition Assay

To determine the efficacy of DNA packaging by polycationic polymer, gel electrophoresis was used as described previously [36]. For the experiments, 1% agarose gels containing 0.83 µg/mL ethidium bromide (EB) were run in TAE buffer (40 mM Tris/HCl, 1% acetic acid, 1 mM EDTA, pH 7.4) for 45 min at 80 V using an Electro-4 electrophoresis unit, Thermo Electron, Waltham, MA, USA. The gels were recorded after irradiation with UV-light using a gel documentation system (BioDocAnalyze, Biometra, Göttingen, Germany). The polyplexes of different N/P ratios (0.5, 1, 2, 5 for retardation assay, and 15 for heparin assay) were prepared as described above, and the volumes of 30 µL, containing 0.6 µg DNA were applied to each slot. To omit the soaring of polyplexes from the slots and to visualize the migration along the lane, 3 µL of loading buffer containing glycerol and bromophenole blue were added immediately prior to application to the gel.

To test the polyplex stability in the presence of competing anions (simulating serum components), they were exposed to heparin of different concentrations for 10 min after the usual incubation procedure of 20 min, then applied to the gel with loading buffer. As control for the visibility of DNA-EB intercalation, free DNA was run on the gel.

3.3.5. Polyplex size- and Charge-Determination via Dynamic Light Scattering (DLS) and Laser Doppler Anemometry (LDA)

3.3.5.1. Hydrodynamic Diameter and Zeta-Potential of pDNA-Polymer Complexes in Isotonic Glucose

Polyplexes used for this analysis were prepared and incubated as described above. The measurements were performed in triplicates for each N/P ratio and polymer. For each

hydrodynamic size measurement (DLS), 50 µL polyplexes were applied directly into a disposable low volume cuvette (Eppendorf, Wesseling-Berzdorf, Germany) and analyzed with the Zetasizer Nano ZS (Malvern, Herrenberg, Germany) equipped with a 4 mW He-Ne laser at a wavelength of 633 nm at 25 °C. The light scattering was detected at a 173° backward scattering angle. The parameters of 5% glucose were applied (refractive index: 1.337, viscosity 1.0351 cP). For zeta potential measurements, the polyplexes were diluted with 750 µL isotonic glucose, applied into a clear zeta U-form cuvette (Malvern, Herrenberg, Germany) and analyzed with the Smoluchowski model, with a dielectric constant of 78.5. Each sample was measured in 5 runs. For both measurements, N/P ratios of 5, 10, 15, and 20 were tested and analyzed with the Zetasizer Nano ZS Software 6.20 (Malvern, Herrenberg, Germany) as reported previously [37].

3.3.5.2. Influence of Isotonic Salt and Glucose Solutions on Aggregation Behavior of Polyplexes (DLS)

To evaluate the impact of ionic strength of the continuous phase on the aggregation behavior of polyplexes, two types of polyplexes were chosen. Polyplexes of the homo-polymer (pDMAEMA115) and the diblock-copolymer (pDMAEMA115-*block*-pHEMA57) were measured concerning hydrodynamic diameters over the period of 1 h with 1 min interval using DLS. The volume and concentration of polyplexes were chosen according to conditions for transfection experiments: 25 µL complex suspension containing 0.5 µg pDNA at N/P 15 were added to 75 µL isotonic glucose or NaCl-solution after incubation for 20 min and measured as described under 3.6. The measurement of each sample was performed twice; the mean values and standard deviation are shown in Figure 7.

3.3.6. Cell Culture

For transfection experiments, confocal laser scanning microscopy (CLSM) and flow cytometry, mouse fibroblasts (3T3) were used that were cultured in DMEM high glucose (PAA Laboratories, Cölbe, Germany), supplemented with 10% fetal bovine serum (Cytogen, Sinn, Germany). For toxicity experiments, L929 mouse fibroblasts cultured in DMEM low glucose (PAA Laboratories, Cölbe, Germany), supplemented with 10% fetal bovine serum (Cytogen, Sinn, Germany) were used according to the USP (Unites States Pharmacopoeia) cytotoxicity test regulations and according to ISO 10993-5. The incubation of both cell lines was performed in a humidified atmosphere with 8% CO_2 at 37 °C. For cell experiments, passages between 10 and 25 were applied.

3.3.7. Cytotoxicity Assays in vitro

3.3.7.1. MTT-Cytotoxicity Assay with Polymers

The toxicity of pDMAEMA-pHEMA diblock copolymers was tested using L929 murine fibroblasts in MTT-assays as previously described, using 2mg/mL MTT (3-(4,5-Dimethylthiazol-2-yl)-2,5-diphenyltetrazoliumbromide)-stock solution [38]. As pure polymers are considered to be more toxic than the polyplexes [12, 35], the harsher conditions were tested by applying the pure polymer dilutions in a concentration range from 0.5 mg/mL to 0.00029 mg/mL to 96-well plates with 8,000 cells per well, seeded 24 h prior to the experiment. As 100% viability control, untreated cells were used. The IC50 values were compared with that of PEI 25k. For each polymer and dilution step, 4 replicates were used. After dissolving the metabolically formed formazane crystals in DMSO, the absorbance was measured using a plate reader (Titertek plus MS 212, ICN, Germany) at wavelengths of 570 and 690 nm. For data evaluation, GraphPadPrism 5.0 (Graph Pad Software, La Jolla, USA) software was used, the x-scale was plotted logarithmically and nonlinear fit with variable slope for data transformation was run to obtain the IC50 values.

3.3.7.2. MTT-Cytotoxicity Assay with pDNA-Polymer Complexes

To directly compare the toxicity of polyplexes to that of polymers only, three pDMAEMA115-derivatives were selected and applied to the cells at N/P 15 for 4 h at transfection conditions (see Section 3.9. Transfection efficiency). After 4 h of incubation, the viability evaluation was performed as described above. Each polymer complex was tested in replicates of four.

3.3.7.3. Toxicity via Protein Assay (Bicinchonic Acid, BCA)

To follow the toxic effect of polymer complexes during the whole transfection period (4 + 44 h), BCA assays were performed according to the manufacturer‘s protocol (Pierce® BCA Assay Kit) parallel to luciferase expression measurements as described below.

3.3.8. Transfection Efficiency

For transfection experiments, 3T3 cells were seeded at a density of 6,000 cells per well in 96-well-plates in 200 µL/well full medium 24 hours prior to transfection. After replacing the old medium with 75 µL of fresh full medium, 25 µL polyplexes per well, containing 0.5 µg DNA, were added to the cells and incubated for 4 h at normal cultivating conditions. The medium was changed 4 hours post transfection to 200 µL fresh medium, and cells were incubated for another 44 hours. After the incubation period, the cells were washed with PBS buffer, lysed with cell culture lysis reagent (CCLR, Promega, Mannheim, Germany) and assayed for luciferase expression with a 10 mM luciferin solution on a LumiSTAR plate reader (BMG Labtech, Offenburg, Germany). In parallel, the lysate samples were analyzed by BCA-Assay according to the manufacturer‘s protocol to determine the protein level. Transfections were performed in replicates of four, and the results are given as mean values +/- SD of relative light units (RLU) normalized to µg protein according to the BCA assay.

3.3.9. Confocal Laser Scanning Microscopy (CLSM)

The intracellular distribution of polyplexes was studied by CLSM as described previously [36] using 3T3 cells and YoYo-1 labeled pDNA-polyplexes of N/P 15. After standard incubation with polyplexes for 4 h, cell fixation and DAPI-staining of cell nuclei followed.

3.3.10. Flow Cytometry

To quantify the intracellular uptake of copolymers transporting pDNA, flow cytometry was employed. 3T3 cells were seeded in 48-well plates at a density of 30,000 cells per well 24 h prior to transfection. For this experiment, polyplexes at N/P 15 were chosen as they were shown to be most effective for transfection and less toxic than polyplexes at N/P 20. To measure pDNA uptake, it was labeled using the intercalating dye YoYo-1 as described previously [36]. In short, polyplex preparation was performed as described for transfection experiments. 3T3 cells were incubated with the polyplexes for 4 h at 37 °C and afterwards washed with PBS. PEI 25k was used as positive control, and as negative control, untreated cells were measured. Trypan blue 0.4% in PBS was used to quench the fluorescence on the cell surface, allowing for measurement of only internalized YoYo-1 fluorescence. After quenching, the cells were washed twice with PBS, trypsinized and fixed with a 1:1 mixture of FACSFlow (BD Biosciences, San Jose, CA) and 4% paraformaldehyde in PBS. The single cell solutions were measured using a FACSCantoII (BD Biosciences, San Jose, CA) with excitation at 488 nm and the emission filter set to a 530/30 bandpass. The gating was adjusted to evaluate 10,000 viable cells for each experiment. The results of three independent experiments were presented as geometric mean fluorescence intensity (MFI) +/- SD. Flow cytometry analysis was performed using FACSDiva™ software (BD Biosciences, San Jose, CA).

3.3.11. Statistics

All analytical tests were conducted in replicates of three or four if not otherwise stated. Results are given as mean values +/- standard deviation (SD). Two-way ANOVA and statistical evaluations were performed using Graph Pad Prism 5.0 (Graph Pad Software, La Jolla, USA) if not stated otherwise.

3.4. RESULTS AND DISCUSSION

3.4.1. Synthesis

3.4.1.1. Synthesis of the Chain Transfer Agent CPT & the Macro Chain Transfer Agent (macroCTA) pDMAEMA

The ^{1}H NMR (nuclear magnetic resonance) spectrum of 4-Cyanopentanoic acid dithiobenzoate (CPT) is displayed in Figure 1(A), for the ^{13}C NMR spectrum, see Supplementary Information Figure S1. Strong agreement with the literature values was found in both cases [23-29]. For this study, four different pDMAEMA homo-polymers designated as pDMAEMA97, pDMAEMA105, pDMAEMA115 and pDMAEMA151 were synthesized. The index denotes the number of repeating units calculated by NMR measurements. For this calculation, the signal of the benzyl group at the end of each polymer strand (7.4–8.1 ppm) was correlated with the signal of the two methylene groups of the side chain (3.5–3.6 + 4.4–4.5 ppm). Shown here are the results from pDMAEMA115 (**1**) while the other homo-polymers behaved similarly. The NMR spectra shown in Figure 1(B) corresponds to that reported in [9]. In the attenuated total reflection (ATR) IR spectra, the two typical ester bands at 1,720 (C=O) and 1,150 (C–O), and the band of the backbone at 2,960 wavenumbers were found.

Figure 1. ^{1}H NMR spectra of (**A**) CPT in $CDCl_3$, (**B**) pDMAEMA in D_2O (**C**) pDMAEMA-*block*-pHEMA in D_2O; the numbers designate the atoms within molecules.

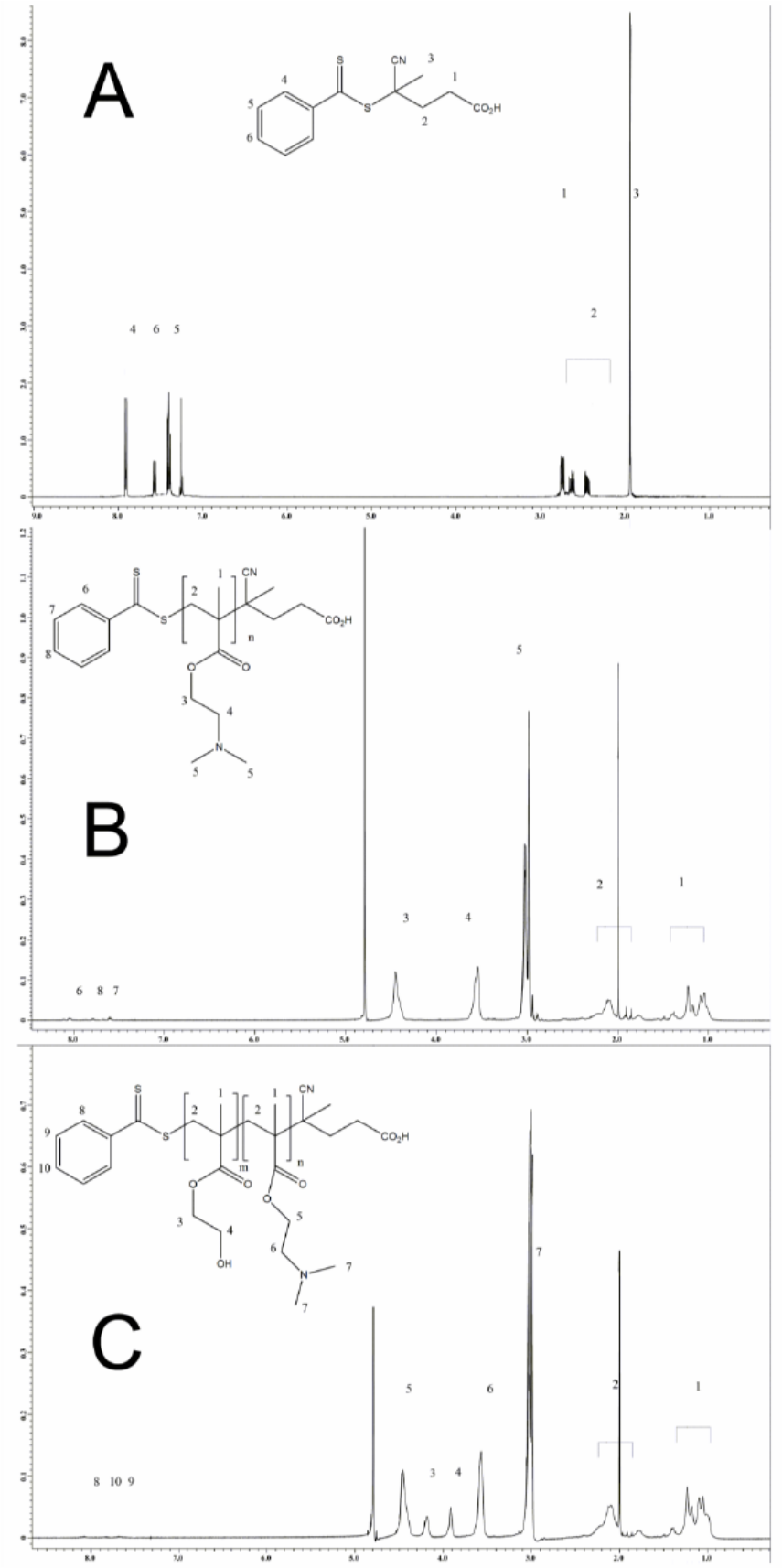

3.4.1.2. Synthesis of pDMAEMA-block-pHEMA Block Copolymers (pDMAEMA-block-pHEMA)

To calculate the number of HEMA repeating units in the polymer, the signal of the known number of methylene groups of the macroCTA was correlated with the signal of the methylene groups of HEMA (3.9–4.1 + 4.2–4.3 ppm). This was possible because the signals of the different parts do not overlap as displayed in Figure 1(C). Additionally, in the ATR IR spectra of the copolymers, the typical band for the hydroxyl group of pHEMA at 3,390 cm^{-1} was found. The ester band at 1,720 and 1,150 cm^{-1} belong to both blocks of the copolymer. The T_g of pDMAEMA [19] (-6 °C) and pHEMA [21] (~70 °C) are known from the literature and decreased, as expected, to lower temperatures for the copolymers with increasing pDMAEMA part. The different block copolymers are shown in Table 1. For illustration of the synthesis of diblock copolymers, see Scheme 1.

Table 1. Molecular weight and nomenclature of synthesized pDMAEMA and pDMAEMA-*block*-pHEMA copolymers, calculated from NMR and GPC.

Name	Polymer	M (NMR) (kDa)	Mn (kDa)	Mw (kDa)	Mw/Mn
1	$pDMAEMA_{115}$	18.3	36.3	39.0	1.08
2	$pDMAEMA_{97}$-*b*-$pHEMA_{11}$	17.0	43.9	45.5	1.04
3	$pDMAEMA_{97}$-*b*-$pHEMA_{24}$	18.5	38.4	40.0	1.04
4	$pDMAEMA_{105}$-*b*-$pHEMA_{24}$	19.9	31.2	31.5	1.01
5	$pDMAEMA_{115}$-*b*-$pHEMA_{6}$	19.1	31.7	32.4	1.02
6	$pDMAEMA_{115}$-*b*-$pHEMA_{57}$	25.7	25.9	26.5	1.02
7	$pDMAEMA_{151}$-*b*-$pHEMA_{91}$	35.7	33.3	34.4	1.03
8	r-pDMAEMA-pHEMA 1.3-1	29.0	26.6	27.4	1.03
9	r-pDMAEMA-pHEMA 4.3-1	29.0	22.4	26.9	1.20

Scheme 1. Synthesis of pDMAEMA-*block*-pHEMA.

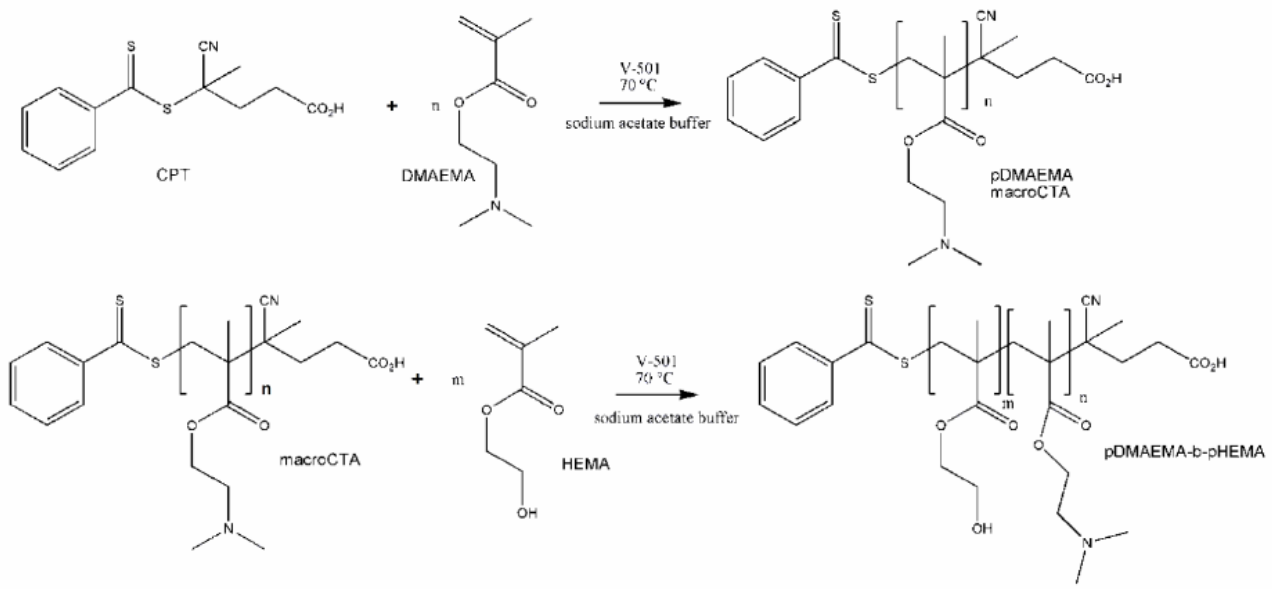

3.4.1.3. Synthesis of pDMAEMA-pHEMA Random Copolymers (r-pDMAEMA-pHEMA)

The synthesis of the random polymers was achieved by simply mixing the monomers before starting the reaction. The weights were calculated as described for the macro CTA by correlating the signal of the benzyl group with the signal of the side chains of the different monomers. Here, the different ratios between the two monomers in the polymer were also calculated. The NMR spectra and the ATR spectra were comparable to the ones of the block copolymers, as expected. The ratio of the monomers is denoted by the last number in the abbreviated term of the polymers as shown in Table 1.

3.4.2. GPC (Gel Permeation Chromatography) Results of the Polymers

Comparing the values in Table 1, there was a discrepancy between the molecular weight calculated by NMR and those values determined by GPC. Since the results for molecular weight depend on the way of calculation, a discrepancy between NMR and GPC was expected for the copolymers with molecular weights of more than 20 kDa. However, the large

differences for the polymers below 20 kDa containing a small amount of pHEMA were unexpected. The calculated refractive index was possibly not correct as these copolymers may interact with the column material leading to incomplete elution. All the polymers showed a PDI around 1, as expected for RAFT polymerization.

3.4.3. Nomenclature of the Synthesized pDMAEMA-block-pHEMA Copolymers

A library of copolymers containing different amounts of DMAEMA (2-(dimethyl amino)ethyl methacrylate and HEMA (2-hydroxyethyl methacrylate) repeating units was synthesized. The polymers were designated and classified as shown in Figure 2 (A, B).

Figure 2. A, B The library of diblock copolymers sorted according to an increasing amount of pDMAEMA (**A**). The proportion and weight of each block-part in the various pDMAEMA-pHEMA copolymers were calculated according to the repeating units (**B**).

A

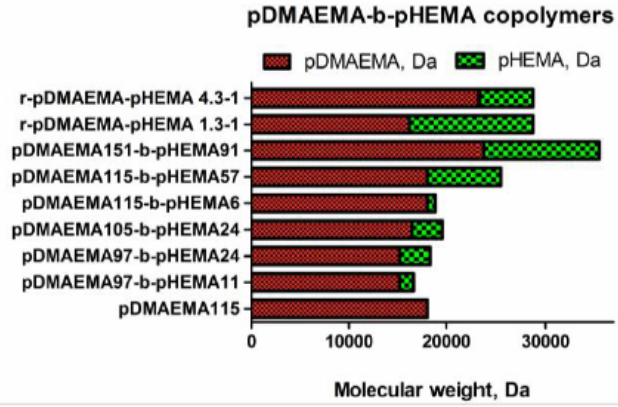

B

Copolymer compositon	Mw of pDMAEMA in copolymer	Mw of pHEMA in copolymer	Total of pDMAEMA in copolymer related to pDMAEMA115	Total pDMAEMA to pHEMA
repeating units, fraction	kDa	kDa	%	w/w
pDMAEMA115	18.3	0	100	1/0
pDMAEMA97-b-pHEMA11	15.3	1.4	84	10.6/1
pDMAEMA97-b-pHEMA24	15.3	3.1	84	4.9/1
pDMAEMA105-b-pHEMA24	16.5	3.1	91	5.3/1
pDMAEMA115-b-pHEMA6	18.3	0.8	100	23.1/1
pDMAMEMA115-b-pHEMA57	18.3	7.4	100	2.4/1
pDMAEMA151-b-pHEMA91	23.7	11.8	131	2/1
random pDMAEMA:pHEMA 1.3:1	16.2	12.5	90	1.3/1
random pDMAEMA:pHEMA 4.3:1	23.3	5.4	129	4.3/1

The synthesized polymers can be divided into three groups: homo-pDMAEMA, linear diblock pDMAEMA-*block*-pHEMA copolymers, and random copolymers with alternating sequence of pDMAEMA and pHEMA. The hypothesis for this work was that there would be a lower limit of the homo pDMAEMA chain length for effective transfection, and that the lack of transfection efficacy could be compensated for by grafting linear pHEMA. A pre-test with a panel of homo-polymers with subsequently decreasing pDMAEMA chain length was performed in form of *in vitro* transfections to point out the limit of transfection capacity of short chain polycations. Together with cytotoxicity data, the results from the transfection pre-test of homo-pDMAEMA 15–290 kDa are presented in Figure S2, Supplementary Information. It was found that a pDMAEMA95 homopolymer of 15 kDa possessing 95 repeating units was ineffective in gene delivery, whereas pDMAEMA406 with 64 kDa efficiently mediated transgene expression. These findings are in line with earlier studies, reporting that a 43 kDa homo-pDMAEMA [9] mediated no significant luciferase expression at N/P 8–20, but that the efficacy as vector could be increased at molecular weights above 112 kDa. Accordingly, in the present study it was found that the pDMAEMA115 homo-polymer of 18.3 kDa was inefficient and therefore chosen as low molecular weight – silent reference vector. The copolymers pDMAEMA115-*block*-pHEMA57 & pDMAEMA115-*block*-pHEMA6 synthesized here contain the same polycationic part, but have increased molecular weights of 25.7 and 19.1 kDa, respectively, due to pHEMA grafting. Moreover, longer and shorter pDMAEMA chains were incorporated into other diblock construct to investigate the effect of pDMAEMA-*block*-pHEMA composition on DNA-complexation, charge, stability, toxicity, transfection efficacy and cellular uptake. The random pDMAEMA-pHEMA copolymers with larger and smaller polycationic parts were also included in the polymer library for investigations of structure function relationships (r-pDMAEMA-pHEMA 4.3–1 and r-pDMAEMA-pHEMA 1.3–1). The created copolymer library allowed for evaluation of the impact

of the pDMAEMA/pHEMA proportion as well as the percentage of the polycationic part in relation to homo-pDMAEMA$_{115}$ concerning vector efficacy *in vitro*.

3.4.4. DNA Complexation Efficiency

3.4.4.1. Agarose Gel Electrophoresis

According to the gel electrophoresis performed with diblock and random pDMAEMA-pHEMA copolymers (Figure 3 (A–D)), the N/P ratio of 2 was sufficient for complexing and immobilizing pDNA in case of all tested polymers. The N/P ratios of 10, 15 and 20 used for transfection experiments showed complete retardation of pDNA (data not shown). No differences were observed concerning the complexation efficiency of homo pDMAEMA115 compared to its diblock derivatives with 6 and 57 pHEMA units, and compared to pDMAEMA105-*block*-pHEMA24. Copolymer pDMAEMA151-*block*-pHEMA91 performed similarly as pDMAEMA115, but showed more complete retardation at N/P 1. Copolymer pDMAEMA97-*block*-pHEMA11 performed similarly to pDMAEMA151-*block*-pHEMA91. Yet, the random copolymers and pDMAEMA97-*block*-pHEMA24 were able to retard DNA at N/P 1 already, outreaching PEI 25k in its complexation properties. Based on the obtained gel electrophoresis data, all tested low molecular pDMAEMA-pHEMA constructs showed good pDNA-complexation even at low N/P ratios. The marginal differences of DNA-retardation at N/P 1 may be evidence of the impact of the polymer structure on interactions with pDNA. One of these slight differences can be seen in Figure 3(C), where pDMAEMA97-*block*-pHEMA24 shows a better complexation of DNA than pDMAEMA97-*block*-pHEMA11 at N/P ratio 1. The efficient complexation ability of the 15.3 kDa polycationic part of diblock copolymer pDMAEMA97-pHEMA24 was unexpected, as a 11.1 kDa homo-pDMAEMA was reported by Jiang *et al.* to be a poor complexer [15].

Figure 3. A, **B**, **C**, **D**. Electrophoretic mobility of free and complexed DNA in agarose gel (Each row starts with free DNA and is continued by N/P 0.5, 1, 2 complexes with the indicated polymers. Polymers are separated by white vertical lines).

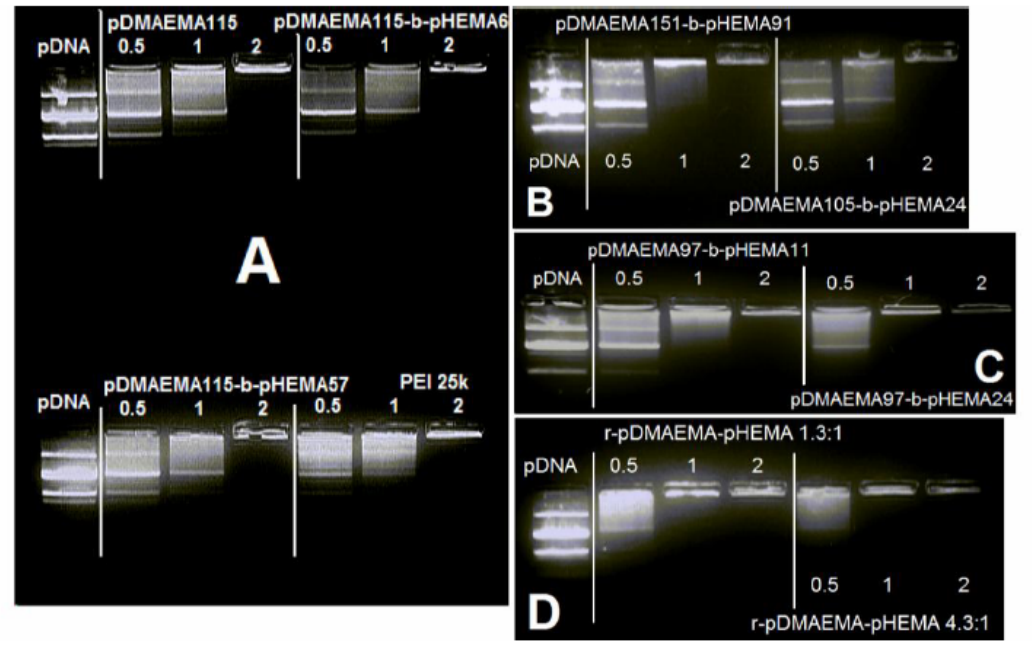

3.4.4.2. Heparin Assay — Stability against Competing Polyanions

The trend observed in gel retardation experiments using polyplexes of lower N/P ratios corresponded well with the heparin competition assay of polyplexes at N/P 15 (Figure 4(A–D)). The copolymers with the same cationic block length of 115 units released DNA upon addition of the same heparin amount of 0.46 international units (IU). The copolymers pDMAEMA151-*block*-pHEMA91, pDMAEMA105-*block*-pHEMA24 as well as pDMAEMA115-derivatives appeared to be more resistant to competition with heparin than PEI 25k at 0.46 IU heparin, whereas pDMAEMA151-*block*-pHEMA91 had a less pronounced fluorescent band in lane 4 (0.46 IU). The random copolymers and pDMAEMA97-*block*-pHEMA11 were even more resistant to the presence of heparin releasing DNA only at higher concentrations of 0.93 IU. The highest resistance to competitive polyanions was observed in case of pDMAEMA97-*block*-pHEMA24, where 1.87 IU of heparin was needed to release DNA from the complex. Taken together, the most stable complexes were obtained using

random copolymers and short chain diblock copolymers with only 97 pDMAEMA units. This may be due to a better interaction of copolymers with DNA thus providing a tighter polyplex structure. All tested copolymer complexes released DNA at heparin concentrations higher than the ones needed for destabilization of PEI 25k polyplexes. This fact can be interpreted as an advantage for protecting genetic material, but as well as a disadvantage, as far as DNA release is concerned at the site of action. Accordingly, decreased DNA release may cause reduced transfection efficiency of the most stable complexes.

Figure 4. A, B, C, D. Heparin assay: displacement of DNA from polyplexes with polyanion on agarose gel.

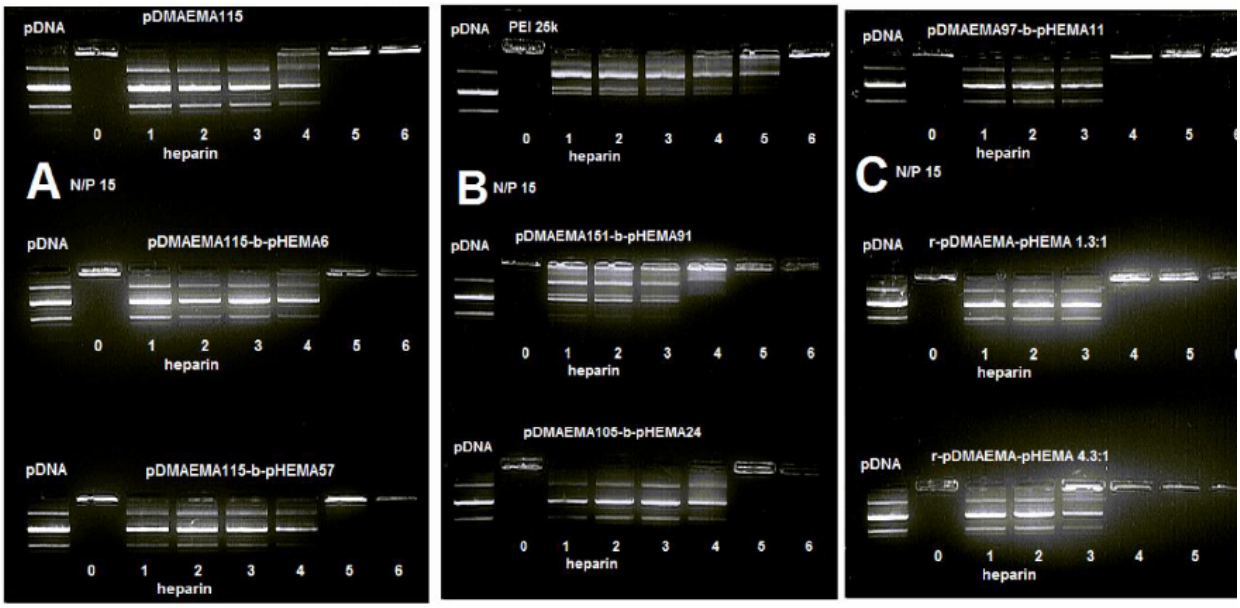

Heparin dilution range in glucose 5%

Conc.No.	IU/polyplex
0	0
1	3.75
2	1.87
3	0.93
4	0.46
5	0.23
6	0.11

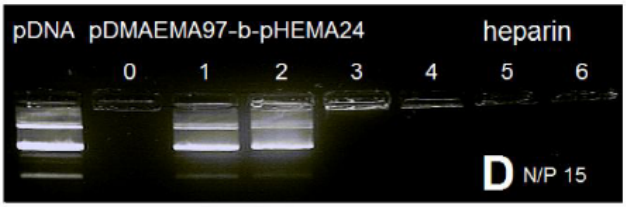

3.4.5. Size and Zeta Potential

3.4.5.1. Size and Zeta Potential of Polyplexes in Isotonic Glucose

Isotonic glucose solution was used to formulate polyplexes with pDNA. For complete self-assembly of polyplexes, a 20 min incubation time was maintained after mixing. In measurements after shorter or no incubation, higher polydispersity indices and larger complex sizes were obtained (data not shown). PEI 25k yielded DNA-polyplexes in the size range <100 nm at all N/P ratios. At N/P ratios of 10, 15 and 20, the polyplex sizes of pDMAEMA-*block*-pHEMA diblock copolymers did not show statistically significant differences in hydrodynamic diameters compared to each other. All polymers were able to complex pDNA into polyplexes with hydrodynamic diameters of 100–170 nm. This is considered a size range suitable for cellular uptake [31, 32]. Larger polyplexes were formed only in case of pDMAEMA105-*block*-pHEMA24 at N/P ratio 10, which may be due to complexation irregularities reflected in the broad standard deviation (Figure 5 (A)). The hydrodynamic diameter of naked plasmid was earlier reported to be in the range of 300–400 nm [12].

The zeta potentials of polyplexes from diblock copolymers ranged from 10 to 30 mV depending on the N/P ratio (Figure 5 (B)). A significant increase of the zeta potential at N/P 20 was only registered for pDMAEMA105-*block*-pHEMA24 and r-pDMAEMA-pHEMA 1.3:1. In general, no reduction in positive charge density could be observed for pHEMA-grafted copolymers in comparison to homo-pDMAEMA, suggesting that the pHEMA chains may not be localized on the polyplex surface but closer to the core of pDMAEMA and pDNA. The polyplex size also remained in the range of homo-pDMAEMA complexes with no obvious disturbance of complexation caused by grafting of pHEMA. Additionally, Figure 6 (A, B) demonstrates similar trends in polyplex size and zeta potential concerning pDMAEMA115-derivatives.

Figure 5. A, B. Polyplex sizes and zeta potentials of all synthesized polymers in isotonic glucose. Significant differences in size and zeta potential comparing N/P 15 *versus* all other N/P 10 and 20 of one polymer according to two-way ANOVA are labeled (***$p < 0.001$, **$p < 0.005$ and *$p < 0.01$).

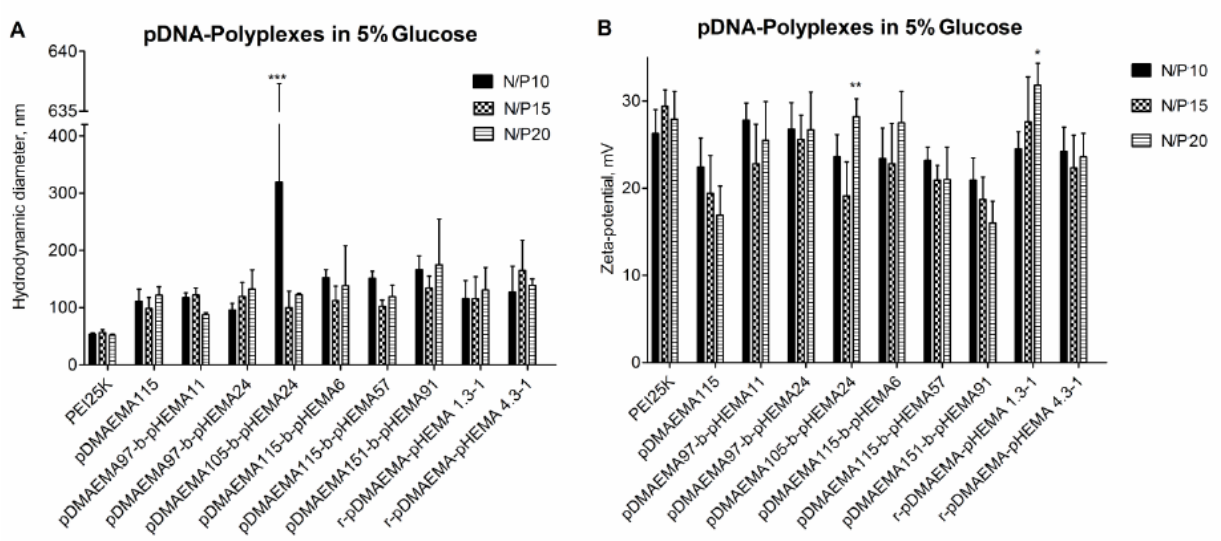

Figure 6. A, B. Polyplex sizes and zeta potential of $pDMAEMA_{115}$ derivatives in isotonic glucose.

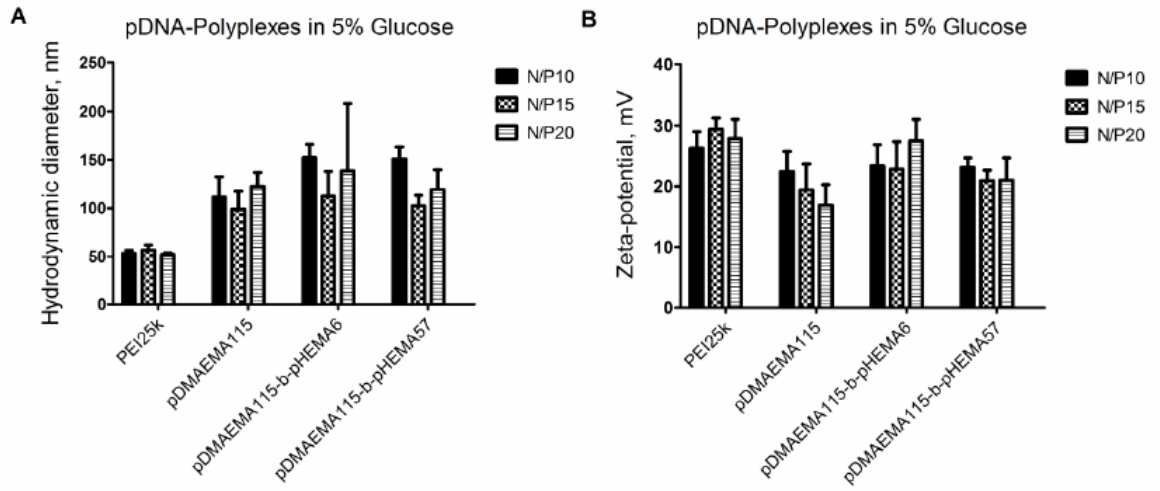

3.4.5.2. Polyplex Aggregation Behavior in Isotonic Salt and Glucose Solution over Time

According to the measurements of hydrodynamic diameters of polyplexes incubated in isotonic glucose and NaCl solution, similar trends were observed for pDMAEMA115 and pDMAEMA115-*block*-pHEMA57. In glucose, both polymer types showed good stability of their polyplexes with pDNA (Figure 7). In high ionic strength solution, on the contrary,

significant polyplex aggregation could be observed and larger sized constructs appeared over time. From the aggregation experiment it may be expected that both types of polymers behaved similarly in cell experiments, as polyplexes of both types aggregated rapidly in the presence of high ionic strength medium. However, the Hennink group previously reported that the transfection efficiency of pDMAEMA polyplexes was not decreased in spite of an observed increase in size in the presence of serum [10, 12].

Figure 7. Polyplex behavior of homo- and diblock-copolymers in isotonic glucose and NaCl as a function of incubation time.

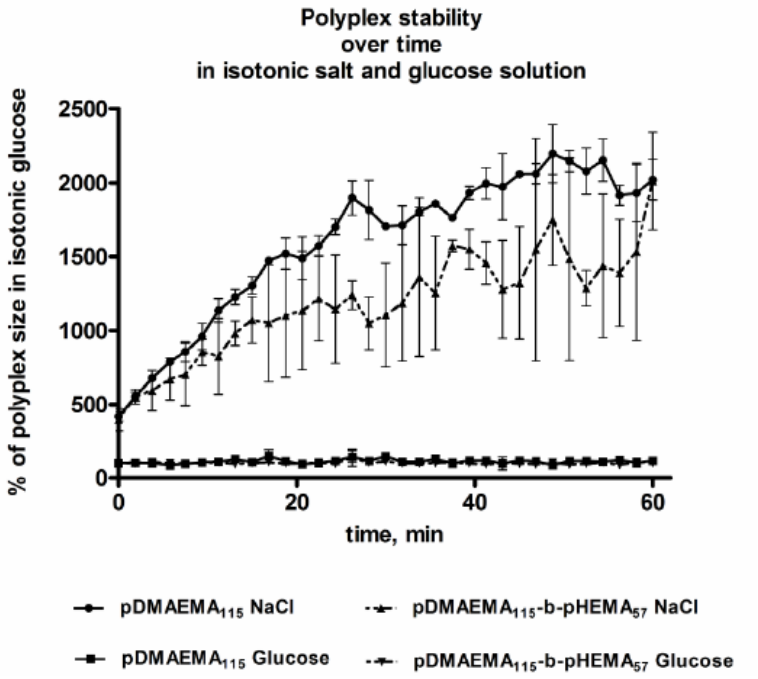

3.4.6. Cytotoxicity of Polymers and Polyplexes in vitro (MTT, BCA)

Cytotoxicity data obtained with MTT assays in L929 mouse fibroblasts indicated a better biocompatibility of pDMAEMA-pHEMA diblock copolymers with IC50 values 1.4–9.7 times higher than that of PEI 25k, depending on the polymer structure (Figure 8 (A,B)). Comparing the IC50-values of the homo-polymers within the library synthesized here, the 18.3 kDa homo-pDMAEMA was nearly five times less toxic (IC50 = 0.043 mg/mL) than 290 kDa

pDMAEMA (IC50 = 0.009 mg/mL) (Figure S2, Supplementary Information). These results were not unexpected as it has been described earlier that the toxicity of homo pDMAEMAs is a function of the molecular weight of the polycation [10]. Cherng *et al.* [12] reported an IC50-value of 0.03 mg/mL determined in XTT-assays for a pDMAEMA homo-polymer of Mw/Mn of 36 × 104/45 × 103 Da in COS-7 cells. Due to the very broad polydispersity (Mw/Mn) of the polymer, however, it cannot easily be compared with the RAFT polymers reported here which all feature PDI values below 1.20 (Table 1). Copolymer pDMAEMA105-*block*-pHEMA24 was 9.7-fold less toxic (***$p < 0.001$), and pDMAEMA115-*block*-pHEMA57 was 7.9-fold less toxic (**$p < 0.01$) than PEI 25k. The lowest IC50 values were obtained with r-pDMAEMA-pHEMA 4.3–1 being only 1.4 times less toxic than PEI 25k. The differences in toxicity between the different diblock-copolymers and homo-pDMAEMA solutions in the Mw range of 17–35.7 kDa (exposure for 24 h, Figure 8 (A,B)), and between complexes with pDNA and solutions of pure pDMAEMA115 homo- or co-polymers (exposure for 4 h, Figure 9) were found to be not significant. The polymers pDMAEMA97-*block*-pHEMA11 and r-pDMAEMA-pHEMA 1.3–1 showed some irregularities in biocompatibility with mouse fibroblasts, resulting in very broad toxicity ranges. These irregularities could possibly be caused by residual impurities from the synthesis (see – Materials and Methods Section 3.4.2. for more details). To further investigate toxicity issues, the protein analysis (BCA assay) following transfection experiments was conferred (see Figure 10). In this assay, a clear trend of decreasing protein values related to blank could be observed towards higher N/P ratios, correlating well with earlier described results [9, 10]. As reported previously, cell membrane destabilization may be one of the reasons for cytotoxicity [9, 10] and is connected with the charge density. The homopolymer pDMAEMA, however, has a lower charge density than PEI 25k. Additionally, grafting of uncharged pHEMA may contribute to the deviation from a linear trend of pDMAEMA-toxicity as a function of the chain length. The toxicity of random copolymers r-pDMAEMA-pHEMA 4.3–1 which was notably higher than that of diblock

copolymers as observed in both MTT and BCA, correlated well with higher polycation content. Surprisingly, no significant differences were found concerning toxicity between pDMAEMA115-derivatives applied as polyplexes or pure polymers of the same concentration (Figure 9). However, Cherng *et al.* also observed only a partial – neutralizing effect of polymer toxicity by plasmid for homo-pDMAEMA of Mw/Mn of 36 × 104/45 × 103 Da in COS-7 cells [12]. PEI 25k was much more toxic as pure polymer than its pDNA complexes (Figure 9), which is in line with earlier reports describing – charge neutralization in polyplexes being able to decrease the toxicity of PEI [33].

The mechanism of interaction of diblock- and random-copolymers with cellular membranes as well as further optimization of the HEMA block-length for better biocompatibility is currently under investigation.

Figure 8. A, **B**. Cytotoxic effects of copolymers in L929 mouse fibroblasts after incubation for 24 h, ***p < 0.001 & **p < 0.01 according to two-way ANOVA.

A

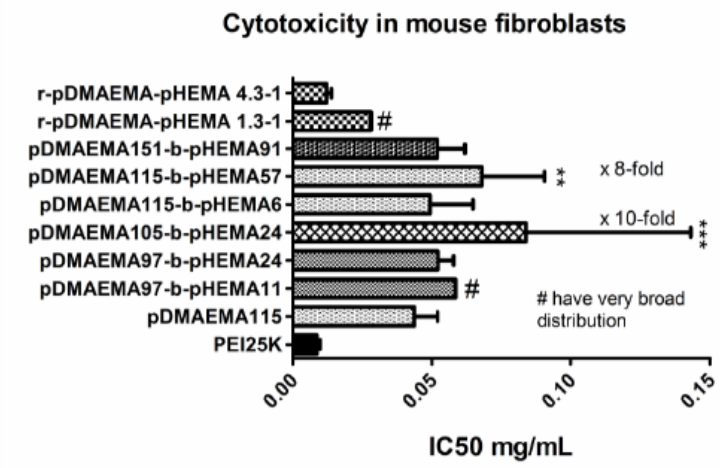

B

Polymers	IC50 mg/mL
PEI 25K	0.009
pDMAEMA115	0.044
pDMAEMA97-b-pHEMA11	~0.059
pDMAEMA97-b-pHEMA24	0.052
pDMAEMA105-b-pHEMA24	0.084
pDMAEMA115-b-pHEMA6	0.049
pDMAEMA115-b-pHEMA57	0.068
pDMAEMA151-b-pHEMA91	0.052
r-pDMAEMA-pHEMA 1.3-1	~0.028
r-pDMAEMA-pHEMA 4.3-1	0.012

Figure 9. Cytotoxicity (MTT) of pDNA-polymer complexes, N/P 15 in L929, exposed for 4 h.

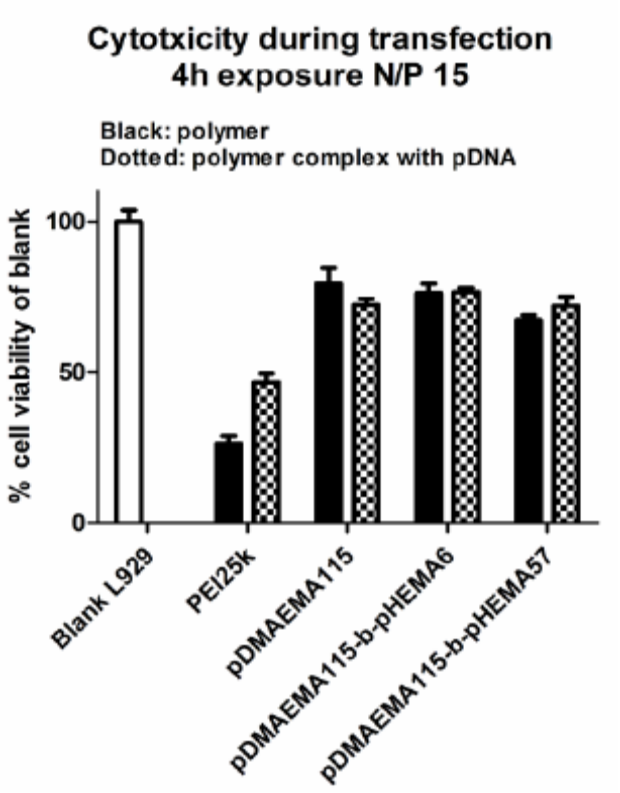

Figure 10. Protein data (BCA assay) from transfection experiments.

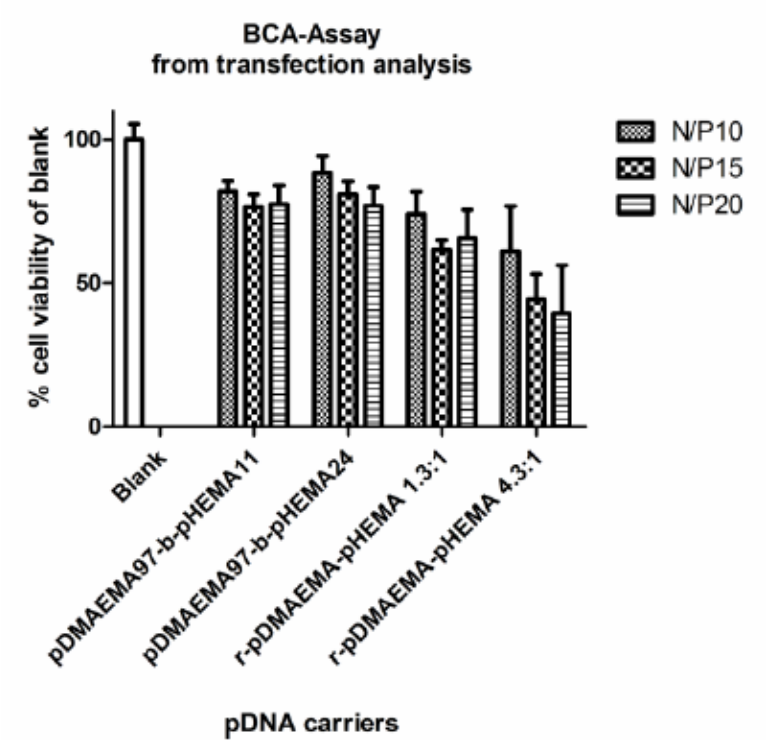

3.4.7. Transfection

Based on the results of the physico-chemical characterization of pDMAEMA-pHEMA polyplexes concerning polyplex size distribution, zeta potential and complexation efficiency, none of the polymers from the tested panel could be excluded as candidate for transfection. However, the *in vitro* transfection experiments using pDNA encoding for luciferase in comparison to PEI 25k as standard presented a different picture. The obtained relative light units (RLU) related to µg protein were statistically evaluated using two-way ANOVA comparing them to blanks. Free DNA did not mediate significant luciferase expression compared to untreated cells (data not shown). Therefore, in further experiments, untreated cells were used as blanks. The p-values are indicated on the bar heads with stars **(****p < 0.05; **p < 0.01;***p < 0.001*). At N/P 10, only one efficient candidate (pDMAEMA151-*block*-pHEMA91) that caused significantly higher transgene expression than naked DNA was observed apart from PEI 25k (see Figure 11). At higher N/P ratios two additional candidates were identified mediating significant transgene expression (pDMAEMA115-*block*-pHEMA57, pDMAEMA115-*block*-pHEMA6). As expected from previous reports, where 43 kDa pDMAEMA was not successful in transfection [9], the homopolymer pDMAEMA consisting of 115 repeating units (18.3 kDa) was found to be an ineffective transfection agent at all tested N/P ratios. On the other hand, its derivatives pDMAEMA115-*block*-pHEMA57 and pDMAEMA115-*block*-pHEMA6 with Mw of 25.7 and 19.1 kDa, respectively, provided transfection efficiency at higher N/P ratios, whereas Jiang *et al.* only achieved moderate transfection results with brushed pDMAEMA-pHEMA copolymers far above 75 kDa at N/P 6 [15]. The diblock copolymers with slightly higher pDMAEMA content (151 units, total Mw of 35.7) were able to mediate transfection already at N/P 10. The random copolymer r-pDMAEMA-pHEMA 1.3–1 (29.0 kDa) yielded no statistically significant luciferase expression over the whole N/P-range tested. Thus, it can be assumed that one of the factors essential for transfection is the number of charged repeating units incorporated within the

diblock copolymer, as a clear trend of increasing transfection efficacy towards higher homo-pDMAEMA molecular weights was already observed earlier [9, 10]. The candidates possessing only 105 or even 97 pDMAEMA repeating units in a pDMAEMA-pHEMA diblock were ineffective, probably due to the lack of positive charge needed to perform transfection. This data strongly agree with the pre-test transfection experiment where homo- and diblock copolymers with 95 and 110 units pDMAEMA were tested and showed RLU values only at blank level (diblock copolymers data not shown, for homopolymers see Figure S2 Supplementary Information).

The unexpected observation that low molecular weight pDMEMA achieves transfection efficiency only after conjugation with pHEMA in a block structure points to the fact that interaction with cells is affected by this arrangement. It was reported that pHEMA possesses good tissue affinity [19] and may therefore have additional – fusogenic interactions with cellular membranes enhancing the uptake of polyplexes. The candidates, pDMAEMA151-*block*-pHEMA91 and pDMAEMA115-*block*-pHEMA57, being successful in transfection carry rather long pHEMA blocks. The w/w proportion of pDMAEMA:pHEMA blocks for pDMAEMA151-*block*-pHEMA91 was 1.7:1 and for pDMAEMA115-*block*-pHEMA57 2:1, suggesting that a two-fold excess of the polycationic part is favorable for transfection. In case of pDMAEMA115-*block*-pHEMA6, the proportion was 19:1 and for r-pDMAEMA-pHEMA 4.3–1 4.3:1, leading to effective transfection only at one N/P ratio (N/P 20 and 15, respectively). Taken together, the most promising copolymers were found to contain at least 18.5 kDa of the polycationic part grafted to pHEMA in a pDMAEMA:pHEMA proportion of 2 to 1. The efficacy of random copolymers was observed to grow with increasing poylcationic part. The favorable impact of pHEMA on transfection efficacy is being further investigated.

Figure 11. Transfection efficacy of copolymers in 3T3 mouse fibroblasts, significant differences to blank (*$p < 0.05$; **$p < 0.01$; ***$p < 0.001$).

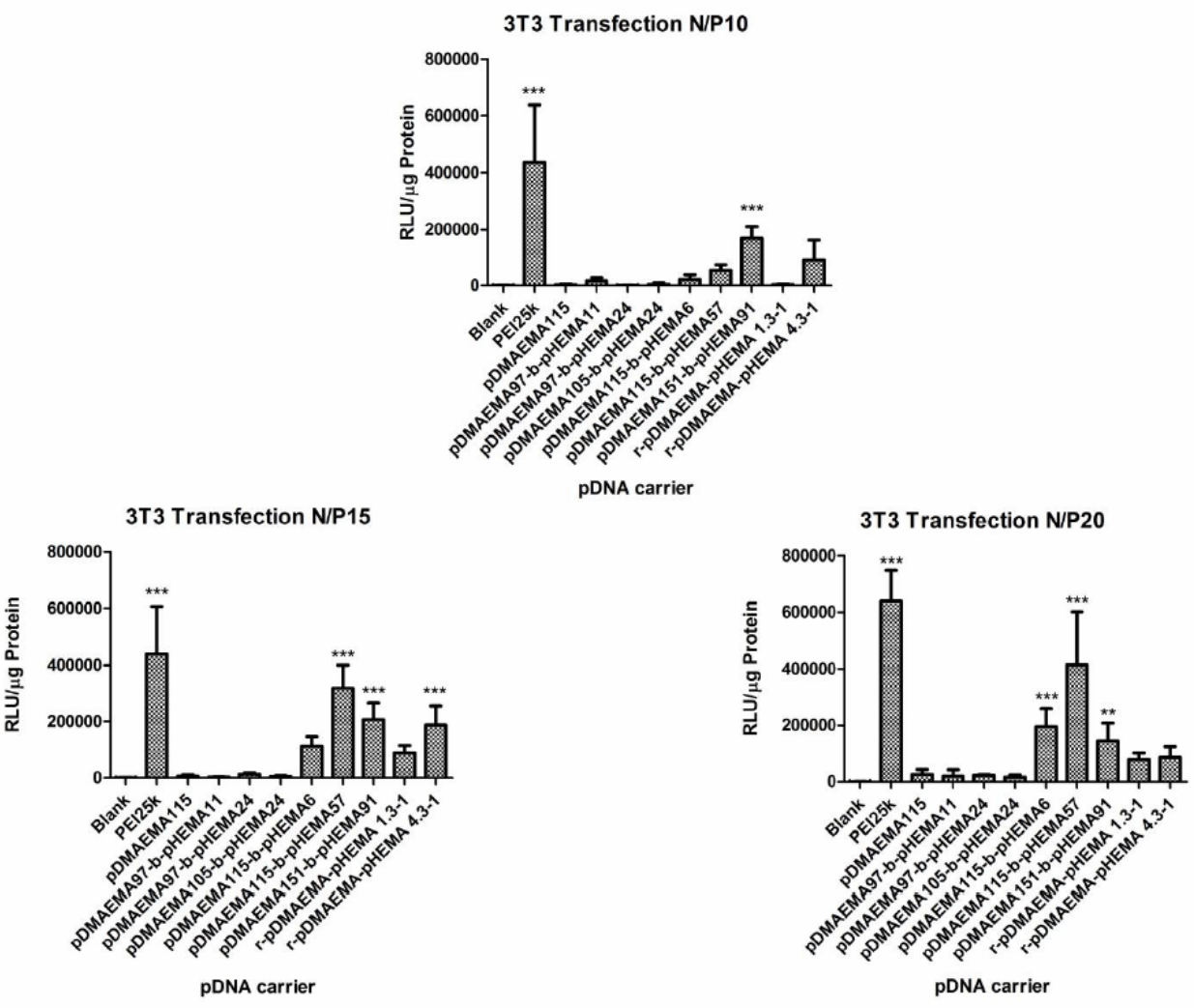

3.4.8. Uptake Efficiency

To gain a more detailed insight into the cell uptake of polyplexes from diblock copolymers, uptake efficiency was tested with fluorescently-labeled DNA in the same cell line as used for transfection at an N/P ratio of 15 (Figure 12). The geometric mean fluorescence intensity values (MFI) obtained in flow cytometry experiments were found to be in agreement with the transfection results. Layman *et al.* observed no influence of pDMAEMA length on cellular uptake in the molecular weight range from 43 to 915 kDa [9]. In this study, however, all

pDMAEMA-pHEMAs successfully transfecting 3T3 cells were taken up to a higher degree than the “silent” ones, suggesting that uptake is a critical step for these polyplexes. The structural analysis implies a favorable effect of pHEMA on cell affinity correlating well with previously reported findings [19], since the pDMAEMA$_{115}$-derivative with a longer pHEMA-graft was taken up to a higher extent than the one with only 6 pHEMA units. Additionally, pDMAEMA$_{151}$-*block*-pHEMA$_{57}$ was also effectively taken up. PEI 25k showed a lower MFI due to its higher toxicity and thus higher percentage of dead cells not gated in the experiment. The same could be speculated regarding r-pDMAEMA-pHEMA 4.3:1.

Figure 12. Cellular uptake of copolymer DNA-complexes with fluorescently labeled DNA, significance of *p < 0.05 and **p < 0.01 compared to PEI 25k according to the two-way ANOVA.

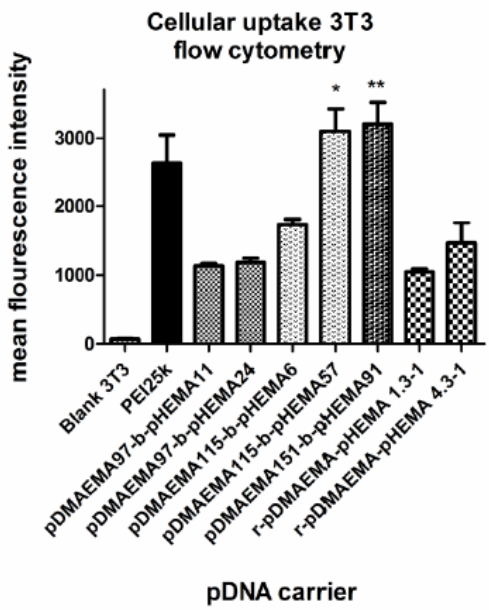

3.4.9. Subcellular Distribution (CLSM, Confocal Laser Scanning Microscopy)

After internalization of polyplexes, the intracellular distribution is of importance. Confocal microscopy was performed to characterize the intracellular polyplex distribution 4 h post exposure to the cells. YoYo-1 labeled pDNA is displayed in green, and DAPI stained nuclei

appear blue, the cell membranes are visualized with transmitted light. The images of all three channels are superimposed.

For this study, polyplexes of diblock copolymers with the most prominent transfection efficiency were depicted at an N/P ratio of 15. In all cases the green fluorescence was clearly observed in the perinuclear area, inside the nucleus as well as diffusely in the cytoplasm. This confirms an effective uptake within the period of 4 hours. Since microscopy does not allow for quantitative analysis, only representative images of transfected cells are shown in Figure 13. Cells treated with PEI-pDNA complexes appeared to be less intensively fluorescent. This may be related to the higher toxicity of PEI 25k at N/P 15 or to the fact that there was less fluorescently labeled DNA in the cytosol, but the DNA was translocated to the nucleus. Especially in cells treated with polyplexes of copolymers, broadly disseminated fluorescence as well as dot-formed green was present. This reflects the presence of polyplexes captured in endosomes as well as pDNA released into cytoplasm. Presence of fluorescence in the perinuclear area and inside the nucleus is a good predisposition for effective transfection. Layman *et al.* showed successful cellular uptake of polyplexes made of pDMAEMA 915 kDa as early as 30 min after application [9]. However, at that time point, only dotted increments were found, indicating endosomal capture of the polyplexes.

Figure 13. Confocal pictures of blank cells (**A**), PEI 25k (**B**), $pDMAEMA_1$ $pHEMA_{57}$ (**C**), $pDMAEMA_{151}$-*block*-$pHEMA_{91}$ (**D**) transfected cells. Green: labeled pDNA, blue—DAPI stained nuclei.

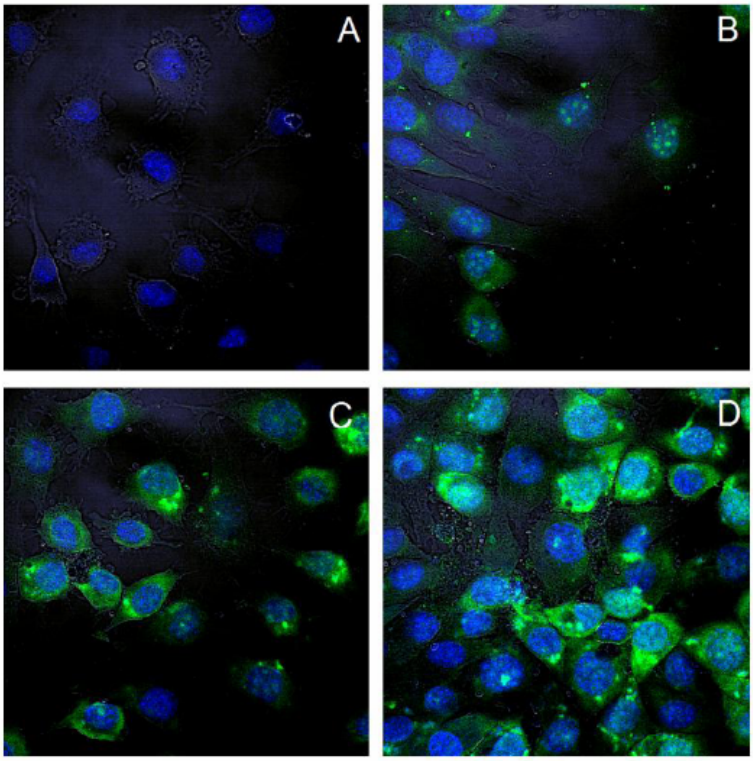

3.5. CONCLUSIONS

It was shown in this study that the *in vitro* transfection ability of low molecular weight pDMAEMA ę18.3 kDa could be improved by grafting low molecular weight pHEMA. The high molecular weight homo-polymers were established as effective pDNA vectors by the Hennink group [10, 12], with the lower limit for efficient homo-polymers being 43 kDa as reported by Layman *et al.* [9]. In agreement with these findings, no transfection for 18.3 kDa homo-pDMAEMA at N/P ratios up to 20 was observed in the experiments described here. Accordingly, this polymer was used as – negative control, whereas its transfection efficiency was succesfully improved by grafting pHEMA. Efficient transfection could be achieved with homo-pDMAEMA of 64 kDa (see Supplementary Information Figure S2). The central idea of

this project was on the one hand to create non-viral vectors with molecular weight below the kidney elimination limit suitable for excretion without previous degradation, and on the other hand decreasing the vector‘s toxicity by reducing the molecular weight of the polycationic part. This approach of improving biocompatibility was successfully performed by Jiang *et al.* [15], using a pHEMA backbone grafted with cleavable short pDMAEMA-chains, resulting in vectors of molecular weight over 75 kDa. In this present study, the molecular weight of efficient copolymers was successfully decreased to 30–35 kDa. The diblock pDMAEMA-*block*-pHEMA bearing only 115 pDMAEMA repeating units became an active transfectant after grafting with pHEMA to the total molecular weight of 19 kDa. The diblock copolymers bearing less than 115 polycation units could not be improved in transfection efficacy despite of pHEMA-grafting. Based only on physicochemical characteristics of the polyplexes (size, zeta potential, and complexation ability), no discrimination between “active” and “inactive” copolymers for DNA transfection could be made, all tested copolymers were potentially appropriate for gene delivery, possessing favorable complexation, cellular uptake and DNA-packaging. Only in transfection experiments, the potential as gene vectors could be discriminated. The cellular uptake and intracellular distribution strongly agree with transfection data, underlining the importance of the – charge and – total Mw balance. The pHEMA-grafting implies to be favorable for polyplexes in terms of cellular interaction and uptake. The toxicity of the homo-polymers was in good correlation with the pDMAEMA block length and thus with charge density. Concluding, the low molecular weight linear diblock pDMAEMA-*block*-pHEMA constructs starting from 19 kDa and possessing at least 18 kDa pDMAEMA, are promising candidates for further investigations in the field of gene delivery. Ongoing studies on *in vivo* transfection experiments, mechanistic aspects of complexation, and kinetic inside the cell are currently under investigation. For cell-type specific transfection, coupling of targeting ligands is being discussed.

3.6. ACKNOWLEDGEMENTS

We are grateful to Eva Mohr (Department of Pharmaceutics and Biopharmacy) for technical support in cell culture work and Tanja Dicke for operating FACS-measurements.

3.7. SUPPLEMENTARY MATERIALS

Figure S1. ^{13}C NMR spectra of (**A**) CPT in $CDCl_3$, (**B**) pDMAEMA in $CDCl_3$ and (**C**) pDMAEMA-b-pHEMA in D_2O; the numbers designate the atoms within the molecules.

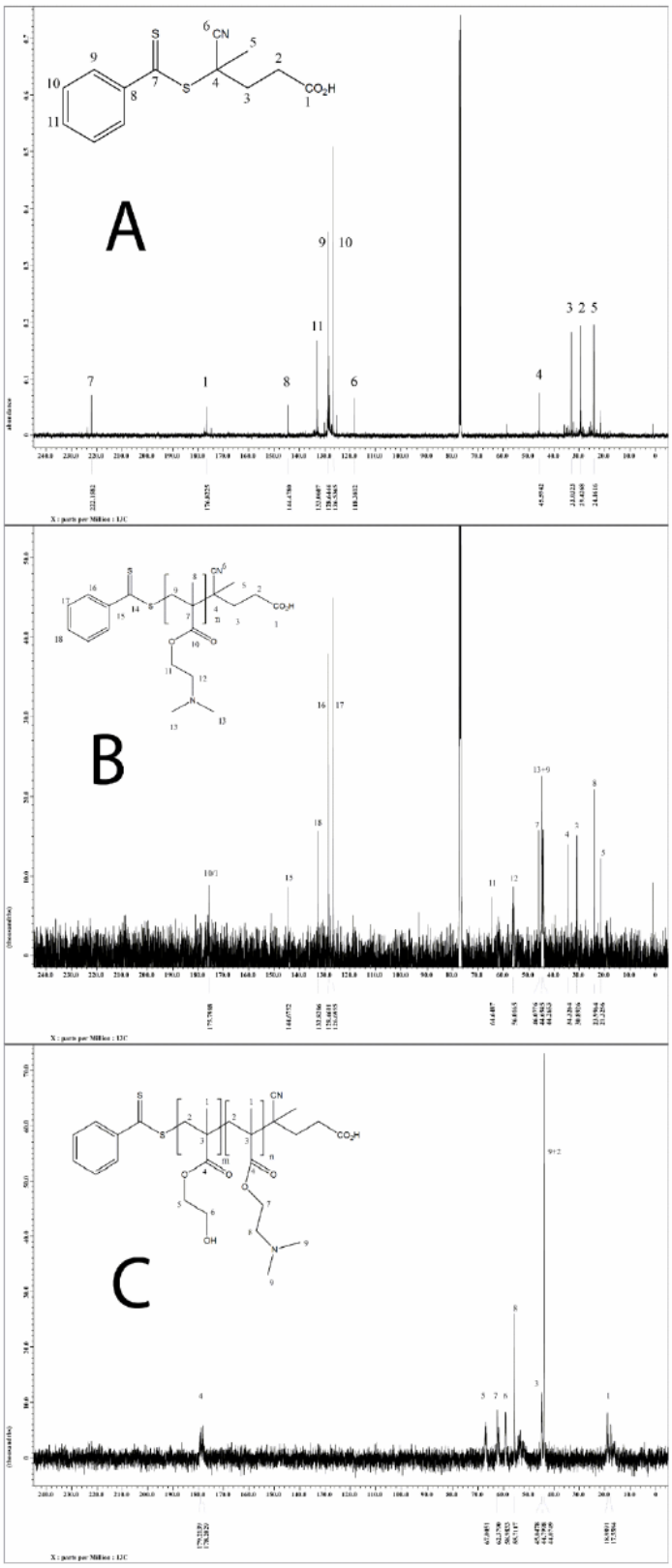

Figure S2. Molecular weight (**A**), transfection efficacy (**B**) and cytotoxicity (**C**) of homo-pDMAEMAs poly(2-(dimethyl amino)ethyl methacrylate).

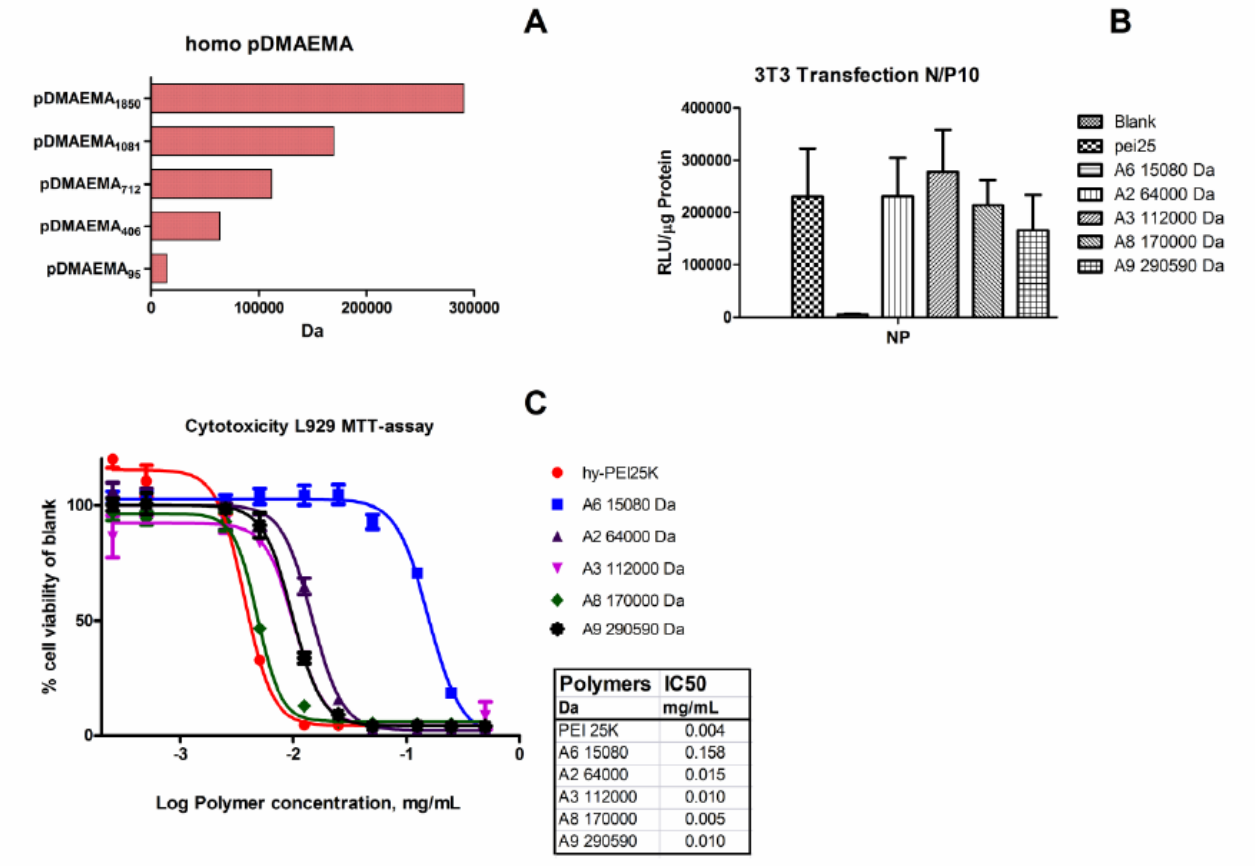

Polymers Da	IC50 mg/mL
PEI 25K	0.004
A6 15080	0.158
A2 64000	0.015
A3 112000	0.010
A8 170000	0.005
A9 290590	0.010

REFERENCES

[1] Morille, M.; Passirani, C.; Vonarbourg, A.; Clavreul, A.; Benoit, J.P. Progress in Developing Cationic Vectors for Non-Viral Systemic Gene Therapy against Cancer. *Biomaterials* **2008**, *29*, 3477-3496.

[2] Mintzer, M.A.; Simanek, E.E. Nonviral Vectors for Gene Delivery. *Chem. Rev.* **2009**, *109*, 259-302.

[3] Neu, M.; Fischer, D.; Kissel, T. Recent Advances in Rational Gene Transfer Vector Design Based on Poly(ethylene imine) and Its Derivatives. *J. Gene Med.* **2005**, *7*, 992-1009.

[4] Kunath, K.; von Harpe, A.; Fischer, D.; Petersen, H.; Bickel, U.; Voigt, K.; Kissel, T. Low-Molecular-Weight Polyethylenimine as a non-Viral Vector for DNA Delivery: Comparison of Physicochemical Properties, Transfection Efficiency and *in vivo* Distribution with High-Molecular-Weight Polyethylenimine. *J. Control. Release* **2003**, *89*, 113-125.

[5] Mao, S.; Neu, M.; Germershaus, O.; Merkel, O.; Sitterberg, J.; Bakowsky, U.; Kissel, T. Influence of Polyethylene Glycol Chain Length on the Physicochemical and Biological Properties of Poly(ethylene imine)-graft-Poly(ethylene glycol) Block Copolymer/SiRNA Polyplexes. *Bioconjugate Chem.* **2006**, *17*, 1209-1218.

[6] Neu, M.; Germershaus, O.; Behe, M.; Kissel, T. Bioreversibly Crosslinked Polyplexes of PEI and High Molecular Weight PEG Show Extended Circulation Times *in vivo*. *J. Control. Release* **2007**, *124*, 69-80.

[7] van de Wetering, P.; Zuidam, N.J.; van Steenbergen, M.J.; van der Houwen, O.A.G.J.; Underberg, W.J.M.; Hennink, W.E. A Mechanistic Study of the Hydrolytic Stability of Poly(2-(dimethylamino)ethyl methacrylate). *Macromolecules* **1998**, *31*, 8063-8068.

[8] Jones, R.A.; Poniris, M.H.; Wilson, M.R. pDMAEMA is internalised by endocytosis but does not physically disrupt endosomes. *J. Control. Release* **2004**, *96*, 379-391.

[9] Layman, J.M.; Ramirez, S.M.; Green, M.D.; Long, T.E. Influence of Polycation Molecular Weight on Poly(2-dimethylaminoethyl methacrylate)-Mediated DNA Delivery *in vitro*. *Biomacromolecules* **2009**, *10*, 1244-1252.

[10] van de Wetering, P.; Cherng, J.-Y.; Talsma, H.; Hennink, W.E. Relation between Transfection Efficiency and Cytotoxicity of Poly(2-(dimethylamino)ethyl methacrylate)/Plasmid Complexes. *J. Control. Release* **1997**, *49*, 59-69.

[11] Wink, T.; de Beer, J.; Hennink, W.E.; Bult, A.; van Bennekom, W.P. Interaction between Plasmid DNA and Cationic Polymers Studied by Surface Plasmon Resonance Spectrometry. *Anal. Chem.* **1999**, *71*, 801-805.

[12] Cherng, J.Y.; van de Wetering, P.; Talsma, H.; Crommelin, D.J.; Hennink, W.E. Effect of Size and Serum Proteins on Transfection Efficiency of Poly ((2-dimethylamino)ethyl methacrylate)-Plasmid Nanoparticles. *Pharm. Res.* **1996**, *13*, 1038-1042.

[13] Arigita, C.; Zuidam, N.J.; Crommelin, D.J.; Hennink, W.E. Association and Dissociation Characteristics of Polymer/DNA Complexes Used for Gene Delivery. *Pharm. Res.* **1999**, *16*, 1534-1541.

[14] Rungsardthong, U.; Ehtezazi, T.; Bailey, L.; Armes, S.P.; Garnett, M.C.; Stolnik, S. Effect of Polymer Ionization on the Interaction with DNA in Nonviral Gene Delivery Systems. *Biomacromolecules* **2003**, *4*, 683-690.

[15] Jiang, X.; Lok, M.C.; Hennink, W.E. Degradable-Brushed pHEMA-pDMAEMA Synthesized via ATRP and Click Chemistry for Gene Delivery. *Bioconjugate Chem.* **2007**, *18*, 2077-2084.

[16] Verbaan, F.; van Dam, I.; Takakura, Y.; Hashida, M.; Hennink, W.; Storm, G.; Oussoren, C. Intravenous Fate of Poly(2-(dimethylamino)ethyl methacrylate)-Based Polyplexes. *Eur. J. Pharm. Sci.* **2003**, *20*, 419-427.

[17] Verbaan, F.J.; Oussoren, C.; Snel, C.J.; Crommelin, D.J.; Hennink, W.E.; Storm, G. Steric Stabilization of Poly(2-(dimethylamino)ethyl methacrylate)-Based Polyplexes Mediates Prolonged Circulation and Tumor Targeting in Mice. *J. Gene Med.* **2004**, *6*, 64-75.

[18] Tagami, T.; Nakamura, K.; Shimizu, T.; Yamazaki, N.; Ishida, T.; Kiwada, H. CpG Motifs in pDNA-Sequences Increase anti-PEG IgM Production Induced by PEG-Coated pDNA-Lipoplexes. *J. Control. Release* **2010**, *142*, 160-166.

[19] Montheard, J.-P.; Chatzopoulos, M.; Chappard, D. 2-Hydroxyethyl Methacrylate (HEMA): Chemical Properties and Applications in Biomedical Fields. *Polym. Rev.* **1992**, *32*, 1-34.

[20] Mabilleau, G.; Moreau, M.F.; Filmon, R.; Basle, M.F.; Chappard, D. Biodegradability of Poly(2-hydroxyethyl methacrylate) in the Presence of the J774.2 Macrophage Cell Line. *Biomaterials* **2004**, *25*, 5155-5162.

[21] You, J.O.; Auguste, D.T. Nanocarrier Cross-Linking Density and pH Sensitivity Regulate Intracellular Gene Transfer. *Nano Lett.* **2009**, *9*, 4467-4473.

[22] Dai, F.; Sun, P.; Liu, Y.; Liu, W. Redox-Cleavable Star Cationic PDMAEMA by arm-First Approach of ATRP as a Nonviral Vector for Gene Delivery. *Biomaterials* **2010**, *31*, 559-569.

[23] Hosseini Nejad, E.; Castignolles, P.; Gilbert, R.G.; Guillaneuf, Y. Synthesis of Methacrylate Derivatives Oligomers by Dithiobenzoate-RAFT-Mediated Polymerization. *J. Polym. Sci. A Polym. Chem.* **2008**, *46*, 2277-2289.
[24] Patton, D.L.; Advincula, R.C. A Versatile Synthetic Route to Macromonomers via RAFT Polymerization. *Macromolecules* **2006**, *39*, 8674-8683.
[25] Xiong, Q.; Ni, P.; Zhang, F.; Yu, Z. Synthesis and Characterization of 2-(Dimethylamino)ethyl Methacrylate Homopolymers via aqueous RAFT Polymerization and Their Application in Miniemulsion Polymerization. *Polym. Bull.* **2004**, *53*, 1-8.
[26] Liu, L.; Wu, C.; Zhang, J.; Zhang, M.; Liu, Y.; Wang, X.; Fu, G. Controlled Polymerization of 2-(diethylamino)ethyl Methacrylate and Its Block Copolymer with N-Isopropylacrylamide by RAFT Polymerization. *J. Polym. Sci. A Polym. Chem.* **2008**, *46*, 3294-3305.
[27] York, A.W.; Kirkland, S.E.; McCormick, C.L. Advances in the Synthesis of Amphiphilic Block Copolymers via RAFT Polymerization: Stimuli-Responsive Drug and Gene Delivery. *Adv. Drug Delivery Rev.* **2008**, *60*, 1018-1036.
[28] Scales, C.W.; Huang, F.; Li, N.; Vasilieva, Y.A.; Ray, J.; Convertine, A.J.; McCormick, C.L. Corona-Stabilized Interpolyelectrolyte Complexes of SiRNA with Nonimmunogenic, Hydrophilic/Cationic Block Copolymers Prepared by Aqueous RAFT Polymerization. *Macromolecules* **2006**, *39*, 6871-6881.
[29] Mitsukami, Y.; Donovan, M.S.; Lowe, A.B.; McCormick, C.L. Water-Soluble Polymers. 81. Direct Synthesis of Hydrophilic Styrenic-Based Homopolymers and Block Copolymers in Aqueous Solution via RAFT. *Macromolecules* **2001**, *34*, 2248-2256.
[30] van de Wetering, P.; Cherng, J.Y.; Talsma, H.; Crommelin, D.J.A.; Hennink, W.E. 2-(dimethylamino)ethyl Methacrylate Based (co)polymers as Gene Transfer Agents. *J. Control. Release* **1998**, *53*, 145-153.
[31] Chen, L.; Li, H.; Zhao, R.; Zhu, J. Study Progress of Cell Endocytosis. *Chin.-Ger. J. Clin. Oncol.* **2009**, *8*, 360-365.
[32] Prokop, A.; Davidson, J.M. Nanovehicular Intracellular Delivery Systems. *J. Pharm. Sci.* **2008**, *97*, 3518-3590.
[33] Merkel, O.M.; Beyerle, A.; Beckmann, B.M.; Zheng, M.; Hartmann, R.K.; Stoger, T.; Kissel, T.H. Polymer-Related Off-Target Effects in Non-Viral siRNA Delivery. *Biomaterials* **2011**, *32*, 2388-2398.
[34] Sahnoun, M.; Charreyre, M.-T.; Veron, L.; Delair, T.; D'Agosto, F. Synthetic and Characterization Aspects of Dimethylaminoethyl Methacrylate Reversible Addition Fragmentation Chain Transfer (RAFT) Polymerization. *J. Polym. Sci. A Polym. Chem.* **2005**, *43*, 3551-3565.
[35] Liu, Y.; Nguyen, J.; Steele, T.; Merkel, O.; Kissel, T. A New Synthesis Method and Degradation of Hyper-Branched Polyethylenimine Grafted Polycaprolactone Block Mono-Methoxyl Poly (ethylene glycol) Copolymers (hy-PEI-*g*-PCL-*block*-mPEG) as Potential DNA Delivery Vectors. *Polymer* **2009**, *50*, 3895-3904.
[36] Germershaus, O.; Mao, S.; Sitterberg, J.; Bakowsky, U.; Kissel, T. Gene Delivery Using Chitosan, Trimethyl Chitosan or Polyethylenglycol-*graft*-Trimethyl Chitosan Block Copolymers: Establishment of Structure-Activity Relationships *in vitro*. *J. Control. Release* **2008**, *125*, 145-154.
[37] Merkel, O.M.; Mintzer, M.A.; Librizzi, D.; Samsonova, O.; Dicke, T.; Sproat, B.; Garn, H.; Barth, P.J.; Simanek, E.E.; Kissel, T. Triazine Dendrimers as Nonviral Vectors for *in vitro* and *in vivo* RNAi: The Effects of Peripheral Groups and Core Structure on Biological Activity. *Mol. Pharm.* **2010**, *7*, 969-983.
[38] Nguyen, J.; Reul, R.; Roesler, S.; Dayyoub, E.; Schmehl, T.; Gessler, T.; Seeger, W.; Kissel, T. Amine-Modified Poly(Vinyl Alcohol)s as Non-viral Vectors for siRNA Delivery: Effects of the Degree of Amine Substitution on Physicochemical Properties and Knockdown Efficiency. *Pharma. Res.* **2010**, *27*, 2670-2682.

CHAPTER 5

Polymer Conformation in Aqueous Solution is Critical for DNA-Vector Formation: Isothermal Titration Calorimetry and Molecular Dynamics Disclose Causes for Variability in Transfection Performance.

Olga Samsonova[1], Adam Biela[2], Serghei Glinca[2], Christian Pfeiffer[1,3], Gerhard Klebe[2] and Thomas Kissel[1]

[1] Department of Pharmaceutics and Biopharmacy, Philipps-Universität, Ketzerbach 63, D-35032 Marburg, Germany, olga.samsonova@staff.uni-marburg.de, kissel@staff.uni-marburg.de

[2] Department of Chemistry, Philipps-Universität, Marbacher Weg 6, D-35032 Marburg, Germany, biela@staff.uni-marburg.de, glinca@staff.uni-marburg.de, klebe@staff.uni-marburg.de

[3] Department of Physics, Philipps-Universität, Renthof 7, D-35032 Marburg, Germany, pfeiffeb@staff.uni-marburg.de

Experimental contribution of OS: ITC-measurements, LDA, TEM

In preparation for Acta Biomaterialia

Abstract:

Low molecular weight poly(2-(dimethyl amino)ethyl methacrylate-*block*-poly(2-hydroxyl methacrylate (pDMAEMA-b-pHEMA) block-copolymers have been proposed as potential gene delivery agents. The interrelation between structure, biocompatibility and transfection efficacy has been described previously. However, reasons for variable transfection efficacy within this polymer family remained unclear, apart from beneficial effects of the pHEMA segment. This study investigates the energetic aspects of polymer-DNA binding by means of isothermal titration calorimetry (ITC), and simulates polymer chain behaviour in water via computational molecular dynamics (MD).

Polymer chain flexibility as reflected in the glass transition temperature (T_g) appeared to be important for binding thermodynamics, as depicted in ITC enthalpy profiles. The T_g increased with growing pHEMA chain length. The T_g above the room temperature reduced the chain flexibility, favouring the formation of hydrogen bonds between polymer and sorrounding water molecules according to Collets protein folding theory (Collet O. J. Chem. Phys. 2011; 134(8):85101-85107). Therefore, pHEMA-rich structure was fixed in a more stretched form in solution. The hydrogen bonds to the solvent molecules counteracted folding, herewith providing better accessibility for positive charge to DNA.

Evaluating the nanovehicle self-assembly process according to mechanistic criteria of polymer conformational state and subsecquent DNA-binding thermodynamics, this study could define high T_g as advantageus polymer parameter favourable for transfection efficacy of a low molecular weight pDMAEMA-b-pHEMA polymer family. The combined use of ITC and MD principles presented here can be interesting for examination of other linear materials for gene delivery application.

1. Introduction

In the course of creating optimal non-viral vectors for gene and drug delivery, many strategies have been exploited, adjusting diverse polymer parameters such as branching grade [1-3], charge density [4], linkage of components with different physico-chemical properties [5, 6] represented in the entire variety of chemical structures [7, 8]. To be efficient in its mission of cargo delivery, it is essential for a drug or gene carrier to fulfil a range of requirements, such as low toxicity, high complexation efficacy, enzyme degradation resistance, and capability for endosomal escape, among others [9]. One of the questions arising from the very first technological step of vector preparation is: how does the polymeric structure behave in a solvent environment? Does it have a preferred conformation in solutions? A further question is how possibly existing conformational transitions can be controlled, and how well do these conformational states assemble with intended cargo? How can we predict these conformational states based on information from chemical structure for more productive carrier tailoring? Adequate and sufficiently sensitive methodology is required to carry out this versatile polymer investigation.

Isothermal titration calorimetry (ITC) is a highly sensitive and precise measuring methodology to characterize ligand binding. It is based on the registration of released or absorbed heat of interaction and can be employed for an elaborate analysis of thermodynamic processes of association. A detailed overview of measurement principles and performance capacities of one of the first computerized ITC-instruments was given by Wiseman et al. as early as 1989 [10]. Nowadays, ITC has established itself in a broad range of applications, including the characterization of micellar systems, interactions of drugs, polymers and proteins with surfactants, the association of nucleic acids with multivalent cations, nanoparticle characterization, as well as the improvement of targeting ligands as reviewed lately by Bouchemal [11]. Several previous studies have already attempted to describe this

problem in respect to transfection efficacy. Thus Choosakoonkriang et al. studied the aspects of PEI/DNA complexation, searching for a relationship between physical characteristics and transfection efficacy. In his study both DNA circular dichroism spectra and ITC monitored polymer-DNA binding interaction, as well as polyplex stability examined via differential scanning calorimetry showed no direct correlation to transfection performance in cells. No DNA conformation change was observed for any of the PEI structures [12]. Nandy et al. simulated PAMAM/DNA interaction computationally, studying the compaction impact of different generation dendrimers on DNA. The binding strength correlated with polymer charge intensity and thus with dendrimer generation. The G3 and G4 dendrimers were more flexible and showed deformation upon binding to DNA, being also less efficient. All generations preserved the native B-form DNA structure [13]. Also for siRNA the interaction of dendritic molecules characterized via ITC and molecular dynamic simulation was published by Jensen et al [14]. Here a good applicability of this technique was shown: simulated rigid sphere behaviour of siRNA of G7 dendrimer, favourable for complexation of siRNA, was in line with experimental data.

Despite broad availability of information on polymers with more complex structures, the short linear co-block polymers have so far been rather scarcely investigated. Here, we focus on linear polymer structure and its conformational aspects, using the pDMAEMA homo- and pHEMA-diblock-copolymer family as example. The low molecular weight pDMAEMA-b-pHEMA diblock copolymers have previously shown considerable capability for transgene expression in vitro [15]. The dependency between performance in cell culture and varying pHEMA-part in polymeric structure could be clearly demonstrated. Nevertheless, the definite reasons for superior performance of pHEMA-containing vectors are still to be understood.

This question has become the objective of this study. Selected candidates from the pDMAEMA/pHEMA polymer family were explored regarding their mechanistic aspect, using a combinational method of isothermal titration calorimetry (ITC) and molecular dynamic

simulation (MD). The ITC was used to characterize the binding interaction between polymer and DNA from an energetic point of view. The MD was applied to assess the conformational rearrangements of polymers in an aqueous environment. The grade of hydrogen bonds development between polymer and solvent molecules and its depandance on glass transition temperature T_g will be discussed from the view of Collet's protein folding theory in water. [16].

2. Materials and Methods

2.1. Materials

Polymers for his study were synthesized in via RAFT polymerization as described previously [15]. Poly(ethylene imine) (Polymin™, 25 kDa, abbreviated as PEI 25k) was a gift from BASF (Ludwigshafen, Germany). For titration experiments herring testes DNA, Type XIV was obtained from Sigma Aldrich Chemie GmbH (Seelze, Germany).

2.2. Isothermal titration calorimetry of DNA with polymers

Isothermal titration calorimetry (ITC) was applied for the investigation of energetic effects detected as heat flow during the polymer-DNA binding process. Both ligands, herring testes DNA (HT-DNA) and polymers, were prepared in double distilled filtered water from pure lyophilized substances without any additives. The ITC measurements were conducted with a MCS titration calorimeter (Microcal, Inc., Northhampton, MA) at a temperature of 25°C. 0.03 mM HT-DNA, based on phosphate, was applied in a temperature controlled measurement cell. Polymer solutions ranged from 0.55 to 5.5 mM based on nitrogen. Prior to application to the cell or syringe respectively, both components involved in titration were degassed under vacuum and with stirring for 7-10 minutes, to avoid artefacts due to gas bubbles and hence possible disturbances of the base line. Polymer was titrated from a 250 µL syringe to DNA in

steps, with 250-300 seconds between injections, to return the temperature to the base line after the registration of the binding heat of each injection peak. The first injection volume was set at 4 µL and not involved in the further data evaluation to avoid possible inaccuracy due to syringe filling etc.; further injections were set at 6 or 8 µL and repeated at least 15 times during one titration run to achieve the DNA-saturation with polymer. Each sample measurement was performed at least twice. ITC-data were analyzed with ORIGIN Software (Microcal Inc.) to prepare final isotherms.

2.3. Molecular dynamics (MD) simulation

The three-dimensional polymer structures of pDMEAMA-derivatives were modelled using MOE [17] and were used as input for molecular dynamic simulations, which were performed with the AMBER 11 software suite [18]. The force field parameters were computed using the *antechamber* program. Amber coordinate, parameter and topology files were generated by *xleap* and the generalized Born solvation model [19] was applied. The resulting systems were minimized and equilibrated at 300 K for 1 ps using 10 Å cutoff. The simulation time was 20 ns, at 300 K and 1 atm with a time step of 1 fs and no cut-off. All simulations were carried out by the *pmemd.cuda* module of the AMBER 11 suite on a single GPU. Dynamic trajectories analysis and geometric data clustering were performed with *ptraj*. Graphical representations of the polymer molecules were prepared using PyMOL [20].

2.4. Laser Doppler Anemometry (LDA)

For zeta potential measurements, polymer solutions of 2.75 mM based on nitrogen were freshly prepared in twice distilled filtered water. The measurement was performed in a clear zeta cuvette (Malvern, Herrenberg, Germany) at 25°C, and analyzed using the Smoluchowski model. Each polymer was measured three times, the amount of runs and the attenuator position were adjusted automatically. The data were presented in relative values, setting the

maximal zeta potential signal equal with the maximally stretched polymer form. Decreasing charge signals were given as per cent of stretched form charge availability and represented indirectly the folding state of the counted molecule.

2.5. Differential scanning calorimetry (DSC)

The glass transition temperature T_g was determined by menas of a DSC device composed of a DSC-7 unit and a control station TAC7/DX (Perkin – Elmer, Waltham, USA). For the measurement, 10 mg of lyphilized substance were sealed in an aluminium DSC pan. The measurement data were obtained from the second heating cycle. The minimal cycle temperature was -40°C and the maximal 120°C, the heating rate was 10°C/min. The data were evaluated with Pyris Software Version 4.01 (Perkin – Elmer).

2.6. Transmission electron microscopy (TEM)

For morphological evaluation of polymer-DNA complexes, 10µL of polyplex formulation were applied to a carbon copper grid (S160-3, Plano, Wetzlar), incubated for 10 minutes, blotted with filter paper and dried overnight. The final polymer concentration in preparation was about 0.2 mg/mL. Prior to complexation with DNA, the polymer was incubated with Copper (II) sulphate in a proportion of about 1µg polymer to 1.4 µL 3% copper solution. The OH-groups of pHEMA complexed Cu^{2+} ions and increased the coiled polymer chain electronic density, improving visibility in TEM (JEM-3010 TEM, JEOL, Eching). The measurement was performed at 300 kV.

3. Results and Discussion

3.1. Thermodynamic monitoring of Polymer-DNA association process (ITC)

To study the binding interaction between components capable of self-assembly, isothermal titration calorimetry [10] was applied here. A binding process is accompanied by changes in heat flow, the direction and intensity of which is dependant on structural features of the interacting components. During step by step addition of polymer to DNA, the spontaneous thermodynamic process of vector formation can be registered in form of peak signals following each injection, detectable until the DNA-saturation point is reached and the signals drop to the base line.

For the thermodynamic study five polymers were selected: poly(ethylene imine) (PEI) 25 kDa, a well established branched transfection agent of high performance [12, 21], pDMAEMA115 (linear polymer with 115 pDMAEMA repeting units), previously “silent” in transfection, and three linear diblock copolymers pDMAEMA115-b-pHEMA6 , pDMAEMA115-b-pHEMA57 and pDMAEMA151-b-pHEMA91 whose transfection efficacy improves along with increasing co-part of pHEMA [15].

Despite the principally equivalent process of polymer-DNA self-assembly, three different types of heat flow profiles could be registered during titration (Fig.1). The purely exothermic profile (downward peaks) was obtained for PEI 25k, the purely endothermic (upward peaks) profile for homo-pDMAEMA, and a combined exothermic-endothermic profile for pDMAEMA-b-pHEMA diblock-copolymers. The molarity of titration solutions was based on nitrogen charge of polymers (+) and phosphate charge of DNA (-). In the final product – a nano-vehicle suspension, at a certain nitrogen to phosphate ratio (N/P) was generated. Depending on the amount of HEMA-repeating units grafted to the pDMAEMA-block, the point at which the heat flow switched direction moved towards higher or lower N/Ps. The most prolonged exothermal interaction was achieved during titration of pDMAEMA115-b-pHEMA57 and pDMAEMA151-b-pHEMA91 to DNA (switch-point at N/P of 8-11 and 6-8 respectively). pDMAEMA115-b-pHEMA6 had the shortest exothermal titration segment (switch-point already at N/P 4-5).

For PEI 25k, the interaction process was completed already at N/P 2.5-3. All pDMAEMA-derivatives, on the contrary, interacted beyond the charge neutralization point with significant amplitude of heat signal registered until N/P 18-20.

Attempts to interpret the uneven heat flow profiles are known from earlier ITC studies involving polymers and genetic material. Wankee et al., for instance, assigned different ITC-phases to DNA conformational transition during polymer binding, and the DNA state changed from an elongated to a collapsed form [22]. Jensen et al. studied siRNA interaction with PAMAM, and interpreted the appearance of the second phase in ITC-curve at higher N/P ratios as aggregation process [14]. Privette et al. experienced the heat flow switch from endothermic to exothermic direction with poly(amidoamine)-derivatives and DNA and also assigned the later interaction phase to the aggregation process; aggregation was supported with dynamic light scattering data and subtracted from further ITC analysis [23].

The segmentation of ITC profile into two enthalpic phases with different sign, in the present study, can neither originate from DNA-conformational changes nor from the nano-vehicle aggregation or sedimentation process. The circular dichroismus spectra (Fig.S1, Appendix) do not give any evidence of any DNA conformation transition: the native B-form, slightly altered, was maintained for all tested polymers over a broad N/P range. The dynamic light scattering and zeta potential data show no abrupt change in size, charge or PDI at the heat flow switch points of the ITC-curve (Fig. S2, Appendix). Both interacting components applied for titration were lowly concentrated (0.0099 mg/mL DNA, 0.0237 mg/mL PEI 25k and up to 0.123 mg/mL pDMAEMA-derivatives depending on structure), thus providing good solubility of titration products up to higher N/Ps.

We assign the enthalpy direction switch in ITC curve profile to polymer conformational changes. Hendriksen et al. observed similar thermodynamic transitions and interpreted them as structural rearrangements of peptides during interaction with lipid membranes [24]. Such transitions during interaction of polymer with genetic material, to our knowledge, have not

been studied previously. In this study the energetically favourable initial phase (exothermic) is likely to represent the stretched form of pDMAEMA-derivatives, during which polymer nitrogen atoms are easily accessible for interaction with DNA. After this polymer conformation is exhausted due to DNA-binding, the interaction with a coiled polymer form begins. This interaction is accompanied by an energy-intensive (endothermic) chain de-folding process, making nitrogens accessible for contact with DNA. This unfavourable segment has to be compensated by increasing entropy of the reaction system to allow spontaneous material assembly after de-folding [25].

PEI 25k is a less flexible polymer, retaining its conformation in solution [26], due to which the sterical accessibility of nitrogens to DNA does not change over the whole titration period. The pDMAEMA115, on the contrary, has an energetically unfavourable start and must support the binding interaction by investing energy into the de-folding process. The diblock copolymers combine both processes, switching to endothermic interaction after utilization of freely available stretched form. More details regarding conformational state, reasons for conformational changes and charge accessibility are discussed in further sections.

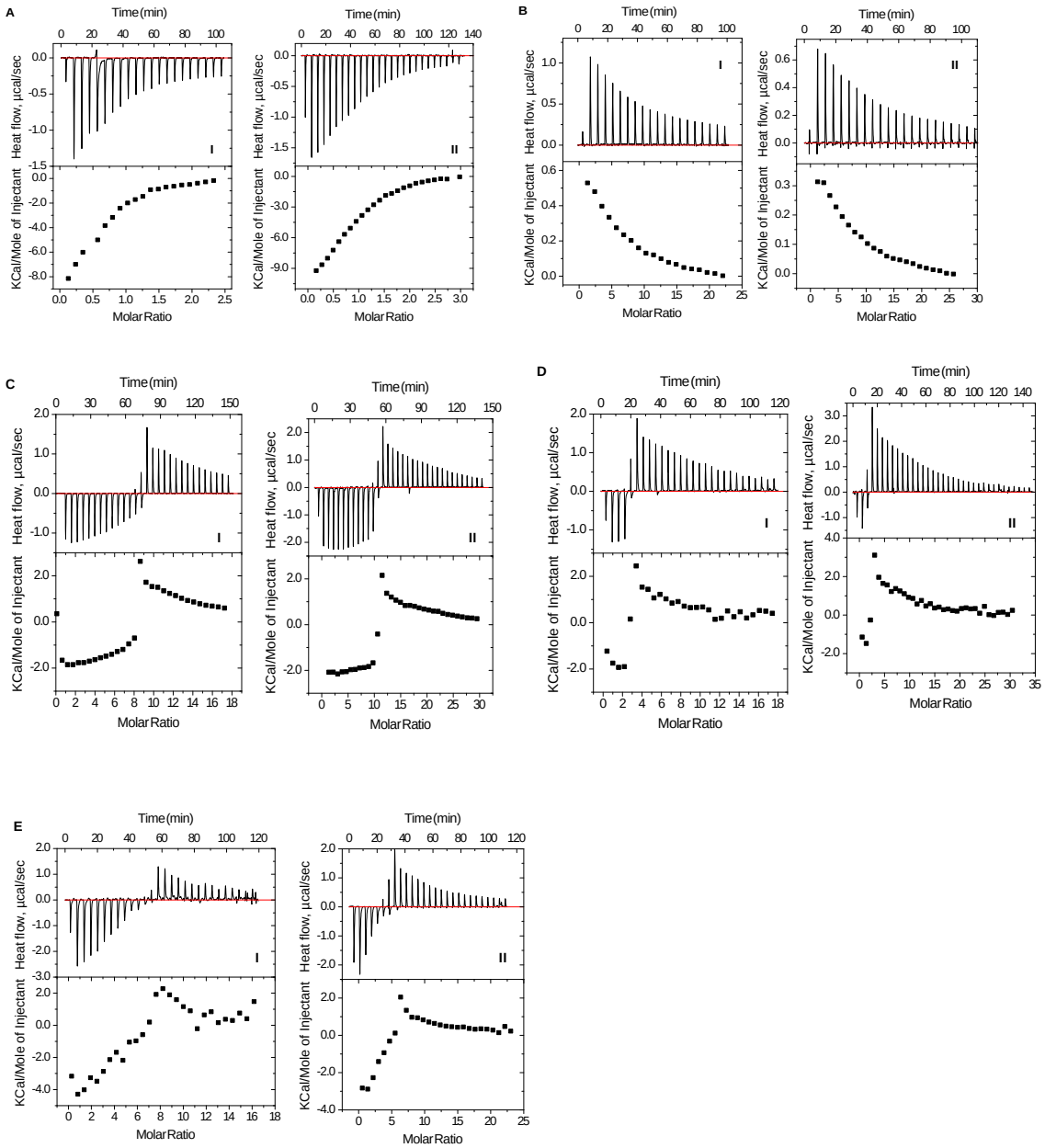

Figure 1: Isothermal titration calorimetry profiles, titration of 0.03mM HT-DNA with 0.55 mM PEI 25k (A), 5.5 mM pDMAEMA115 (B), 2.75 mM (C I) and 5.5 mM (C II) pDMAEMA115-b-pHEMA57, 4 mM (D I) and 5.5 mM (D II) pDMAEMA115-b-pHEMA6, 2.75 mM (E I) and 5.5 mM (D II) pDMAEMA151-b-pHEMA91

3.2. Energetically preferred polymer conformation state in water (MD and ZS)

For MD simulations, one polymer without and two polymers with different amounts of HEMA-repeating units were selected: pDMAEMA115, pDMAEMA115-b-pHEMA6 and pDMAEMA115-b-pHEMA57. The polymer chain rearranged itself considerably during the MD simulation. In order to obtain representative frames of each polymer's geometric

movement, dynamic trajectories were clustered into 10 groups. The clustering procedure was based on the root mean square deviation (RMSD) of the polymer's backbone atom coordinates. The RMSD is a commonly used method for measuring the average distance between atoms of two molecules. Results from the cluster analysis clearly demonstrate that during the simulation stretched polymers collapse into more energetically favorable globular conformations, however, the polymers gain the final energetically favourable state on different time scales (Fig.2). This final conformation is most likely to be the polymers' "natural state" upon dissolution in water. Any geometrical rearrangements of this conformational state would be energetically unfavourable and therefore require energy investment.

For each frame which emerged from the clustering analysis, the water accessible surface area [27] for atoms with positive partial charge (ASAplus) was calculated by MOE [17]. According to these calculations the accessibility of charges on the molecule surface decreased from 100% (related to the first frame) to 63% for pDMEAMA115-b-pHEMA57 and to about 40-50% for pDMAEMA115-b-pHEMA6 and pDMAEMA115 final conformations (last frame) (Fig.3). The length and width of the polymer chains in linear and coiled conformation changed even more drastically (Tbl.1). For example the length of pDMAEMA115-b-pHEMA57 contracted itself nearly 4.1-fold from 36.97 nm to 9.11 nm, of homo-pDMAEMA about 4.4-fold (26.28 to 6.12 nm).

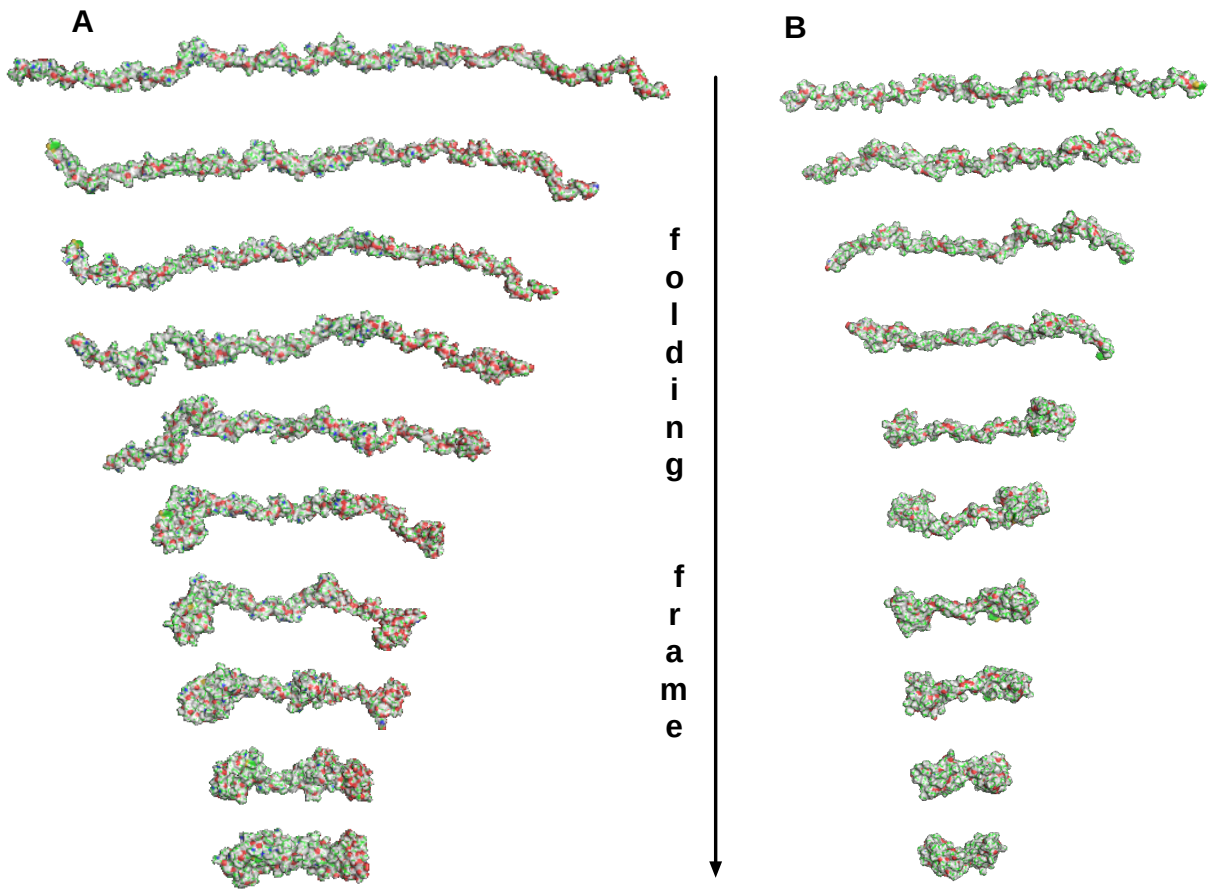

Figure 2: Molecular dynamic folding frames of pDMAEMA115-b-pHEMA57 (A) and pDMAEMA115 (B) during the MD simulation. The collapse of both polymers proceeds on different time scales. pDMAEMA115-b-pHEMA57 reaches the final frame after 10.4 ns and pDMAEMA115 after 7 ns.

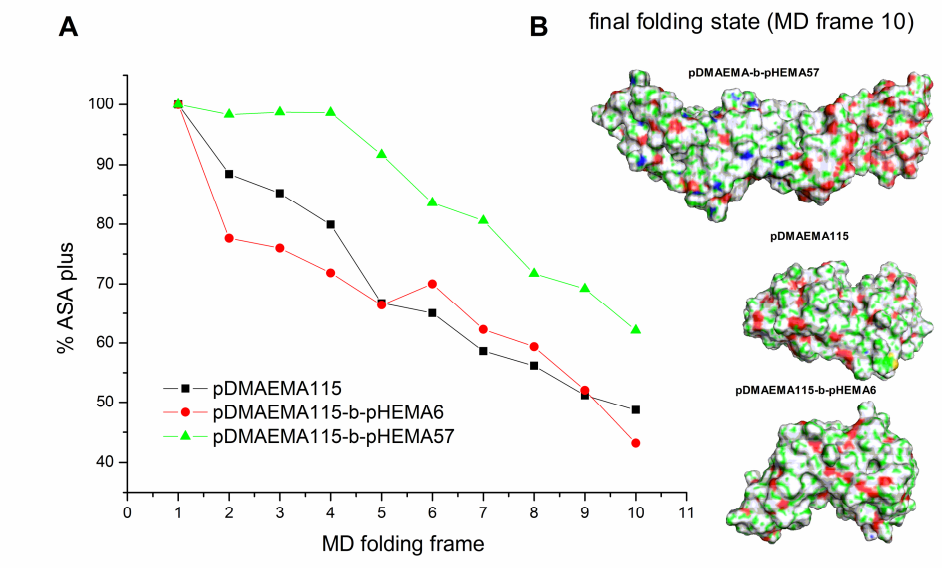

Figure 3: Reduction of overall positive charge accessibility upon molecule folding over 10 frames. The surface area with positive partial charge (ASAplus) accessible for water has been computed by MOE and is shown as a value relative to the first frame of the MD simulation (A). Accessible surface after maximal folding (B).

	stretched form		folded form	
Name	long (nm)	across (nm)	long (nm)	across (nm)
pDMAEMA115	26.28	1.46	6.12	3.99
pDMAEMA115-b-pHEMA6	23.67	2.39	5.61	3.57
pDMAEMA115-b-pHEMA57	36.97	1.61	9.11	3.76

Table 1: Distances between the most remote points of molecules in stretched (first frame) and folded state (last frame), determined from MD simulation.

To assess the conformation state distribution in a practical experiment, the zeta potential of polymer constructs available in water were measured. Due to the folding of polymer chains, overall accessible nitrogen charge declined. Thus the most stretched state appeared the most charged, the most coiled appeared least charged. The highest value of zeta potential of each polymer measured in water solution was related to the unfolded polymer molecule state (100% nitrogen charge accessibility). The presence of molecules with lower zeta potential was interpreted as polymer chain folding, resulting in partial sterical blockage of charge. The distribution of polymer chain conformations in water could be indirectly accessed experimentally via zeta potential measurement, and zeta potetial/folding state correlation building (Fig.4). According to these findings, PEI 25k molecules had a single distribution peak with about 80% charge availability. This was expected, as PEI 25k is a globular molecule of branched structure and rather inflexible, representing a single conformation state [26]. All three pDMAEMA-derivatives showed multi-peak distributions. pDMAEMA115 had the broadest distribution of conformational states, probably due to the highest chain flexibility and dynamicity in solution. Its derivatives with 6 and 57 pHEMA repeating units were more clearly split into two conformational states, one smaller, representing the stretched state, another with a higher amount of counts. For pDMAEMA115-b-pHEMA6 and pDMAEMA115-b-pHEMA57 the final folded state with about 43 and 48 % of the total charge availability. Homo-pDMAEMA also had a second peak at 43% charge availability, with the highest peak appearing at about 63%, which corresponds to a middle folding frame

of MD. The zeta potential data deviated slightly from the MD charge availability prognosis, and are likely to give a more dynamic picture with intermediate folding states. The findings resulting from both methods agree in that the folding does not undershoot the charge accessibility of 30% for all tested polymer structures. Comparing the absolute zeta potential values, it is important to underline that the maxima of PEI 25k and pDMAEMA115-b-pHEMA57 mostly overlap, which may be an indicator of optimal charge availability as they were both superior in transgenic expression [15] (Fig.S3, Appendix).

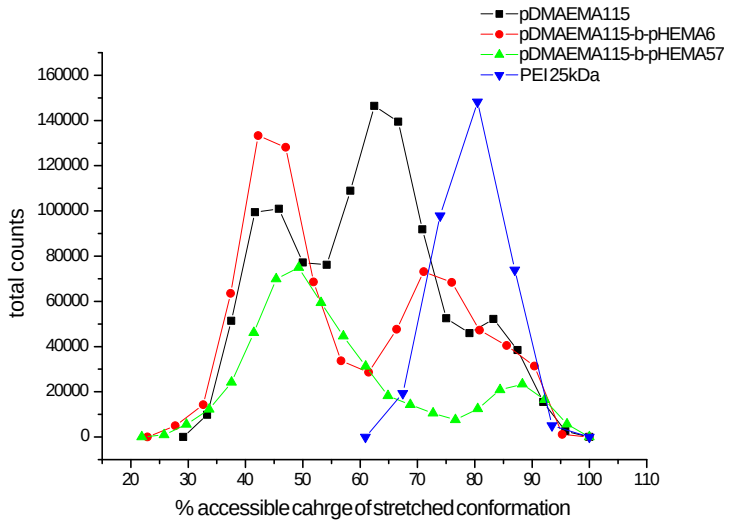

Figure 4: The zeta potential of polymer solutions in water (2.75 mM based on nitrogen) was measured, the highest value for each polymer was assigned to the unfolded polymer molecule state with 100% charge accesibility. Charges beneath this value represent polymer molecules in a more folded state, where nitrogen charges are partly sterically blocked.

3.3. Glass transition temperature of polymers (T_g)

Usually the glass transition temperature T_g is used as a parameter indicating the mobility of polymer chains. Here we make use of another effect described in detail by Collet et al. in relationship to protein folding in water [16]. According to Collet, the stability of hydrogenic bonds between some compound and solvent molecules depends on the T_g of this compound. The higher above the solvent temperature the T_g is, the more likely it is for hydrogenic bonds

to remain intact. Bonds to the surrounding environment protect the compound from sterical collapse, letting it retain a more stretched geometry. Above the T_g, the hydrogen bounds rupture spontaneously and compound chains turn into a "natural" coiled state. This phenomenon applies to pDMAEMA-derivatives, as the pHEMA content increases the T_g. Pure pHEMA has a T_g about 70°C [28], homo-pDMAEMA about -6°C [29]. The pDMAEMA115-b-pHEMA6 has a T_g of 23°C, which predestined the large part of chains to fold in water at 25°C. This behaviour could be traced in MD during this study. The pDMAEMA115-b-pHEMA57 with T_g of 53°C was less folded according to computer stimulation in comparison to pDMAEMA115-b-pHEMA6. The branched polyethyleneimine 25 kDa (PEI 25k) was not simulated in MD. Even though its T_g is a lot lower (-25°C) [30, 31], it does not follow this folding rule due to its highly branched and inflexible structure [26].

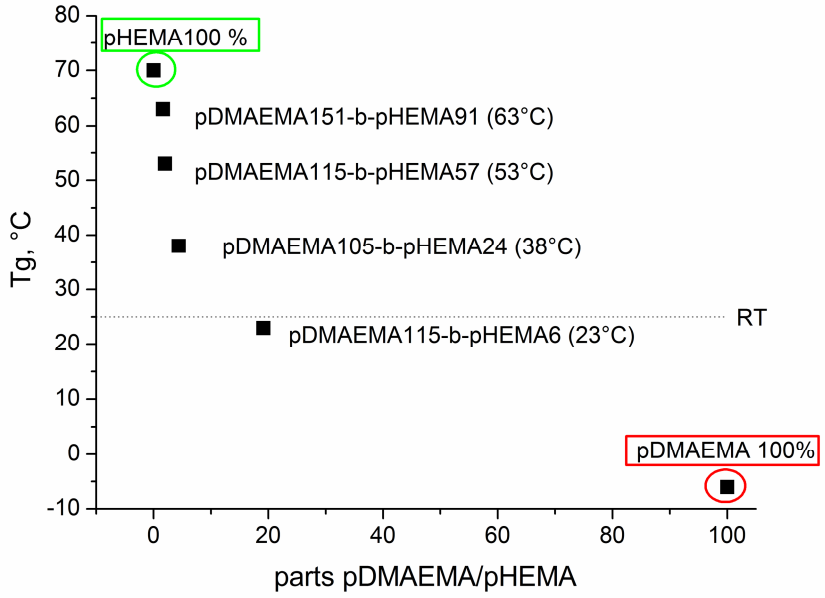

Figure 5: Glass transition temperature (Tg) of pDMAEMA-derivatives depending on pDMAEMA/pHEMA proportion in diblock, room temperature (RT) is indicated as horizontal dotted line

3.4. Depiction of "patchy" polyplex structure

As the dynamic light scattering could only give an idea concerning the size, but not concerning the shape and morphology of polymer complexes with DNA (polyplexes), transmission electron microscopy (TEM) was able to fill this gap (Fig.6). In TEM images the polyplexes appeared as constructs with an irregular boundary line in about 100 nm size range, which is in agreement with dynamic light scattering measurements (DLS) (Fig. S2, Appendix). Moreover, the polyplexes appear to have a “patchy” surface structure. The polyplex increments with higher electronic density sized 5-10 nm were expected artefacts, representing the coiled polymer conformations associated with a polyplex surface. The presence of folded pDMAEMA-b-pHEMA57 chains in the solution was already indicated by the polymer conformation state in water (MD, DLS). The excess of polymer at N/P15 did not allow the polymer chains to make tight contact with DNA, here only adsorptive attachment of folded polymer chains occurred. In ITC curve, the N/P 15 is situated on a falling endothermic heat flow slope, indicating the energetically expensive de-folding process to decrease here.

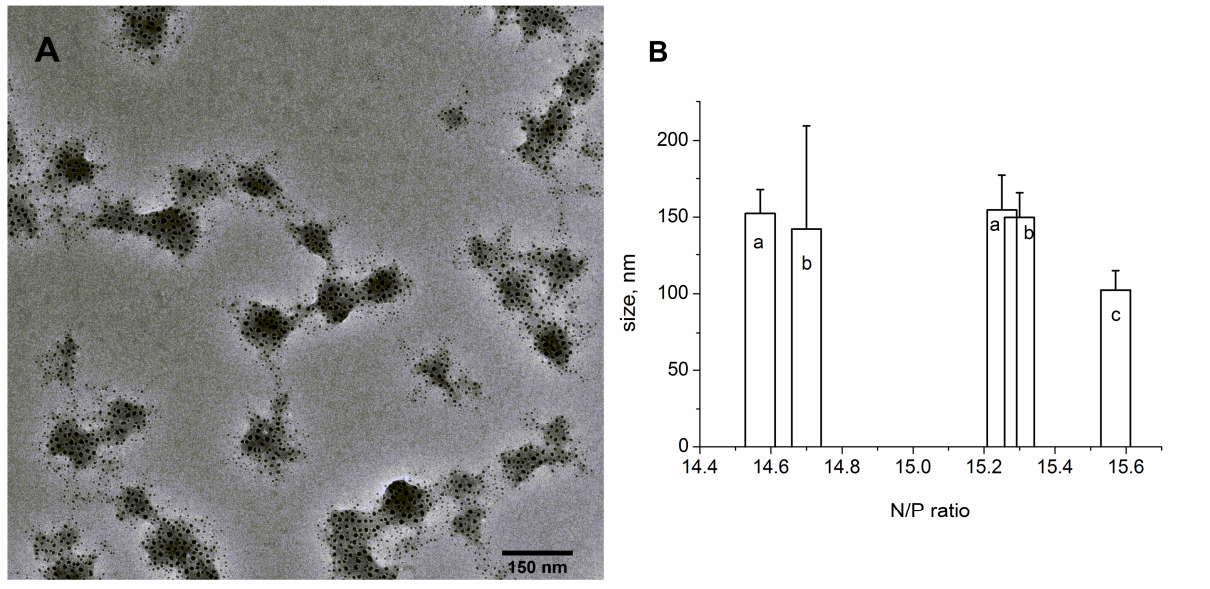

Figure 6: Transmission electron microscopic pictures of pDMEMA115-b-pHEMA/DNA complexes of N/P 15, the structures with irregular contour are polyplexes, rounded increments of 5-10 nm are coiled polymer chains on their surface (A). Hydrodynamic diameters of pDMAEMA115 (a), pDMAEMA115-b-pHEMA57 (b) and PEI 25 kDa (c) complexes with DNA, N/P ratios taken directly from ITC titration curve and hence uneven (B).

4. Conclusions

In this study we could shed light on the mechanistic differences of the self-assembly process of low molecular weigth homo-pDMAEMA and pDMAEMA-b-pHEMA block-copolymers with DNA. The folding behavior of polymers in solution and their binding thermodynamics correlated well with the previously described differences in transfection performance.

The conformational state of linear molecules was proven to be critical for self-assembly with DNA. The availability of a stretched conformation with the highest nitrogen accessibility was essential for energetically favourable interaction with DNA and correlated with the glass transition temperature T_g. The pHEMA-rich methacrylate derivatives with higher T_g were the "energetically cheapest" interaction partners as revealed by ITC. Due to their ability to retain more hydrogen bonds to solvent molecules than homo-pDMAEMA, they remained fixed in a more stretched conformational state as MD could show. The de-folding process had endothermic character and most probably had to be compensated by entropy increase to allow a spontaneous self-assembly reaction. This means that the linear polymers are handicapped for DNA-binding, as they are preferably in a folded state in solutions.

Here we introduced a possibility to explore the polymer-DNA self-assembly process using both ITC and MD methodology elucidating polymer characteristics benefitial for transfection purposes. Establishing correlation between polymer flexibility and favourable binding energetics can be recommended as an effective and sensitive approach for further development and evaluation of non-viral vectors for gene therapy and drug delivery.

Acknowledgements

The authors thank Prof. Essen for the opportunity to perform the CD-measurements, and Wolfgang Große for an excellent support at spectrometer apparatus operation. Prof. Klebe is greatly acknowledged for providing possibility of the isothermal titration calorimetry measurements; Damla Sahin is cordially thanked for her diligent participation in computational polymer structure modelling. Further thanks go to TEM operator Michael Hellwig (MWZM).

SUPPLEMENTARY MATERIALS

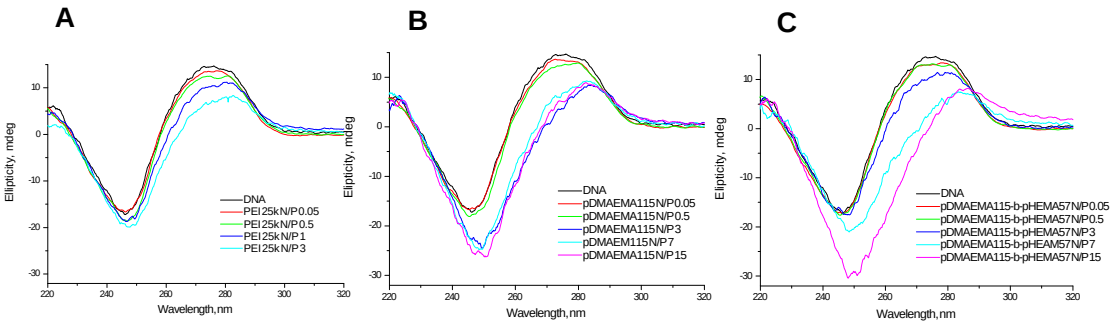

Figure S1: Circular dichroismus spectra of PEI 25k Da (A), pDMAEMA115 (B), pDMAEMA115-b-pHEMA57 (C) with DNA complexes at different nitrogen to phosphate ratios (N/P). Native DNA is added as reference in each graph (black line). N/P 7 and 15 for PEI not shown, as there was no ITC signal, thermodynamic interaction ended before N/P 3.

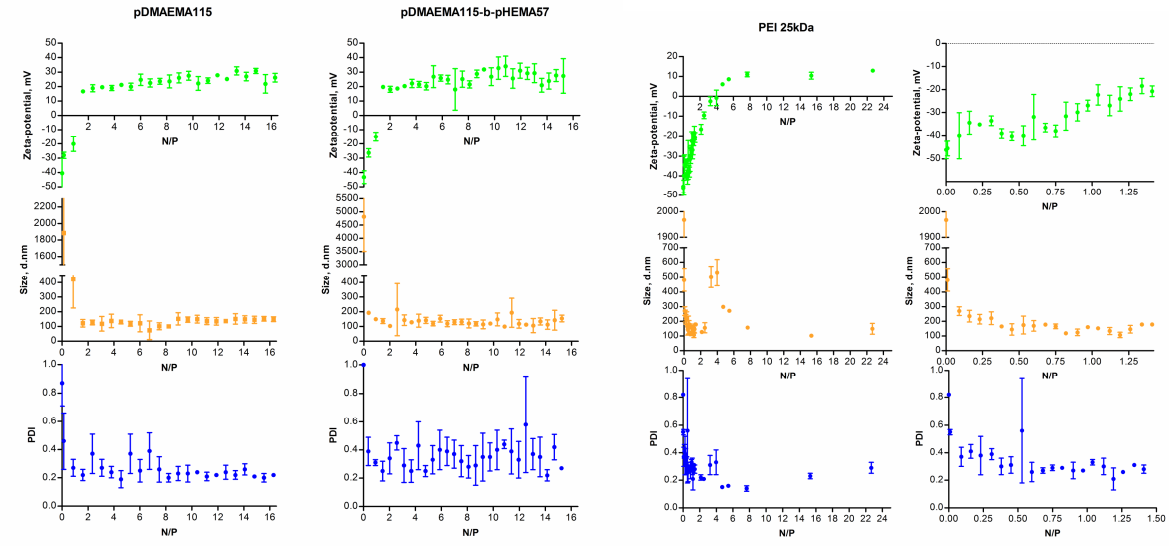

Figure S2: Zeta potential, Size and PDI data of polymer-DNA complexes, N/Ps are matching the titration steps in ITC.

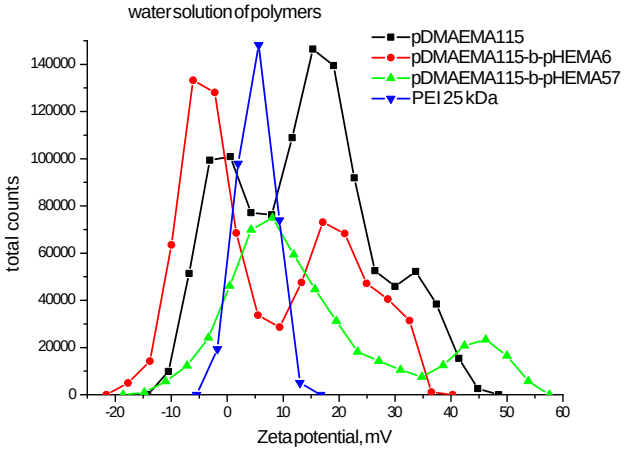

Figure S3: Absolute values of zeta potential of polymer 2.75 mM solutions in water

REFERENCES

[1] Liu Y, Nguyen J, Steele T, Merkel O, Kissel T. A new synthesis method and degradation of hyper-branched polyethylenimine grafted polycaprolactone block mono-methoxyl poly (ethylene glycol) copolymers (hy-PEI-g-PCL-b-mPEG) as potential DNA delivery vectors. Polymer 2009;50:3895-3904.

[2] Sun C, Tang T, Uludag H, Cuervo JE. Molecular Dynamics Simulations of DNA/PEI Complexes: Effect of PEI Branching and Protonation State. Biophys. J. 2011;100:2754-2763.

[3] Schallon A, Jerome V, Walther A, Synatschke CV, Mueller AHE, Freitag R. Performance of three PDMAEMA-based polycation architectures as gene delivery agents in comparison to linear and branched PEI. React. Funct. Polym. 2010;70:1-10.

[4] Alatorre-Meda M, Taboada P, Hartl F, Wagner T, Freis M, Rodriguez JR. The influence of chitosan valence on the complexation and transfection of DNA: The weaker the DNA-chitosan binding the higher the transfection efficiency. Colloids Surf., B 2011;82:54-62.

[5] Endres TK, Beck-Broichsitter M, Samsonova O, Renette T, Kissel TH. Self-assembled biodegradable amphiphilic PEG-PCL-lPEI triblock copolymers at the borderline between micelles and nanoparticles designed for drug and gene delivery. Biomaterials 2011;32:7721-7731.

[6] Liu Y, Samsonova O, Sproat B, Merkel O, Kissel T. Biophysical characterization of hyper-branched polyethylenimine-graft- polycaprolactone-block-mono-methoxyl-poly(ethylene glycol) copolymers (hy-PEI-PCL-mPEG) for siRNA delivery. J. Controlled Release 2011;153:262-268.

[7] Mintzer MA, Simanek EE. Nonviral Vectors for Gene Delivery. Chem. Rev. (Washington, DC, U. S.) 2009;109:259-302.

[8] Kaneda Y, Tabata Y. Non-viral vectors for cancer therapy. Cancer Sci. 2006;97:348-354.

[9] Kang HC, Lee M, Bae YH. Polymeric gene carriers. Crit. Rev. Eukaryotic Gene Expression 2005;15:317-342.

[10] Wiseman T, Williston S, Brandts JF, Lin LN. Rapid measurement of binding constants and heats of binding using a new titration calorimeter. Anal. Biochem. 1989;179:131-137.

[11] Bouchemal K. New challenges for pharmaceutical formulations and drug delivery systems characterization using isothermal titration calorimetry. Drug Discov Today 2008;13:960-972.

[12] Choosakoonkriang S, Lobo BA, Koe GS, Koe JG, Middaugh CR. Biophysical characterization of PEI/DNA complexes. J. Pharm. Sci. 2003;92:1710-1722.

[13] Nandy B, Maiti PK. DNA compaction by a dendrimer. J. Phys. Chem. B 2011;115:217-230.

[14] Jensen LB, Mortensen K, Pavan GM, Kasimova MR, Jensen DK, Gadzhyeva V, Nielsen HM, *et al.*. Molecular characterization of the interaction between siRNA and PAMAM G7 dendrimers by SAXS, ITC, and molecular dynamics simulations. Biomacromolecules 2010;11:3571-3577.

[15] Samsonova O, Pfeiffer C, Hellmund M, Merkel OM, Kissel T. Low molecular weight pDMAEMA-block-pHEMA block-copolymers synthesized via RAFT-polymerization: potential non-viral gene delivery agents? Polymers (Basel, Switz.) 2011;3:693-718.

[16] Collet O. How does the first water shell fold proteins so fast? J. Chem. Phys. 2011;134:85101-85107.

[17] Molecular Operating Environment (MOE), 2010.10; Chemical Computing Group Inc., 1010 Sherbooke St. West, Suite #910, Montreal, QC, Canada, H3A 2R7, 2010.

[18] Case DA, Darden TA, Cheatham TE, III, Simmerling CL, Wang J, Duke RE, Luo R, Walker RC, Zhang W, Merz KM, Roberts B, Wang B, Hayik S, Roitberg A, Seabra G, Kolossváry I, Wong KF, Paesani F, Vanicek J, Liu J, Wu X, Brozell SR, Steinbrecher T, Gohlke H, Cai Q, Ye X, Wang J, Hsieh MJ, Cui G, Roe DR, Mathews DH, Seetin MG, Sagui C, Babin V, Luchko T, Gusarov S, Kovalenko A, and Kollman PA (2010), AMBER 11, University of California, San Francisco.

[19] Tsui V, Case DA. Theory and applications of the generalized Born solvation model in macromolecular simulations. Biopolymers 2001;56:275-291.

[20] The PyMOL Molecular Graphics System, Version 1.2r2pre, Schrödinger, LLC.

[21] Kichler A, Leborgne C, Coeytaux E, Danos O. Polyethylenimine-mediated gene delivery: a mechanistic study. J Gene Med 2001;3:135-144.

[22] Kim W, Yamasaki Y, Jang W, Kataoka K. Thermodynamics of DNA Condensation Induced by Poly(ethylene glycol)-block-polylysine through Polyion Complex Micelle Formation. Biomacromolecules 2010, 11: 1180-1186

[23] Prevette LE, Lynch ML, Reineke TM. Amide Spacing Influences pDNA Binding of Poly(amidoamine)s. Biomacromolecules 2010;11:326-332.

[24] Henriksen JR, Andresen TL. Thermodynamic Profiling of Peptide Membrane Interactions by Isothermal Titration Calorimetry: A Search for Pores and Micelles. Biophys. J. 2011;101:100-109.

[25] Lobo BA, Davis A, Koe G, Smith JG, Middaugh CR. Isothermal Titration Calorimetric Analysis of the Interaction between Cationic Lipids and Plasmid DNA. Arch. Biochem. Biophys. 2001;386:95-105.

[26] Merkel OM, Zheng M, Mintzer MA, Pavan GM, Librizzi D, Maly M, Hoffken H, *et al.*. Molecular modeling and in vivo imaging can identify successful flexible triazine dendrimer-based siRNA delivery systems. J Control Release 2011;153:23-33.
[27] Connolly ML. Solvent-accessible surfaces of proteins and nucleic acids. Science (Washington, D. C., 1883-) 1983; 221:709-713.
[28] Kataoka K, Ito H, Amano H, Nagasaki Y, Kato M, Tsuruta T, Suzuki K, *et al.*. Minimized platelet interaction with poly(2-hydroxyethyl methacrylate-block-4-bis(trimethylsilyl)methylstyrene) hydrogel showing anomalously high free water content. J. Biomater. Sci., Polym. Ed. 1998;9:111-129.
[29] Keszler B, Kennedy JP, Mackey PW. Amphiphilic networks. VI. Swelling and sustained release of poly(N,N-dimethylacrylamide)-l-polyisobutylene, poly(N-N-dimethylamino ethylmethacrylate)-l-polyisobutylene and poly(2-hydroxyethyl methacrylate)-l-polyisobutylene networks. J. Controlled Release 1993;25:115-121.
[30] Santini CMB, Johnson MA, Boedicker JQ, Hatton TA, Hammond PT. Synthesis and bulk assembly behavior of linear-dendritic rod diblock copolymers. J. Polym. Sci., Part A: Polym. Chem. 2004;42:2784-2814.
[31] Weyts KF, Goethals EJ. New synthesis of linear poly(ethylenimine). Polym. Bull. (Berlin) 1988;19:13-19.

CHAPTER 6

Summary and Outlook

SUMMARY

In this thesis, novel polycationic vectors for therapeutic gene delivery were introduced with the focus on structure-function relationship in both physicochemical and biological aspects. First the transfection related differences of classical vectors with high and low branching grade and charge density: PEI and PLL, were examined under pH-alternating tumor tissue conditions. Further structural design for siRNA delivery was proposed on base of PEG-PCL-PEI multifunctional self-assembly ABC-construct, showing the importance of total hydrophilic-lipophilic balance for efficient gene silencing performance. For DNA delivery a new low molecular weight di-block pDMAEMA derivative was synthesized and characterized, proving it to be a low toxic and efficient vector. The relationship between pHEMA-content and polymer chain flexibility was assessed via molecular dynamics simulation (MD). The thermodynamic polymer-DNA binding characteristics, monitored via ITC, appeared to depend on glass transition temperatue (T_g). The use of both MD and ITC methodologies provided new information on the cargo-carrier self-assembly process in solution, relevant to transfection performance of diblock-copolymers.

Chapter 1 introduced to the general goals and executive instruments of gene therapy, as well as potentially addressable disease scope, with a special focus on cancer treatment. The pH-alteration and cell cycle phase impact on transfection process in tumor tissue, as well as EPR-effect were discussed. Advantages and requirements on polycationic gene carriers were presented, followed by short portrait of classical polymers with their advantages and optimisation needs. Strategies of vector optimisation were discussed following the ways of prolonged circulation, toxicity decrease and modified membrane activity.

Chapter 2 investigated the impact of environmental pH on transfection efficacy of polymeric carriers on example of classical representatives PEI and PLL. Both transfection and culture medium were varied from physiological to pathologically lowest pH-condition, proceeding in four steps: 7.4, 7.0, 6.7, and 6.3. Physicochemical and biological parameters either showed significant alternations in respond to pH-shift. The effects were partly oppositely directed, as it could be monitored in separated medium- and transfection pH-conditions. Compared to physiological conditions, acidic transfection medium reduced gene expression 1.6~7.7-fold, whereas acidic culture medium enhanced transfection efficiency 2.1~2.6-fold at the same time. Findings of this study strongly suggest to take tumor acidity in consideration when developing materials for gene carrier purposes. The specific biological charcteristics of acidified tissue should also not be neglected, as they modify transfection efficacy performance.

Chapter 3 analyzed the structure-function relationship of mono-methoxyl-poly(ethylene glycol)-block-poly(ε-caprolactone) (mPEG-PCL) modified hyperbranched PEI copolymers (hy-PEI-PCL-mPEG) as vectors for siRNA delivery. These ABC constructs were amphiphilic and could build stable polyplexes. The PCL-segment length as well as PCL-PEG-grafting density had the most noticable impact on buffer capacity, colloidal stability and siRNA binding affinity. From a library of (hy-PEI-PCL-mPEG) polymers, hy-PEI25k-(PCL900-mPEG2k)1 was distinguished as the most successful candidate for siRNA delivery making it perspective for in vivo experiments.

In **Chapter 4** the block-lengths and molecular weights of poly(2-(dimethyl amino)ethyl methacrylate-*block*-poly(2-hydroxyl methacrylate) family were varied to determine the minimal requirements on polycationic part for transfection. The lower limit was set with homo-pDMAEMA of 115 repeating units. The homo-pDMAEMA115 was ineffective in

transfection, its performance in vitro was increased significantly with pHEMA-grafting. The RAFT-synthesized diblock copolymers were in the range of 17–35.7 kDa, being 1.4–9.7 times less toxic than PEI 25 kDa and potentially extractable via kidney without prior degradation need. Here the low molecular weight pDMAEMA polymers, previously believed to be unsuitable as DNA vectors, were improved in their transfection capability keeping the toxicity in acceptable range, making them attractive candidates for further investigation in terms of therapeutic gene delivery.

In **Chapter 5** the correlation between polymer rigidity, pHEMA-content and glass transition temperature (T_g) was determined. The ability to retain stretched conformation in solution, demonstrated with MD, reflected the conformational state importance in interaction with DNA, where the energetical aspect of binding was assessed with ITC. Highly flexible homo-polymer molecules required additional energy investments for de-folding process prior to self-assembly with DNA to form a functional nano-vehicle. The correlation of preferentially exothermic ITC-profiles with pHEMA-co-block length underlined repeatedly the beneficial effect of pHEMA-grafting on transfection performance improvement. The findings about polymer structure-dependant conformational state in water and the polymer thermodynamic speciality of interaction with DNA could explain the differences in transfection performance observed previously.

OUTLOOK

Basing on the results described in **Chapters 2** to **4**, strategically different ways of farther gene delivery candidates investigations can be followed. The knowledge obtained on impact of acidified tumor tissue conditions on polymeric transfection in **Chapter 2** can be propagated on a broader range of more complex polycationic carriers like PEG-PCL-PEI for siRNA form **Chapter 3** or pDMAEMA-pHEMA for DNA delivery from **Chapter 4**. This option may disclose more details on vector specificity in transfection conditions nearer to pathological situation and hence help optimize the vector design in a more directed way.

Another important step for vectors proven to be efficient in vitro is to launch to the animal experiment phase. The factors essential for the perspective to join clinical studies should be obtained: biocompatibility, biodistribution and circulation time etc.

For more precise understanding of intermolecular interactions and sterical effects of polycationic carriers on DNA and siRNA interaction ITC and MD studies are reasonable including the comparative siRNA/DNA binding study as well as thermodynamical screening of binding potential under different conditions (varying ionic srength-, serum protein content and medium pH) to uncover potential handicaps of synthesized constructs.

ZUSAMMENFASSUNG

In der vorliegenden Arbeit wurden innovative polymerische Vektoren, die für die Durchführung von Gentransfers entwickelt gewesen sind, vorgestellt. Hierbei richtete sich der besondere Akzent auf den Zusammenhang zwischen Struktur und Funktion sowohl aus physikalisch-chemischen als auch biologischen Blickpunkten. Zuerst wurden die für eine Transfektion relevanten Unterschiede von klassischen Vektoren mit hohem und niedrigem Verzweigungsgrad - PEI und PLL - unter alternierenden pH-Bedingungen von Krebsgewebe untersucht. Weiter wurde strukturelles Design für siRNA-Transfer auf Basis von PEG-PCL-PEI, einem multi-funktionellen selbst-assoziierenden ABC-Konstrukt, mit Betonung der Wichtigkeit der gesamten Hydrophilie-Lipophilie-Bilanz für effiziente Stilllegung der Genfunktion vorgeschlagen. Für Transport und Zustellung von DNA wurde ein neuer niedermolekularer diblock pDMAEMA-Abkömmling synthetisiert und charakterisiert, wonach der Vektor sich als effizient und geringfügig toxisch erwiesen hat. Der Zusammenhang zwischen pHEMA-Gehalt und Flexibilität der Polymerkette konnte mittels Dynamischer Simulation (MD) aufgeklärt werden. Die Besonderheiten zu thermodynamischen Aspekten von Polymer-DNA Bindung, die an die Glaspunkttemperatur (T_g) gekoppelt zu sein scheinen, wurden mittels ITC beobachtet. Sowohl die MD als auch die ITC- Methodiken lieferten neue Informationen zum Cargo-Carrier-Selbstorganisationsprozess in Lösung, welche wichtig in Bezug auf die Transfektionsleistung der Diblock-Copolymere sind.

Kapitel 1 stellte die allgemeinen Ziele und Ausführungsinstrumente der Gentherapie sowie die potenziell adressierbaren Krankheiten mit besonderem Akzent auf Krebstherapie vor. Hier wurden die Einflüsse von verschiedenen Zellzyklusphasen bei alternierenden pH-Werten auf den Transfektionsprozess im Tumorgewebe sowie der EPR-Effekt diskutiert. Die Anforderungen an polykationische Genvektoren wurden dargestellt, gefolgt von einem kurzen

Portrait der klassischen Polymere mit deren Vorteilen und Optimierungsnotwendigkeiten. Optimierungsstrategien für Vektoren wurden in Bezug auf verlängerte Zirkulation, Toxizitätsminderung und modifizierte Membranaktivität erörtert.

Kapitel 2 beschäftigte sich mit der Untersuchung der Einflüsse von Umgebungsazidität auf die Effizienz von polymerischen Genträgern am Beispiel der klassischen Vertreter PEI und PLL. Sowohl das Transfektions- als auch das Kultivierungsmedium wurde von der physiologischen bis hin zur pathologisch niedrigsten Azidität - in vier pH-Stufen 7.4, 7.0, 6.7, und 6.3 - variiert. Die physikalisch-chemischen und biologischen Kenngrößen zeigten beide bedeutende Veränderungen als Reaktion auf den pH-Shift. Wie es sich aus der Betrachtung der Kultivierungs- und Transfektionsmedien unter getrennten Bedingungen abgezeichnet hat, waren die Effekte teilweise entgegen gerichtet. Das angesäuerte Transfektionsmedium verringerte die Genexpression um etwa 1.6~7.7-mal im Vergleich zu physiologischen Bedingungen, wobei das angesäuerte Kulturmedium gleichzeitig die Transfektionseffizienz um etwa 2.1~2.6-mal erhöhte. Die in dieser Studie erworbenen Befunde zeigen, dass die Berücksichtigung des aziden Milieus in der Tumorumgebung sehr empfehlenswert bei der Materialentwicklung für Gentransportzwecke ist. Die spezifischen biologischen Eigenschaften von azidem Gewebe sollten nicht vernächlässigt werden, weil sie die Transfektionsleistung beeinträchtigen.

Kapitel 3 untersuchte den Zusammenhang zwischen Struktur und Funktion von mit Mono-methoxyl-poly(ethyleneglycol)-block-poly(ε-caprolacton) (mPEG-PCL) modifizierten hoch verzweigten PEI-co-polymeren (hy-PEI-PCL-mPEG) als siRNA-Vektoren. Die ABC-Konstrukte waren amphiphil und konnten stabile Komplexe bilden. Die PCL-Segmentlänge sowie die PCL-PEG-Armanzahl hatten meist deutlichen Einfluss auf Pufferkapazität, kolloidale Stabilität und Bindungsaffinität zu RNA. Aus der Biblothek von (hy-PEI-PCL-

mPEG) Polymeren hat sich hy-PEI25k-(PCL900-mPEG2k)1 als erfolgreichster Kandidat für den Transport von siRNA hervorgehoben und somit Perspektiven für Tierexperimente eröffnet.

In **Kapitel 4** wurden die Blocklängen und Molekularmassen der poly(2-(dimethyl amino)ethyl methacrylate-*block*-poly(2-hydroxylmethacrylate)-Familie variiert, um die für eine erfolgreiche Transfektion notwendigen Mindestanforderungen an den polykationischen Anteil zu bestimmen. Durch pHEMA-Kopplung konnte das bis dahin zu Transfektionszwecken unbrauchbare homo-pDMAEMA115 bedeutend in seiner in vitro Leistungsfähigkeit verbessert werden. Die mittels RAFT synthetisierten Diblockcopolymere lagen im Bereich von 17–35.7 kDa und waren um 1.4–9.7-mal weniger toxisch als PEI 25 kDa sowie auf Grund ihrer Größe für renale Ausscheidung ohne vorherige Metabolisierung geeignet. Somit wurden die niedermolekularen pDMAEMA - früher als erfolglose DNA-Vektoren bezeichnet - in deren Transfektionspotential bei gleich niedriger Toxizität gestärkt, was sie zu interessanten Kandidaten für weitere Untersuchungen in Rahmen der therapeutischen Genzuführung macht.

In **Kapitel 5** wurde die Wechselbeziehung zwischen Polymersteifigkeit, pHEMA-Anteil und Glaspunkt-Temperatur (T_g) bestimmt. Der mittels MD im Wasserkraftfeld simulierte Faltungsprozess der Polymerketten reflektierte die Bedeutung der Polymerkonformation während der DNA-Bindung. Mittels ITC konnten auch die energetischen Aspekte dieses Bindingsprozesses ersichtlich gemacht werden. Hoch flexible Moleküle des Homopolymers benötigten eine zusätzliche Energieinvestition für den Entfaltungsprozess, um mit DNA zu funktionstüchtigen Nanovehikeln assoziieren zu können. Der Zusammenhang zwischen dem hohen Anteil an exothermen Segmenten in ITC-Profilen und der Länge des pHEMA-co-Blocks betonte zum wiederholten Male den günstigen Einfluss der pHEMA-Anknüpfung auf

die Transfektionseffizienz. Die Befunde über den Zusammenhang zwischen Polymerstruktur, dessen räumlicher Anordnung in Wasser, und der Besonderheit der thermodynamischen Bindung dieser Polymerkonformation zu DNA könnten Aufschluss über die zuvor bobachteten Varitionen in Transfektionseffizienz geben.

AUSBLICK

Basierend auf den in **Kapitel 2** bis **4** beschriebenen Ergebnissen können weitere Untersuchungen im Bereich Gentransfer in strategisch verschiedenen Richtungen verfolgt werden. Die **in Kapitel 2** gewonnenen Erkenntnisse über den Einfluss von sauren Bedingungen im Tumorgewebe auf die polymerische Transfektion können auf ein weiteres Spektrum noch komplexerer polykationischer Trägersysteme ausgebreitet werden, wie z.B. PEG-PCl-PEI für siRNA aus **Kapitel 3** oder pDMAEMA-pHEMA für DNA-Transfer aus **Kapitel 4**. Diese Vorgehensweise kann mehr vektorspezifische Details über die Transfektionseffizienz in pathologisch nahen Bedingungen offenbaren und somit zu einer feineren und gezielteren Gestaltung der Vektoren beitragen.

Ein anderer wichtiger Schritt ist der Übergang zur tierexperimentellen Phase mit in vitro als erfolgreich etablierten Polymeren. Die für die Teilnahme an klinischen Studien erforderlichen Parameter, wie z.B. Bioverträglichkeit, Bioverteilung und Zirkulationsdauer, sind noch zu ermitteln.

Zum detaillierteren Verständnis von intermolekularen Interaktionen und sterischen Effekten polykationischer DNA- und siRNA-Träger sind weitere ITC- und MD-Studien sinnvoll, inclusive der Vergleichsstudie von siRNA/DNA-Polymer-Bindung, sowie thermodynamischem Screening des Bindungspotentials unter unterschiedlichen Bedingungen (variierende Ionenstärke, Serumproteingehalt und Medium-pH), um potentielle Engpässe der synthetisierten Konstrukte aufzudecken.

APPENDICES

LIST OF PUBLICATIONS

2012 Han Chang Kang[1], Olga Samsonova[1], Sun-Woong Kang, You Han Bae
[1]*contributed equally*
The *effect of environmental pH on polymeric transfection efficiency*
research article
accepted in Biomaterials 33 (2012) 1651-1662

2011 Thomas Endres, Moritz Beck-Broichsitter, Olga Samsonova, Thomas Renette, Thomas Kissel
Controlling the self-assembly structure of mPEG-PCL-lPEI triblock copolymers for drug and gene delivery: from micells to nanoparticles
research article
published in Biomaterials 32 (2011) 7721-7731

2011 Yu Liu[1], Olga Samsonova[1], Brian Sproat, Olivia Merkel, Thomas Kissel
[1]*contributed equally*
Biophysical characterization of hyper-branched polyethylenimine-graft-polycaprolactone-block-mono-methoxyl-poly(ethylene glycol) copolymers (hy-PEI-PCL-mPEG) for siRNA delivery
research article
published in Journal of Controlled Release 153 (2011) 262-268

2011 Olga Samsonova[1], Christian Pfeiffer[1], Markus Hellmund, Olivia Merkel and Thomas Kissel
[1]*contributed equally*
Low Molecular Weight pDMAEMA-block-pHEMA Block-Copolymers Synthesized via RAFT-Polymerization: Potential Non-Viral Gene Delivery Agents?
research article
published in Polymers 3 (2011) 693-718

2010 Olivia M. Merkel, Meredith A. Mintzer, Damiano Librizzi, Olga Samsonova, Tanja Dicke, Brian Sproat, Holger Garn, Peter J. Barth,O Eric E. Simanek and Thomas Kissel
Triazine Dendrimers as Nonviral Vectors for in Vitro and in Vivo RNAi: The Effects of Peripheral Groups and Core Structure on Biological Activity
research article
published in Molecular Pharmaceutics 7 (2010) 969–983

2010 Han Chang Kang, Olga Samsonova, You Han Bae
Trafficking microenvironmental pHs of polycationic gene vectors in drug-sensitive and multidrug-resistant MCF7 breast cancer cells
research article
published in Biomaterials 31 (2010) 3071–307

RECENT POSTERS AND ORAL PRESENTATIONS

Nov 2011	Olga Samsonova, Adam Biela, Serghei Glinca, Yu Liu, Thomas Kissel BIT'S 1st Annual Symposium of Drug Delivery Systems, Shenzhen, China Oral presentation *Isothermal Titration Calorimetry as an Exclusive Tool for Transfection Efficacy Prediction of Polymeric vectors in Vitro*
Mar 2011	Olga Samsonova, Christian Pfeiffer , Adam Biela and Thomas Kissel Controlled Release Society Local Chapter Meeting, Jena, Germany Poster *Low molecular weight pDMAEMA-b-pHEMA copolymers as non-viral vectors: a mechanistic study*
Oct 2010	Olga Samsonova, Yu Liu, Olivia Merkel and Thomas Kissel ESF-UB Conference in Biomedicine and Nanomedicine: Reality Now and Soon, Sant Feliu de Guixols, Spain Poster *Biophysical characterization of hyper-branched PEG-PCL-PEI copolymers for siRNA delivery*
Jul 2010	Olga Samsonova, Christian Pfeiffer, Olivia Merkel and Thomas Kissel Materialforschungstag Mittelhessen in Marburg, Germany Poster *pDMAEMA-pHEMA as potential non-viral carriers for gene transfer synthesized via RAFT-polymerization*

CURRICULUM VITAE

Personal Information

Name	Samsonova, Olga
Date	21th May 1982
Place of birth	Kharkiv, Ukraine
Home address	Wagnergasse 26, Schwalmstadt, Germany
E-mail	olga.samsonova@staff.uni-marburg.de sov@dr.com
Nationality	Ukrainian, permanent residence in Germany since Feb 2003

Work experience

since Aug 2009	PhD candidate in the working group of Prof. Dr. Thomas Kissel, Department of Pharmaceutics & Biopharmacy, Philipps-Universitaet Marburg, Ketzerbach 63, 35032 Marburg, Germany Area of research: ***non-viral gene and drug delivery*** Teaching activity: practical training in Pharmaceutical Technology: preparation of sterile dosage forms (7th semester pharmacy students)
May – Jul 2009	Full-time pharmacist at Stadtapotheke Treysa, Marktplatz 11, 34613 Schwalmstadt-Treysa, Dr. Bernd Adam, customer service
Nov 2008 – Apr 2009	Pharmacy trainee at Stadtapotheke Treysa, Dr. Bernd Adam
May – Oct 2008	DAAD research scholar at the working group of Prof. Dr. You Han Bae GPEN (Globalization of Pharmaceutics Education Network) program Area of research: ***non-viral gene delivery*** Project supervisor Dr. Han Chang Kang Dept. of Pharmaceutics & Pharmaceutical Chemistry, University of Utah, 421 Wakara Way, Suite 318, Salt Lake City, Utah 84108, USA.

Skills and competences

Native speaker	***Russian, Ukrainian***
Other languages	***English***, high proficiency in oral and writing skills (TOEFL, FCE)
	German, high proficiency in oral and writing skills (Feststellungsprüfung, Mittelstufeprüfung, Zertifikat Deutsch)
	Finnish, basic skills in reading, writing, and spoken language

Education and Training

Oct 2009	MSc in Pharmacy (Diplom), Martin-Luther-Universitaet Halle, Germany (defended with distinction, grade 1) Thesis title: ***„Effect of extracellular pH on polymeric transfection of tumor cell lines“***, this thesis is based on research work at the University of Utah
since Jun 2009	Pharmacist's License (Berufserlaubnis als Apothekerin)
May 2009	3rd Pharmaceutical State Examination
Apr 2008	2nd Pharmaceutical State Examination
Apr 2004 – Apr 2008	Studies at the Philipps-Universitaet Marburg, Germany Field of study: Pharmacy Sep – Dec 2006: Erasmus exchange student at the University of Kuopio, Finland. Subject of studies: Pharmaceutical Technology & Biopharmacy + Courses in Multiculturalism, English and Finnish
Mar 2003 – Feb 2004	Studienkolleg Hannover – preliminary studies for foreign applicants without immediate admittance to higher education in Germany (M-course: German, Biology, Physics, Mathematics and Chemistry). Qualified for enrollment to University via Feststellungsprüfung (Grade 1.4)
Sep 1999– Feb 2003	BSc studies at the National Pharmaceutical University of Ukraine, Department of clinical pharmacy (Kharkiv, Ukraine), only preliminary grades available
Jun 1999	Graduation from Academic Secondary School No.45 in Kharkiv, Ukraine with distinction (Grade 1.0 according to German system)

Member in

SciMento	Mentoring program for women in natural sciences in Hessen, providing courses for professional development accessory to academics, such as: human resources and project management, scientific writing, public speech coaching, etc.
MARA	Marburg University Research Academy, Graduate Center for Life Sciences. Program scope for members includes workshops, presentations and lectures in issues relevant to career development
CRS	Controlled Release Society/ Local Chapter Germany (Saarbrücken, Germany) aims to exchange knowledge on innovative therapeutical delivery systems, assist young scientists in their professional development, organizes conferences, symposia and workshops

Hobbies

Open air leisure sports: cycling, voleyball, jogging, hiking etc.

ACKNOWLEDGMENTS

Herewith I would like to express my deepest gratitude to the supervisor of my doctoral thesis Prof. Dr. Thomas Kissel, for his continuous and efficient help with words und deeds in developing and coordinating of projects described above. I thank him cordially for giving me an opportunity to join his working group, for his trust in me and motivating mentoring during the whole research period. I appreciate his constant readiness for scientific discussions and his experienced advice. The unique opportunity to learn a broad range of analytical and cell culture methods is greatly appreciated as well. I also thank Prof. Dr. Kissel for providing me sufficient space for individual creativity and the possibility to develop own concepts. Last but not least I would like to thank him for enabling me the research visit to the University of Utah in 2008 and opening me a world of international science.

I cordially thank Prof. Dr. Carsten Culmsee for the role of second thesis referee and carrying out the function of examination board chairman.

My best thanks goes to Prof. Dr. Maike Petersen and Prof. Dr. Gerhard Klebe for their readiness to join the examination board as minor field study examiners at my thesis defense.

My special thanks go to Prof. Dr. You Han Bae and Prof. Dr. Han Chang Kang for an inspiring and productive cooperation.

I would like to grately thank all my cooperation partners, who brought vivid variability in my research projects: Christian Pfeiffer, Markus Hellmund and Dr.Yu Liu for synthesizing polymer libraries of pDMAEMA and PEG-PCL-PEI, as well as their excellent support in chemical questions. I cordially thank Dr. Olivia Merkel for introducing me into a broad range of cell culture techniques, productive discussions as well as proof reading of publications. I greatly appreciate the creative advice of Dr. Moritz Beck-Broichsitter on multiple strategic and methodical questions during physicochemical studies. I forward my best thanks to Adam

Biela and Serghei Glinca from Prof. Dr. Klebe’s working group for their exellent support in questions of isothermal titration calorimetry and computer modeling.

I greatly thank Elena Bohn for her patient proofreading of my PhD thesis.

My farther thanks go to Eva Mohr for support in cell culture questions, as well as to Julia Michaelis for providing me with literature materials.

I would like to thank all members of Prof. Kissel’s and Prof. Bakowsky’s working groups for a friendly and creative atmosphere and great time together!

My parents I deeply thank for their support over the whole time of my studies in Germany and especially the PhD phase, for their patience, believing in me and setting a good spirit for all my endeavours.

ERKLÄRUNG

Ich versichere, dass ich meine Dissertation

“Self-assembling polycations for gene delivery:
Effects of polymer structure and environmental pH”

selbständig ohne unerlaubte Hilfe angefertigt und mich dabei keiner anderen als der von mir ausdrücklich bezeichneten Quellen bedient habe.

Die Dissertation wurde in der jetzigen oder einer ähnlichen Form noch bei keiner anderen Hochschule eingereicht und hat noch keinen sonstigen Prüfungszwecken gedient.

Marburg, den 6.01.2012

.....

Olga Samsonova